Dissertation

Molecular mechanisms of photo(chemo)therapy and mTOR inhibition in two mouse models of psoriasis

submitted by

Nitesh Pralhad SHIRSATH

for the Academic Degree of

Doctor of Philosophy

(PhD)

at the

Medical University of Graz

Department of Dermatology

under the Supervision of

Prof. Dr. Peter WOLF

2017

Table of content

Declaration and Disclosures IV
ABBREVIATIONS V
ABSTRACT VII
ZUSAMMENFASSUNG IX
1. INTRODUCTION 1
1.1 Psoriasis 1
1.2 Phototherapy and its immunomodulating effects 3
1.3 Imiquimod (Aldara) 6
1.4 Imiquimod psoriasis mouse model 7
1.4 Cellular senescence 10
1.5 mTOR signaling 11
2. STUDY PART 1: TO ELUCIDATE THE THERAPEUTIC EFFECTS OF PUVA AND UVB TREATMENT USING THE IMIQUIMOD MODEL OF PSORIASIS 13
2.1 MATERIALS AND METHODS 15
2.1.1 Animals 15
2.1.2 PUVA and UVB treatment and MPD determination 15
2.1.3 Double skin fold measurements 16
2.1.4 Tissue collection 16
2.1.5 Histologic evaluation 17
2.1.6 Immunohistochemistry 17
2.1.7 Immunoscoring 18
2.1.8 Senescence associated (SA) ß-Galactosidase (ß-Gal) Staining 18
2.1.9 Multiplex immunfluorescent analysis 18
2.1.10 Bead immunoassay 19
2.1.11 RNA isolation 19
2.1.12 RNA microarray and pathway analysis 19
2.1.13 Neutrophile chemotaxis assay 20
2.1.14 Statistical analysis 21
2.2 RESULTS 22
2.2.1 Identification of the minimal phototoxic dose (MPD) 22
2.2.2 Both treatment and pretreatment with PUVA and UVB reduces the susceptibility of mouse skin to mount a psoriatic response to IMQ 22
2.2.3 Histopathological assessment of psoriatic phenotype development 24

2.2.4 PUVA pretreatment influences Th1/Th2/Th17 cytokine and chemokines profile in IMQ-treated mice 25
2.2.5 Microarray for differential expressed genes, biological function and pathway analyses 26
2.3 DISCUSSION 29
2.4 FIGURES 33
2.5 TABLES 52
3. STUDY PART 2: REGULATION AND FUNCTIONAL IMPORTANCE OF MAMMALIAN TARGET OF RAPAMYCIN IN PSORIATIC SKIN LESIONS 56
3.1 MATERIALS AND METHODS 58
3.1.1 Mice and Treatment 58
3.1.2 Chemicals and reagents 59
3.1.3 Immunohistology examination and staining 60
3.1.4 Quantification of macroscopic vascularization 60
3.1.5 Multiplex immunfluorescent analysis 60
3.1.6 Flow Cytometry 61
3.1.7 Complete blood count 61
3.1.8 Bead immunoassay 61
3.1.9 Statistical analysis 61
3.2 RESULTS 63
3.2.1 Activation status of mTOR signaling components in psoriatic skin of K5.hTGFb1 transgenic mice 63
3.2.2 Deactivation of mTOR signalling promotes keratinocyte differentiation while cytokine-mediated induction leads to inhibition 63
3.2.3 Hyperactivation of mTORC1 signaling by agonist, MHY1485, inhibits differentiation leading to psoriasis-like skin morphology 65
3.2.4 Topical mTOR inhibition ameliorates skin and systemic symptoms of imiquimod-induced psoriasis 66
3.2.5 Rapamycin reduces inflammation induced by dermal mTOR signalling 67
3.2.6 Topical rapamycin treatment normalizes the epidermal differentiation pattern and extravasation of immune cells 68
3.2.7 Topical rapamycin reverse the shift from lymphoid to myeloid cells in imiquimod model of psoriasis 69
3.2.8 Topical rapamycin treatment precludes any adverse systemic effects 70
3.3 DISCUSSION 71
3.4 FIGURES 77
3.5 TABLES 97

4. THESIS CONTRIBUTIONS 98
5. ACKNOWLEDGEMENTS 99
6. REFERENCES 100

Declaration and Disclosures

Hereby, I disclose that part of the results included in this dissertation was published in the Experimental Dermatology (Shirsath, N., Mayer, G., Singh, T. P. & Wolf, P. 2015. 8-methoxypsoralen plus UVA (PUVA) therapy normalizes signalling of phosphorylated component of mTOR pathway in psoriatic skin of K5.hTGFbeta1 transgenic mice. Exp Dermatol, 24, 889-91), Acta-Dermatology and Venereology (Bürger, C., Shirsath, N., Lang, V., Diehl, S., Kaufmann, R., Weigert, A., Han, Y. Y., Ringel, C. & Wolf, P. 2017. Blocking mTOR signalling with rapamycin ameliorates imiquimod-induced psoriasis in mice) and Plosone journals (Bürger, C., Shirsath, N., Lang, V., Berard, A., Diehl, S., Kaufmann, R., Boehncke, W. H. & Wolf, P. 2017. Inflammation dependent mTORC1 signaling interferes with the switch from keratinocyte proliferation to differentiation. PLoS One, 12, e0180853) and is being reproduced in the thesis with the confirmation from the co-authors.

I hereby declare that this dissertation is my own original work and that I have fully acknowledged by name all of those individuals and their organizations that have contributed to the research for this dissertation in the acknowledgement section. The inclusion of such materials was done under the permission of the publisher and the respective copywrite holder. Throughout this dissertation and in all related publications I followed the guidelines of “Good Scientific Practice”.

October 2017

ABBREVIATIONS

AMP, Antimicrobial peptide;

Bregs , Regulatory B cells;

CDKIs, Cyclin-dependent kinase inhibitors;

cDC, Conventional dendritic cell;

cis- UCA, urocanic acid;

DC, Dendritic cell;

DDR, DNA damage response;

4E-BP1, Eukaryotic initiation factor 4E-binding protein 1;

ECP, Extracorporeal photopheresis;

ELISA, Enzyme-Linked Immunosorbent Assay;

ERK, Extracellular regulated kinase;

Flt3l, Fms-like tyrosine kinase 3 ligand;

FOXP3, Fork head box P3;

GM-CSF, Granulocyte/macrophage colony-stimulating factor;

IFN, Interferon;

IGF-1, Insulin-like growth factor 1;

IL, Interleukin;

IRF, IFN regulatory factor;

LC, Langerhans cell;

LPS, Lipopolysaccharide;

MAPK, Mitogen-activated protein kinase;

moDC, Monocyte-derived DC;

mTOR, Mammalian (or mechanistic) target of rapamycin;

mTORC, mTOR complex;

miR, Micro-RNA;

NF-κB, Nuclear factor κB;

pDC, plasmacytoid DC;

PASI, Psoriasis Area Severity Index;

PI3K, Phosphoinositide 3-kinase;

PIP3, Phosphatidylinositol 3,4,5-trisphosphate;

PLE , Polymorphic Light Eruption;

PUVA, Psoralen + UVA;

RANKL, Receptor activator of NF-κB ligand;

Raptor, Regulatory associated protein of mTOR;

Rictor, Rapamycin-insensitive companion of mTOR;

SASP, Senescence-associated secretory phenotype;

STAT3, Signal transducer and activator of transcription 3;

siCTRL, Silencing RNA control;

siRNA, Silencing RNA;

TG, Transgenic;

TGF-β, Transforming growth factor β;

Th1-cells, T helper 1 cells;

Tregs, Regulatory T cells;

TLR, Toll-like receptor;

TNFα, Tumour necrosis factor α;

TSC, Tuberous sclerosis complex;

γδ T cells, Gamma delta T cells ;

UV, Ultraviolet;

UVB, Ultraviolet light B;

WT, Wild Type;

ABSTRACT

The pathophysiology of psoriasis is associated with epidermal thickening, hyperproliferative keratinocytes along with aberrant induction of IL-23/Th17 axis. This uncontrolled cellular proliferation of keratinocytes has been recently identified to be modulated by mammalian target of rapamycin (mTOR), which has emerged as a major effector molecule for proliferation and differentiation defects. mTOR may also play a role in the anti-psoriatic effects in photo(chemo)therapy, a standard treatment of psoriasis. However, the mechanisms involved in the therapeutic effects of photo(chemo)therapy and the role of mTOR signaling in functional regulating the pathogenesis of psoriasis are not yet fully understood.

In the first part of the thesis, the factors responsible for the photo(chemo)therapeutic effects of psoralen+UVA (PUVA) photochemotherapy and UVB irradiation were investigated, using the imiquimod (IMQ) psoriasis mouse model. Mouse skin was treated with repetitive sub-phototoxic doses of PUVA or UVB before or during topical IMQ administration. Here, PUVA to a greater degree than UVB not only suppressed the IMQ-induced psoriatic phenotype but also pretreatment (before IMQ administration) with PUVA did to a greater degree than UVB suppress the susceptibility of murine skin to respond to IMQ. Microarray analysis showed enrichment of senescence pathway-related genes after PUVA pretreatment. PUVA downregulated baseline levels (before IMQ treatment) of IFN-gamma, IL-17 and IL-9, cytokines that drive psoriatic inflammation. However, the anti-psoriatic effect of PUVA was lost when the interval between last PUVA exposure and first IMQ administration was extended from 3 to 7 days. These findings highlight that PUVA primes the skin in such a manner as to shift the balance in favour of a reduced responsiveness to IMQ.

In the second part of the thesis, the pathogenic role of mTOR signalling and its regulatory functions in psoriasis pathology were investigated. Being a conserved serine-threonine kinase, mTOR acts primarily via the regulation of protein synthesis. This was confirmed in this part of the study where mTOR signaling hyperactivation in the psoriatic skin of K5.hTGFβ1 transgenic mice was normalized after PUVA therapy. Furthermore, by using an mTOR agonist in mice, it was

proved that specific activation of mTOR leads to abnormal epidermal organization with disturbed involucrin distribution which is a marker of terminal differentiation. These findings not only identify mTOR pathway as an important signal integrator pivotal in the psoriatic pathomechanisms but also advocated it as a promising anti-psoriatic target. This was tested by using its antagonist rapamycin, topically applied in the IMQ model of psoriasis. Locally applied rapamycin could not only inhibit the mTOR signaling in the skin but also diminish the epidermal barrier and differentiation defect of psoriatic skin.

Together, these results help better understanding the therapeutic mechanisms of photo(chemo)therapy and illuminate the role of mTOR signaling in the pathophysiology of psoriasis and its response to treatment.

ZUSAMMENFASSUNG

Die Pathophysiologie der Psoriasis steht in Verbindung mit einer verdickten Epidermis, bedingt durch Hyperproliferation von Keratinozyten und eine abnormale Induktion der IL-23/Th17-Achse. Diese unkontrollierte zelluläre Proliferation von Keratinozyten wurde jüngst erkannt durch “Mammalian Target of Rapamycin” (mTOR) moduliert zu werden, ein Effektormolekül, welches entscheidend für Proliferations- und Differenzierungsdefekte ist. mTOR könnte auch eine Rolle bei der anti-psoriatischen Wirkung der Photo(chemo)therapie spielen, einer Standardbehandlung der Psoriasis. Die Mechanismen der therapeutischen Wirkung der Photo(chemo)therapie und die Rolle der mTOR-Signalkette bei der funktionellen Regulierung der psoriatischen Pathogenese sind noch nicht zur Gänze erforscht.

Im ersten Teil dieser Arbeit wurden die für die photochemotherapeutische Wirkung der Psoralen+UVA (PUVA)-Photochemotherapie und UVB-Bestrahlung verantwortlichen Faktoren im Imiquimod (IMQ)-Psoriasis-Modell untersucht. Die Haut von Mäusen wurde dazu wiederholt mit unterschwelligen phototoxischen Dosen von PUVA oder UVB vor oder während der topischen Verabreichung von IMQ untersucht.

PUVA unterdrückte in einem stärkeren Ausmaß als UVB nicht nur den durch IMQ hervorgerufenen psoriatischen Phänotyp, sondern auch die Vorbehandlung (vor der Verabreichung von IMQ) mit PUVA unterdrückte in größerem Ausmaß die Empfänglichkeit von Mäusehaut auf IMQ zu reagieren. Eine Microarray-Analyse ergab nach PUVA-Vorbehandlung eine Anreicherung von Genprodukten, die mit Seneszenz in Verbindung stehen. PUVA (verabreicht vor der Gabe von IMQ) regulierte die Ausgangsspiegel von IFN-gamma, IL-17 und IL-9 hinunter - Zytokinen, welche die psoriatische Entzündung vorantreiben. Der anti-psoriatische Effekt von PUVA ging allerdings verloren, wenn das Intervall von der letzten PUVA-Bestrahlung bis zur ersten Verabreichung von IMQ von 3 auf 7 Tagen verlängert wurde. Diese Ergebnisse unterstreichen, dass PUVA die Haut auf eine Weise verändert, aus der sich eine veränderte Balance mit verminderter Reaktionsbereitschaft auf IMQ ergibt.

Im zweiten Teil der Arbeit wurden die pathogenetische Rolle der mTOR-Signalkette und deren regulatorische Funktion in der Pathologie der Psoriasis untersucht. Als eine konservierte Serin-Threonin-Kinase agiert mTOR in erster Line über die Regulierung der Proteinsynthese. Dies bestätigte sich in diesem Teil der Arbeit, zumal die Hyperaktivierung von mTOR in psoriatischer Haut von K5.hTGFβ1 transgenen Mäusen sich nach Behandlung mit PUVA normalisierte. Darüber hinaus zeigte sich durch die Verwendung eines mTOR-Agonisten bei Mäusen, dass die spezifische Aktivierung von mTOR zum abnormalen Aufbau der Epidermis mit gestörter Verteilung von Involucrin, einem Marker der terminalen Differenzierung, führt. Diese Ergebnisse identifizieren die mTOR-Kette nicht nur als einen wichtigen Integrator mit? entscheidender Rolle bei den psoriatischen Pathomechanismen, sondern sprechen auch für die Kette als vielversprechendes Angriffsziel einer anti-psoriatischen Therapie. Dies wurde durch die Verwendung des mTOR-Antagonisten Rapamycin mittels topischer Verabreichung im IMQ-Modell studiert. Lokal aufgebracht, vermochte Rapamycin nicht nur die mTOR-Reaktionskette zu hemmen, sondern auch den epidermalen Barriere- und Differenzierungsdefekt psoriatischer Haut zu vermindern.

Die Ergebnisse dieser Arbeit helfen, die therapeutischen Mechanismen der Photo(chemo)therapie besser zu verstehen und durchleuchten die Rolle der mTOR-Reaktionskette in der Pathophysiologie der Psoriasis und deren Ansprechen auf die Behandlun.

1. INTRODUCTION

1.1 Psoriasis

Psoriasis is a common, chronic autoimmune skin disorder which affects approximately 3-4% of the world's population with frequency rates influenced by geographic location and age (Chandran and Raychaudhuri, 2010, Crow, 2012, Di Meglio et al., 2014). Its pathology is a result from the interplay of immune system, predisposing genetic factors and environmental triggers. This leads to phenotype which is characterized by focal formation of inflamed, raised plaques that shed scales from excessive growth of epithelial cells with hyperplasia of epidermal keratinocytes (KC), vascular hyperplasia, ectasia, infiltration of T lymphocytes, neutrophils, and other types of leukocytes in the affected skin (Guttman-Yassky et al., 2011, Boehncke and Schon, 2015). Interestingly, it shares immunologic and genetic features with other autoimmune inflammatory conditions such as inflammatory bowel disease; rheumatoid arthritis and multiple sclerosis, which pathologies all involve Th1 and Th17 cells (Fitch et al., 2007, Fiorino and Omodei, 2015). While the immunopathogenesis is not completely understood, there are complex underlying mechanisms, which involve the communication between three main cellular players (KC, myeloid dermal dendritic cells (DDC) and T cells) and their products (Chamian et al., 2005, Di Meglio et al., 2014).

The immunopathological events of psoriasis can be broadly divided into initiation and maintenance phase. Clinically innate cytokine interferon-α has been identified as an important inducer of psoriasis concomitant with plasmacytoid dendritic (pDCs) cells increased in early psoriatic lesions which has been validated in pertinent animal models (Funk et al., 1991, Nestle et al., 2005, Yao et al., 2008). KCs release the cationic antimicrobial peptide (AMP) LL-37 which binds to self DNA/RNA fragments activating then the subset of circulatory DC and TLR7/9-bearing pDC, which otherwise is absent in human healthy skin (Lande et al., 2007). As a result of this many proinflammatory cytokines are released by activated KCs like interleukin (IL)-1b, IL-6, TNF-α and chemokines (e.g., IL-8 [CXCL8], CXCL10, and CCL20) which causes maturation and activation of DDC (Nestle et al., 2009, Singh et al., 2016). These cells act as an antigen presenting

mature DDC for naive T cells which amplify the signals for plaque progression. This as it creates an IL-23/IL-17 inflammatory environment in which DC and macrophage-derived IL-23 promotes T-helper 17 (Th17) and cytotoxic-T 17 (Tc17) cell effector functions which ultimately form the classical IL-23/ IL-17 axis. Additionally, many other key players like cytotoxic CD8 T cells, as a source of disease-relevant cytokines like IL-17A, TNF, IFNg, and IL-22 in the epidermis (Hammar et al., 1984, Hijnen et al., 2013), and Gamma delta T cells (γδ-T cells), a major resource of IL-17 via alternative IL-22 pathway (Laggner et al., 2011, El Malki et al., 2013), maintain the disease and thereby interface between effectors of the innate and adaptive immune system that shapes the psoriatic phenotype.

Being heterogeneous in nature psoriasis exists in several distinct forms which are classified into four main types identified as: plaque, guttate, generalized pustular, and erythrodermic (Di Meglio et al., 2014). Additionally, several further sub phenotypes are identified according to its distribution (localized vs. widespread), location anatomically (flexural, scalp, palms/ soles/nail), size (large vs. small) and thickness (thick vs. thin) and disease activity (active vs. stable) as proposed by the International Psoriasis Council (Griffiths et al., 2007). Approximately 70 to 80 percent of patients with psoriasis suffer from mild disease form (plaque psoriasis) defined by Psoriasis Area Severity Index (PASI) ≤ 10. The therapeutic approach in controlling psoriasis depends completely on the severity of the disease. 8-methoxypsoralen plus UVA (PUVA) and narrowband UVB (NB-UVB) phototherapies are well-established and generally effective treatments for mild to chronic plaque psoriasis, with therapeutic efficacy supposedly dependent on selected dose and frequency of irradiation (Ibbotson and Farr, 1999, Legat et al., 2004, Tanew et al., 1999). Topical agents such as corticosteroids, vitamin D analogues, retinoids and calcineurin inhibitors are mainly used for the treatment of mild forms of psoriasis. While for moderate-to-severe psoriasis (affecting large body surface areas) a well-established treatment regimen is the combination of topical agents and phototherapy or systemic drugs (Nast et al., 2012, Mendonca and Burden, 2003).

1.2 Phototherapy and its immunomodulating effects

Phototherapy is a valuable option in the treatment of many psoriatic and nonpsoriatic conditions (Roelandts, 2002, Roelandts, 2005, Moller et al., 2005, Walker and Jacobe, 2011). The phototherapeutic effect of UV energy depends on the spectrum of radiation emitted by the different light sources. This UV spectrum can be subdivided into UV-A (315–400 nm), UVB (280-315nm) and UVC (100-280nm) (Hockberger, 2002, Gupta et al., 2013) (Fig.1). PUVA photo(chemo)therapy consists of the oral or topical administration of psoralen with subsequent UVA irradiation. PUVA is therapeutically effective in many skin diseases like chronic eczema, graft-versus-host disease after allogeneic bone marrow transplantation, mastocytosis, and vitiligo. It also can prevent many photodermatoses (light-induced skin diseases), including polymorphic light eruption (PLE ("sun allergy")) (Jampel et al., 1991, Bulat et al., 2011, Radack et al., 2015, Schweintzger et al., 2015a). Also, UVB irradiation is also one of the oldest treatment options in psoriasis, including heliotherapy, broadband UVB, and narrowband UVB. Despite the introduction of biologics, PUVA photochemotherapy and UVB have kept their eminent place in the armamentarium of dermatological treatments for psoriasis and remains a mainstay for mild to unmanageable and very severe forms of psoriasis. However, the mechanisms of action of photo(chemo)therapy are still incompletely understood (Singh et al., 2010, Ling et al., 2016, Wolf, 2016). Classically, the focus of phototherapy research was based on intercalating effects of psoralen in DNA causing the its photochemical reaction along with anti-proliferative effect through programmed cell death in T lymphocytes in both the epidermal and dermal psoriatic tissues (Vallat et al., 1994, Duthie et al., 1999, Santamaria et al., 2002, Wong et al., 2013). This effect was consistently paired with its cellular driven immunosuppressive effect mediated via T cells (Elmets et al., 1983). The relation of immune suppression linked to regulatory T cells (Tregs) (Schwarz, 2008, Schweintzger et al., 2015a) and more recently by regulatory B cells (Bregs) (Byrne and Halliday, 2005) depend on doses and frequency of the therapy. Having said that, reduced frequency and emigration of Langerhans cells (LC) from the epidermis due to UV-R (Noonan et al., 1984) is paired with reduced stimulation of secretary phenotype like growth factors and nitric oxide which regulates keratinocyte proliferation (Morhenn, 1997) along with

mast cells derived histamine which thereby contributes in immune suppression (Hart et al., 2001).

The therapeutic understanding of phototherapeutic mechanisms has emerged a lot over the last years (Patra et al., 2016, Wolf et al., 2016b). This includes the understanding of suppressive effects via isomerization of urocanic acid (UCA) (De Fabo and Noonan, 1983) that acts through the 5-HT_{2A} receptor (Wolf et al., 2016a) and induction of reactive biophospholipids like platelet activating factor (PAF) which by binding to the PAF receptor results in downstream induction of IL-10 (Wolf et al., 2006). Locally and systemically, UV-R have shown to upregulate cytokines such as TNF-α, IL-10, IL-4, IL-33, and prostaglandin E_2 (Shreedhar et al., 1998, Wolf et al., 2000, Byrne et al., 2011) which leads to infiltration of suppressor macrophage and neutrophils in healthy skin (Cooper et al., 1992). In diseases skin exposure to UVB (Johnson-Huang et al., 2010, Racz et al., 2011) or PUVA (Coimbra et al., 2010, Singh et al., 2010, Ravic-Nikolic et al., 2011, Singh et al., 2011) have positively modulated antipsoriatic cytokines such as IL-4 and IL-10 and downregulated propsoriatic cytokines like TNF- α, interferon-gamma, IL-9, IL-23 and its downstream effector cytokines IL-17 and IL-22.

These findings were further scrutinised and validated in in vivo setting. In the TGF-beta1 transgenic psoriatic mouse model the role of PAF in the psoriatic skin was linked to systemic Th17 downregulation and abolishment of disease manifestations (Singh et al., 2011). Recently, both UVB and UVA have showen to cause systemic immune suppression by activating the 5-HT_{2A} receptor (Wolf et al., 2016a). In the field of KC biology work by Weatherhead et al (using computational two-dimensional modelling of epidermis) suggested that UVB's mechanism in resolving psoriatic plaques may possibly be explained by apoptosis of stem and transit-amplifying cells alone.

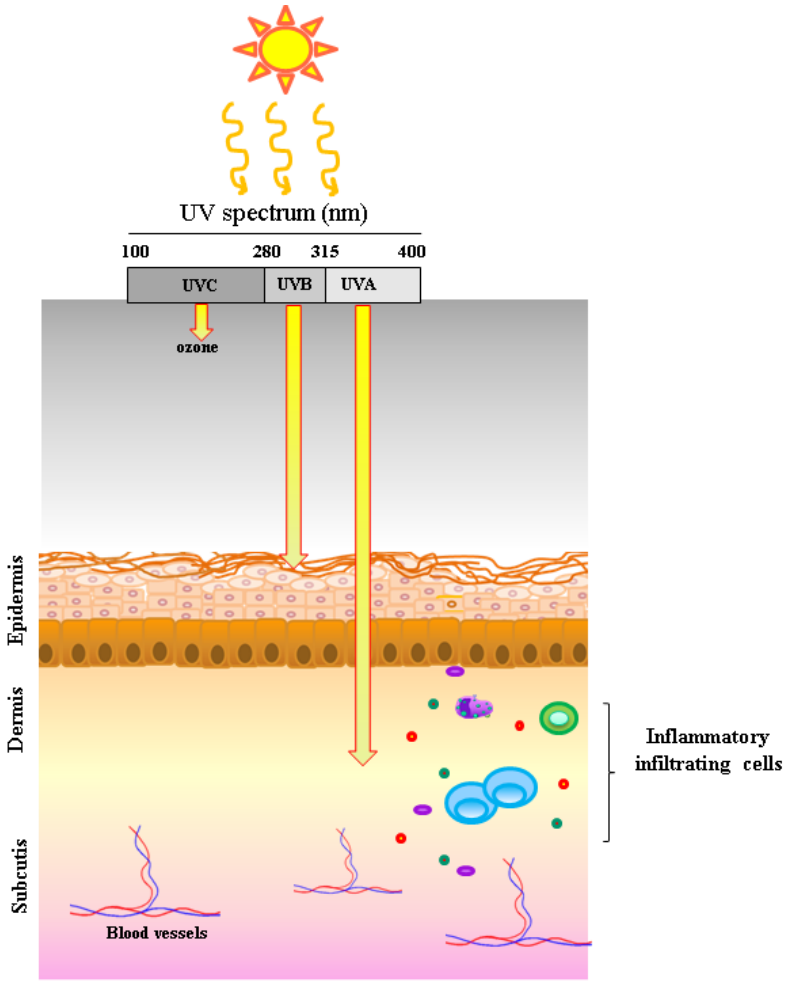

Fig. 1 Skin composition and penetration of solar ultraviolet rays (UVR) into the skin. The skin is divided into three main section which includes epidermis, dermis, and subcutis. UVC with the highest energetic photons is blocked by the ozone layer while UVB carries intermediate energetic photons that damage DNA in epidermal cells. UVA carries low energetic photons but penetrates deeply into the skin and damages the collagen and elastic tissue. This may leads to infiltration of inflammatory cells like leukocytes, mast cell and cytokines.

1.3 Imiquimod (Aldara)

Imiquimod (IMQ) is an imadazoquinoline derivative which was originally developed as a low molecular weight nucleoside analogue which is known as potent inducer of IFNs to provide antiviral activity (Chollet et al., 1999, Chi et al., 2017) through the activation of Toll like receptors (TLR). They belong to a class of pattern recognition receptors which forms a connecting link in innate immunity and adaptive immunity. There are in total 11 TLRs known where some are expressed in the intracellular endosomes (TLR3, 7, 8, and 9), while the remaining are localized on the plasma membrane (TLR1, 2, 4, 5, 6, 10, and 11TLRs) (Hennessy et al., 2010). In general, these TLRs are expressed by many innate immune cells and epithelial cells where IMQ is an agonist specifically for the TLR 7 receptor (Vacchelli et al., 2013). The TLR7 can be triggered not only by ssRNA, but also by immune modifiers with similar structure to nucleosides (Maeda and Akira, 2016). This powerful immune stimulatory action has been potentially used in the anti-tumor therapy. However, based on the highly hydrophobic nature and low molecular weight, IMQ was developed for topical administration (Chollet et al., 1999) where it acts through these receptors to provide its therapeutic effects. IMQ was protective in a vaginal guinea-pig HSV-2 infection model, concomitant with the induction of Type-I IFN. I also can lead to systemic response protecting against subcutaneous, lung, and colon tumors when it is given orally (Sidky et al., 1992).

Though the antitumor efficacy of IMQ is still not fully understood, it is known to be associated with the MYD88-dependent pathway (Chi et al., 2017). This leads to induce tumor regression following infiltration of pDCs (Drobits et al., 2012) not only in transplantable melanomas but also in a variety of murine tumors, both localized and systemically (Sidky et al., 1992). Thus this formed the base for promoting its clinical use. It has been approved by the Food and Drug Administration (FDA) as a therapeutic agent for basal cell carcinoma and genital warts (Beutner et al., 1999, Vacchelli et al., 2012). Its repetitive use for these indication has reportedly induced psoriatic lesions in humans (Tyring, 2001). The pro-psoriatic action of IMQ was later confirmed in a mouse model (van der Fits et al., 2009).

1.4 Imiquimod psoriasis mouse model

Topical application of IMQ in mice has been shown to induce skin inflammation and pathology in mice closely resembling plaque-type psoriasis in humans. It leads to infiltration of the skin by key players from the innate and adaptive immune system such as neutrophils, mononuclear cells, CD4+ T cells (especially Th17 cells), CD11c+ DCs, plasmacytoid DCs. The phenotypic psoriatic changes of transient nature dependent on IL-23/IL-17 (Flutter and Nestle, 2013). Thus, from the time of its initial description by the Van der Fits group (van der Fits et al., 2009) until today, it has become a model of acute skin inflammation with reproducible, psoriasis-like pathology. The model is commonly used for preclinical studies to test anti-psoriatic agents (Hawkes et al., 2017). The model has helped to establish fundamental concepts regarding the pathophysiology of psoriasis. Notably, IMQ exposure does result in diverse outcome in different mouse strains where for instance BALB/c mice exhibit a more rapidly development of psoriatic phenotype being flakier and more inflamed compared to C57BL/6 mice (van der Fits et al., 2009). In C57BL/6 mice IMQ can lead to severe side effects of dehydration which is recoverable by injection of PBS. These differences in outcome after IMQ exposure of different transgenic mouse strains were nicely characterised recently by Flutter and Nestle (Flutter and Nestle, 2013). Usually, a psoriatic IMQ response can be seen nicely after 3 to 4 days of treatment (Walter et al., 2013).

The cellular mediators that initiate psoriatic changes in first 24h include neutrophils, mast cells and Langerhans cells whereas 2 to 4 days after IMQ exposure, more neutrophils are accompanied by macrophages and from day 4 to 5 onwards γδ T cells, being IL-17 producing cells, start to peak up to day 7 (Heib et al., 2007, Flutter and Nestle, 2013).

TLR7 is known to be crucial for the early cutaneous response that recruits the IFN-gamma producing pDC. Whereas the inflammatory mediators IL-17 family members and IL-22 appear 24h after IMQ administration following the expression of upstream effector cytokine IL-23, which is also induced within first 24 h (van der Fits et al., 2009, Van Belle et al., 2012). Remarkably, IL-1 receptor and TNF- α signalling does not seem to be required for inflammation in this model and the absence of the former (IL-1) is compensated by secretion of another other IL-1

family member, IL-36 and its sub-types (IL-36α, β, and γ) (Tortola et al., 2012, Drobits et al., 2012). Mechanistically, IMQ has been shown to regulate through a number of separate pathways, all of which are overlapping as shown in Fig 2. While the principal mode of action of IMQ is through TLR7 signaling (Hemmi et al., 2002), vehicle-dependent and TLR7 and MyD88 signaling-independent responses are also been reported (Walter et al., 2013). While the former works through NF-κB signaling in a MyD88-dependent fashion activating TLR7 receptors in macrophages and DCs. Downstream the activation of STAT1 and STAT3 pathways leads to cytokine production by DCs (Larange et al., 2009). The latter act either by promoting inflammasome activation in keratinocytes, which are TLR7/8 negative (Kollisch et al., 2005), by the vehicle, isostearic acid or by adenosine receptors for which IMQ acts as an antagonist (Schon et al., 2006).

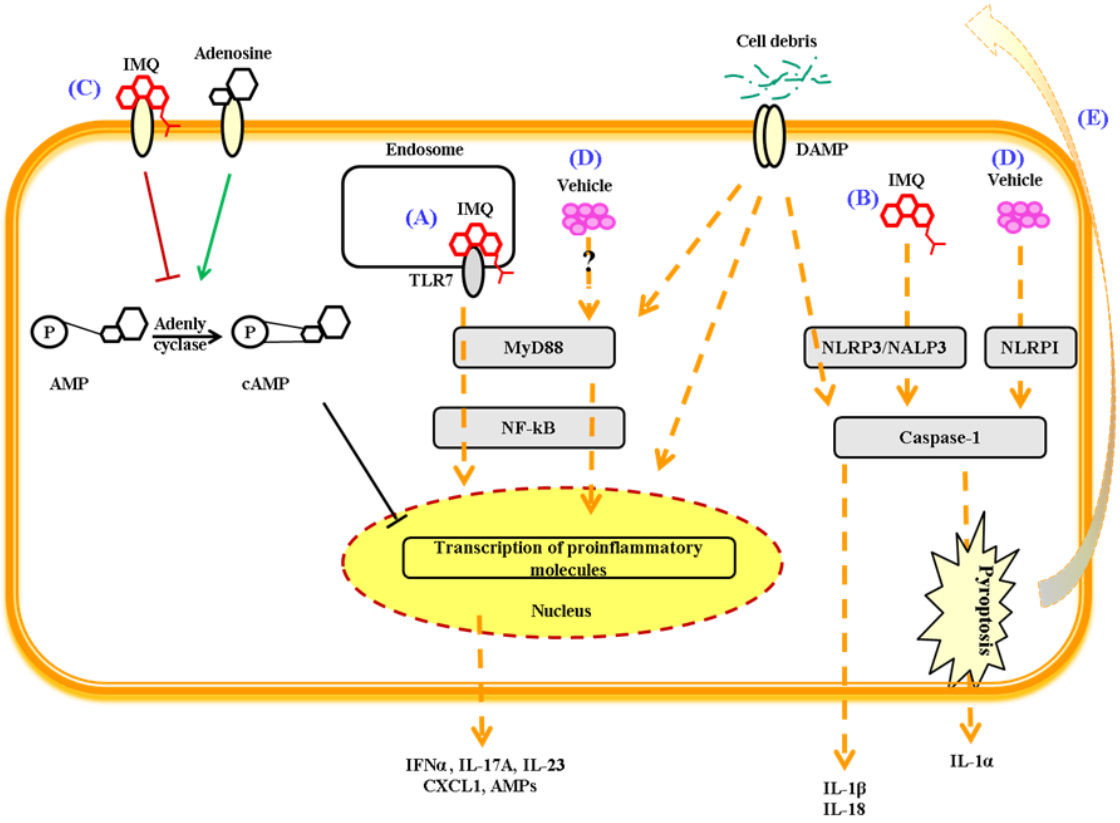

Fig. 2 Aldara™ (IMQ)-induced inflammation and its mode of action. IMQ can activate the immune system via a number of different pathways including: (A) TLR7- dependent MyD88 pathway activation in immune cells, (B) NALP3 activation of the inflammasome, (C) antagonism of adenosine receptor signaling leading to reduced levels of anti-inflammatory cyclic AMP (cAMP), (D) direct activation of the inflammasome or MyD88 pathways through unknown receptors by the vehicle isostearic acid, (E) IMQ or vehicle-driven cell death leading to the release of preformed IL-1α, which may in turn activate other nearby cells. IMQ, imiquimod; DAMP, danger-associated molecular pattern; AMP, antimicrobial peptide. Reproduced from (Flutter and Nestle, 2013) with permission of John Wiley and Sons publisher.

1.4 Cellular senescence

Cellular senescence is a multi-layered response of cells to a variety of stressors that lead to halt of proliferation of cells (Childs et al., 2015). In cell biology, this process of ceasing is also referred to as replicative senescence which distinguishes cells in senescence (a permanent cessation of division) from cells in quiescence (a temporary cessation of division) (Coates, 2013). Notably, this further leads to production of proinflammatory and matrix-degrading molecules, known as the senescence-associated secretory phenotype (SASP) (Coppe et al., 2010). These senescent cells biochemically are known to display increased lysosomal enzyme activities called as senescence-associated β-galactosidase (SA ß-gal) activity which is a common downstream effector marker of the senescent cells. Senescent cells are inable to incorporate BrdU and display increased levels of p16/INK4A, p21/CDKN1A, and their upstream regulatory protein p53 which ultimately leads to cell cycle arrest (Coates, 2013). This fate decision after DNA damage to undergo cellular senescence due to ultraviolet radiations occurs more commonly via the tumor suppressor p53 (Tavana et al., 2010). Moreover, the process of senescent development is sequential where p21 expression increases when the majority of cells are under cell cycle arrest, whereas p16 expression escalates in the terminal stages of senescence when all cells have lost their growth potential (Alcorta et al., 1996). However, nothing is known about whether these CDKIs regulates or influences the SASP or its paracrine effects (Coppe et al., 2010). Further on, senescence effect can be acute and chronic, which are regulated majorly through three pathways. The most common is the telomerase associated-pathway which leads to induction of DNA damage markers such as gH2AX and 53BP1 found at the telomeres; the central pathway is oxidative stress due to ROS and NF-κB signalling that induces senescence; lastly**,** oncogene-induced senescence which is driven by Ras and Raf, or loss of tumour suppressors such as PTEN, inducing senescence (Gorgoulis and Halazonetis, 2010). These oncogenic signal through the MAPK cascade induce p16 expression leading to an irreversible form of senescence.

1.5 mTOR signaling

PI3-kinase (PI3-K) and mammalian target of rapamycin complex 1 (mTORC1) are fundamental components of immune cell-signaling networks. They play an instrumental role in skin normal homeostasis and morphogenesis (Ding et al., 2016), especially in the regulation of keratinocyte differentiation and epidermal stratification (Deane and Fruman, 2004, Pankow et al., 2006, Ding et al., 2016). It has been long time hypothesized that the PI3-K/Akt/mTOR cascade might play a role in the pathogenesis of psoriasis with its hyperproliferative KCs with differentiation defects (Nestle et al., 2009), by not only regulating the function of immune cells but also intrinsic alterations within the epidermis (reviewed in (Huang et al., 2014)). In addition, the PI3-K/mTOR pathway is likely to play a role in Th1-Th2-Th17 imbalance in psoriasis pathogenesis (Huang et al., 2014). While mTOR signalling as a downstream effector has emerged as a major effector and signal integrator molecule of cell proliferation and differentiation (Zhao et al., 2010). It has been shown to control the immune response, not only in myeloid cells but also in keratinocytes by contributing to cytokine production (Laplante and Sabatini, 2012). Overall it drives a complex networking which apparently has contrasting roles on mTOR (Gunzl and Schabbauer, 2008) as inhibition of mTORC1 is also known to activate the upstream PI3K–AKT pathway through a feedback loop via ribosomal protein S6 kinase 1 (S6K1)(Brognard et al., 2007).

This pathway is classically targeted by rapamycin, also known as sirolimus, which was initially investigated as an antifungal agent and later as immunosuppressant (Saunders et al., 2001) and anti-tumorigenic agent. Rapamycin binds to the cytoplasmic protein FKPB-12, which interacts with mTORC1, thus blocking the mTOR target proteins S6 and partly 4E-BP that are essential for protein synthesis and thereby for cell growth and proliferation (Nashan, 2002). This is mainly because rapamycin does not inhibit the preliminary step of substrate recruitment but blocks the right configuration of some substrates to the catalytic cleft which explains that it has been more effective in blocking S6K1 than 4E-BP1 (Shimobayashi and Hall, 2014). This has encouraged the development of the ATP-competitive dual-mTOR inhibitor Torin 1 (Chiarini et al., 2015). The aberrant activation of mTOR in different cancers and also in epidermal tumours has

promoted the investigation of rapamycin as an antitumorigenic agent and enabled further development of a range of small molecule inhibitors that may prove effective in disease control (Laplante and Sabatini, 2012).

There are not many large scale trials to validate the potential of rapamycin as an effective topical agent in psoriasis (Ormerod et al., 2005) and few studies tested its anti-psoriatic effect after oral administration (Frigerio et al., 2007, Reitamo et al., 2001, Wei and Lai, 2015). However, topical rapamycin treatment for tuberous sclerosis complex (TSC) is well documented recently. Reportedly here topical rapamycin have shown remarkable efficacy in treating angiofibromas of patients with TSC (Fogel et al., 2015). At molecular level in TSC, genetic mutations of the TSC1 gene at chromosome 9 or the TSC2 gene at chromosome 16 inhibit the association of their protein product, tuberin and hamartin respectively, which leads to an aberrant upregulation of the mTOR signalling pathway. Interestingly, topical rapamycin has shown remarkable efficacy in treating angiofibromas of patients with TSC (Tanaka et al., 2013). Altogether, this highly advocates the use of topical rapamycin as anti-psoriatic modality. This was tested herewith in the IMQ model which has shown mTOR activity similarly as in human psoriasis (Chamcheu et al., 2016, van der Fits et al., 2009). Moreover the model seems to be an useful tool in testing topical drugs and their effects on barrier integrity (Lin et al., 2015) (Roller et al., 2012).

2. STUDY PART 1: TO ELUCIDATE THE THERAPEUTIC EFFECTS OF PUVA AND UVB TREATMENT USING THE IMIQUIMOD MODEL OF PSORIASIS

Aims

8-methoxypsoralen-UV-A (PUVA) and UVB are well-established treatment options for mild to chronic plaque psoriasis (Ibbotson and Farr, 1999, Legat et al., 2004, Tanew et al., 1999). PUVA has a significant higher clearance rate paired with longer remission period compared to UVB (Ling et al., 2016, Wolf, 2016), though the molecular mechanisms behind these differential anti-psoriatic effects are not well understood. The aim of this thesis part was to investigate the effects of these two phototherapy modalities and the mechanisms involved in the IMQ mouse model. Additionally the molecular gene signature and changes in serum cytokine and chemokine network, responsible for the therapeutic effect were assessed. Also, how PUVA in comparison with UVB treatment suppresses and prevents the onset of IMQ-induced inflammation was determined.

The study and the data that is shown in this section of the dissertation have been submitted for publication to Acta-Dermatology-Venereology and are currently under review. The respective paper is entitled “PUVA diminishes imiquimod-induced psoriatic phenotype with gene expression signature associated with senescence” (by N. Shirsath, K. Wagner, S. Roos, M. Schlederer, C. Ringel, L. Kenner, B. Brüne and P. Wolf). The permission to use this data in my PhD thesis was obtained from the co-authors.

2.1 MATERIALS AND METHODS

2.1.1 Animals

BALB/c mice were purchased from Charles-River and were housed in the animal facility of the Centre for Medical Research, Medical University of Graz, Austria. All the procedures to which the mice were subjected were approved by the Austrian Government, Federal Ministry for Science and Research, through protocol no. BMWF-66-010/0032-11/3b/2013. Female mice at the age of 7–8 weeks were shaved on the back skin 48 h before the start of experiment. Aldara® (IMQ) 5% cream (MEDA Pharmaceuticals, Vienna, Austria) was used for inducing psoriatic skin changes on the shaved back of mice. All animals were maintained with alternating 12-h light-and-dark cycles and controlled temperature and humidity in facilities approved by the Austrian government. Water and food were provided ad libitum. Mice were euthanized with an overdose of isoflurane and all efforts were made to minimize suffering.

2.1.2 PUVA and UVB treatment and MPD determination

The mice were painted on their dorsal skin with 200 µl of 8-methoxypsoralen (8-MOP) (Sigma-Aldrich, St. Louis, MO) made in ethanol at a concentration of 0.1 mg/ml or with vehicle (95% ethanol) or were left untreated. The mice were then kept in standard cages to allow penetration of 8-MOP for 15 min in individual compartments. UVA irradiation was then performed using a Waldmann UV236A irradiation system carrying two fluorescent PL 36W/09-PUVA light tubes (emission range, 315–400 nm; peak, 365 nm; Waldmann Medizintechnik, Villingen-Schwenningen, Germany) at a mean irradiance of 8.55 mW/cm^2 at a distance of 15 cm from the dorsal skin of the mouse to the glass cover of irradiation system positioned upside down on the top of the cage. The irradiance was monitored by a Waldmann PUVA photometer, which is calibrated for the irradiation system. For UVB, radiation was performed using a Waldmann 236 light source (Waldmann Medizintechnik, Villingen- Schwenningen, Germany), equipped with two

Waldmann UV6 fluorescent tubes (emission range 280–360 nm; peak, 320 nm) and positioned upside down on top of cage (Singh et al., 2014). The light source emitted a spectrum of approximate 40% UVB and 60% UVA radiation; where 99% of the light source that caused erythema was derived from the UVB region (280–320 nm), as determined by spectral measurement (MSS 2040 UV spectral radiometer, Fröndenberg, Germany) and calculation of the CIE-weighted erythema spectrum (Schweintzger et al., 2015b). The mean UVB irradiance of the lamp was 1.7 mW/cm^2, which was measured by using Waldmann UV photometer with UV6 detector head, appropriate to the radiation device.

2.1.3 Double skin fold measurements

The macroscopic effect of PUVA and UVB irradiation was evaluated by measuring the double skin-fold thickness of dorsal skin of the mice with a spring-loaded engineer's micrometer (Mitutoyo Corporation) before the start of the experiment and certain days during the experiment and on the day of sacrificing. Skin swelling (S) was determined by subtracting the skin thickness of control (Group VIII) from the treated group. Additionally, the percent suppression of skin swelling for PUVA or UVB treated groups was determined by the following formula: $(1-(S_{IMQ+PUVA \text{ or } UVB} / S_{IMQ})) \times 100$ (Burger et al., 2017).

2.1.4 Tissue collection

Mice were sacrificed at the time point indicated in Fig. 2.4.4 and samples of dorsal skin, spleen, lymph nodes, and blood were collected. Approximately 1 cm^2 of central dorsal skin per mouse was excised, fixed immediately in 4% buffered formaldehyde, processed routinely, and sectioned at 4 mm for haematoxylin and eosin (H&E) staining. In addition, tissue was submerged in RNA later solution (Applied Biosystems, Foster City, CA) and stored at -70˚C for later mRNA analysis.

2.1.5 Histologic evaluation

Skin samples were fixed in 4% formaldehyde; paraffin embedded and stained with H&E. Epidermal hyperplasia was assessed by counting epidermal cell layers and measuring the thickness of the epidermis from the basal layer to the stratum. For quantification of epidermal thickness and layers, 5 randomly selected locations per H&E-stained cross-section of dorsal skin from each mouse were examined under the microscope at magnification 20X (scale bar 100μm). All measurements were performed in a blinded manner. Results were first averaged per mouse and then averaged per treatment group in the statistical analysis. The percent suppression in the increase of epidermal layers and skin thickness for specific groups was determined in analogous way as suppression of skin swelling with formula as given above. Representative images were acquired by using a DP71 digital camera (Olympus, Melville, NY) attached to an Olympus BX51 microscope.

2.1.6 Immunohistochemistry

Paraffin-embedded sections were stained for p21 and p16. De-waxed and rehydrated tissue sections were heated in 0.01M citrate buffer at pH 6.0 in an autoclave, followed by an endogenous peroxidase activity block in 3% hydrogen peroxide in PBS. Afterwards, blocking steps were performed using the Avidin/Biotin blocking kit (Vector laboratories, SP2001), super block (Empire Genomics, IDSTM003) and mouse block (Empire Genomics, IDSTM003). The blocked sections were incubated with the primary antibody p21 (Santa Cruz; sc-397) in a 1:100 dilution or p16ink4a (Abcam, ab54210) in a 1:50 dilution at 4°C overnight. The detection was done with the I Detect Super Stain System HRP (Empire Genomics, IDSTM003) and the specific signal was visualized with 3-amino-9-ethylcarbazole (ID laboratories, BP1108) followed by a counterstaining with haematoxylin.

2.1.7 Immunoscoring

The membranous and cytoplasmic/endogenous levels of p21 and p16 protein were analysed and grouped by the nuclear staining intensity in (0, +, ++, +++) and the percentage of positive cells within the epidermis. A relative intensity score was derived by multiplying the grade of nuclear intensity with the percentage of positive cells for p21 and p16 protein per sample and section.

2.1.8 Senescence associated (SA) ß-Galactosidase (ß-Gal) Staining

The SA-ß-gal staining was performed on cryo-cut samples using the commercial kit from Cell Signalling (9860). The cyro-cut tissues were cut at 5µm thickness and thawed at room temperature for 30min. These samples were fixed for 15min and stained with ß-gal staining solution on the slides with the incubation at 37°C overnight in a humid chamber with light protection. Then the slides were mounted with Geltol mounting gel and covered with glass coverslip for further analysis. Semi-quantitative analysis was made by counting the quantity of ß-gal^{+} cells in dermis and epidermis per sample and section.

2.1.9 Multiplex immunfluorescent analysis

The Opal^{TM} 6-Color Fluorescent IHC Kit (Perkin Elmer) was used according to the manufacturer's instructions. Slides were stained with antibody specific for DC maturation marker, MHC-II (Abcam). CD3, (Abcam) and Ly6-B (BioRad) antibodies were also used together with MHC-II to get better separation of the MHC-II positive population. For image acquisition, Vectra® 3 automated quantitative pathology imaging system (Perkin-Elmer and Inform software) was used to detect the relative abundance of cells expressing the marker protein in the epidermis and dermis upon tissue segmentation.

2.1.10 Bead immunoassay

Procarta 26-Plex bead immunoassay from Affymetrix eBioscience (EPX260-26088-901) for detecting IFN gamma, IL-12p70, IL-13, IL-1 beta, IL-2, IL-4, IL-5, IL-6, TNF-α, GM-CSF, IL-18, IL-10, IL-17A, IL-22, IL-23, IL-27, IL-9, GRO alpha, IP-10, MCP-1, MCP-3, MIP-1 alpha, MIP-1 beta, MIP-2, RANTES and eotaxin was used according to the manufacturer's specifications. Analysis was done with five parametric curve fitting (Bio-Rad, Hercules, CA). Standard curves for each analyte were generated by using the reference analyte concentration supplied by the manufacturers.

2.1.11 RNA isolation

Total RNA was extracted with the miRNeasy Kit (Qiagen, Hilden, Germany; Cat. No. 217004) including DNase treatment steps on the column according to protocol and homogenized with MagNA Lyser Green Beads (Roche, Cat No: 03358-941-001) using the MagNA Lyser (Roche). RNA was quantified by measuring absorbance at 260 and 280 nm and quality was secured with a ratio between RNA and protein of 1.9 – 2.09 using a Nano Drop (checked on the Bio-Analyzer BA2100 (Agilent; Foster City, CA; Cat.No. 5065-4476)).

2.1.12 RNA microarray and pathway analysis

GeneChip® Mouse Gene 2.0 ST Arrays (Affymetrix; Santa Clara, CA; Cat No. 902118) were used for whole transcript amplification in comparison to 3'IVT amplification, which depends on best quality RNA. We used 500ng of the total RNA for the amplification. Protocol was followed according to the manual. We analysed the amplified cDNA again on the BioAnalyzer BA2100 (Agilent, Foster City, CA) using the RNA 6000 Nano LabChip (Agilent; Foster City, CA; Cat.No. 5065-4476). The given fragment size of < 2000nt for overall samples were kept for ss-cDNA synthesis, fragmentation and labelling. These were hybridized for 18h at

45°C as suggested by the manual while rotating in the hybridization oven. Washing and staining (GeneChip® HT hybridization, Wash and Stain Kit; Affymetrix, Santa Clara, CA; Cat No. 900720) was done with the Affymetrix Genechip® fluidics station 450 according to the manual (protocol on fluidics station: FS450_0002). Arrays were scanned with the Affymetrix GeneChip scanner GCS3000. To evaluate the hybridization controls and pre-analysis, Affymetrix Expression Console EC 1.3.1 was used with no technical outlier arrays been detected. Raw data is available at the Gene Expression Omnibus with GEO; with accession number GSE100774. Statistical analysis for this data set was done with the Partek Software v.6.6 (Partek Inc, St Louis, MO). CEL files with the probe intensity data were imported using robust multi-chip average (RMA) algorithm. This included background correction, quantile normalization across all arrays; median polished summarization based on log transformed expression values. Differences among groups were tested with 1-way ANOVA. For pathway analysis we used 194 transcripts showing a significant p-value<0.05 and a fold change +/- 1.5 between Group V and Group. Ingenuity Pathway Analysis software (Ingenuity Systems) was used for pathway analysis performed with following settings: Species = Mouse AND (confidence = Experimentally Observed OR High (predicted)).

2.1.13 Neutrophile chemotaxis assay

Murine bone marrow derived neutrophils were suspended in assay buffer (PBS with Ca2+/ Mg2+ supplemented with 0.1% BSA, 10 mM glucose, 10 mM HEPES, pH 7.4) at 2 x 10 6 cells/ml. 50 µl cell suspension per well were placed onto the top plate of an AP48 micro Boyden chemotaxis chamber with a 5µm pore-size polycarbonate filter (Neuro Probe, Gaithersburg, MD) and were allowed to migrate towards 30 µl of a chemoattractant, placed in the bottom wells of the plate, for 1h at 37°C in a CO2 incubator. The membrane was carefully removed and migrated cells were enumerated by flow cytometric counting. The chemotactic index was calculated as the ratio of the number of migrated neutrophils in

chemoattractant-containing wells divided by the number of neutrophils that migrated to assay buffer alone.

2.1.14 Statistical analysis

Each experiment was repeated at least once with similar results. Data presented are expressed as means ± SEM. Statistical differences among experimental groups were determined by use of ANOVA or paired or unpaired t-test after testing for normality, whatever appropriate. The statistical test chosen for each experiment is indicated in the figure legend. Statistical significance was set at $p \leq 0.05$ and levels of significance were given as $*p \leq 0.05$; $**p \leq 0.01$; $***p \leq 0.001$; and $****p \leq 0.0001$.

2.2 RESULTS

2.2.1 Identification of the minimal phototoxic dose (MPD)

The MPD is defined as the smallest UVA dose required to produce a clearly defined and noticeable erythema after psoralen photosensitization, at 48 hours (Legat et al., 2004). Clinically, as per the original European PUVA study protocol the MPD is employed as the starting dose to initiate PUVA therapy. Because erythema can be sometime difficult to read in the skin of mice, skin swelling was used as a surrogate end point for PUVA- and UVB-induced inflammation and erythema. For repetitive use of PUVA, sub-inflammatory dosage was identified (Singh et al., 2010) and employed for the treatment regime in the current study. The MPD in BALB/c mouse was determined by exposing the dorsal skin to the increasing UVA dosages after topical psoralen administration or UVB irradiation. The study was performed to assure that clinically relevant dosages are used in the experiments. The kinetic and dose-response study revealed that the significant skin swelling after light exposure was present at 48 hours at dose of 0.5 J/cm^2 for PUVA and 0.4 J/cm^2 for UVB. However, sub-phototoxic dose level of 0.25 J/cm^2 (mean exposure time 29 s) and 0.2 J/cm^2 (mean exposure time 120 s) for PUVA and UVB, respectively, were used twice a week for two weeks (Fig.2.4.1).

2.2.2 Both treatment and pretreatment with PUVA and UVB reduces the susceptibility of mouse skin to mount a psoriatic response to IMQ

Before using the IMQ model of inflammation, the stability of IMQ-induced psoriatic phenotype development and inflammation was determined (Fig.2.4.2). To do so, IMQ was applied in two cycles, first for a period of 5 days which led to stable and significant higher inflammation compared to untreated control until day 10. However, the effect dropped, leading to normalization the skin. As it is a well-documented fact, that the model is an acute model of approximate 10 days of inflammation (Flutter and Nestle, 2013), a second cycle of IMQ application was started from day 11 (but with only 3 topical applications until day 13) that sustained inflammation until day 17. Thus, this study formed the base for using the IMQ

model for over the period of 17 days to study PUVA therapeutic effect. In the first study part, IMQ was applied to the mouse dorsal skin along with PUVA and UVB treatment for over the period of 16 days. It was observed that PUVA and UVB treatment both reduced psoriatic inflammation in the model. The double skin fold thickness measurement revealed that IMQ-induced psoriatic inflammation was inhibited when repetitive sub-phototoxic PUVA or UVB exposures were given simultaneously along with two cycles of IMQ, over the period of 16 days Fig.2.4.3. During the first cycle of IMQ application, skin swelling was maximally suppressed on day 5 by 90.5% and 54.8% at 0.25 J/cm^2 and 0.5 J/cm^2 PUVA, respectively, and by 57.5% at 0.2 J/cm^2 UVB (Fig.2.4.3A & B). However, during the second cycle of IMQ application the suppression on day 16 was 67.1% and 80.8% at 0.25 J/cm^2 and 0.5 J/cm^2 PUVA, respectively, and 19.4% at 0.2 J/cm^2 UVB (Fig.2.4.3 C). Meanwhile, the sub-phototoxic dose of 0.25 J/cm^2 PUVA have shown greater efficacy than the phototoxic dose of 0.5 J/cm^2 PUVA; therefore, the sub-phototoxic dose of 0.25 J/cm^2 PUVA and 0.2 J/cm^2 UVB (.i.e. at the level of 50% of the MPD) was used in all succeeding studies.

Further on, to explicate the mechanism of phototherapy in psoriatic inflammation, mouse skin was pretreated with PUVA or UVB before start IMQ application to investigate whether the therapeutic effects are direct or indirect. As outlined in the study plan (Fig. 2.4.4), PUVA pretreatment with one single exposure (Group VII) as well as PUVA or UVB pretreatment with 4 repetitive exposures over two weeks was given until 3 days (or more) before the start of an IMQ cycle over 3 days (Groups II and IX). In order to study the duration of the therapeutic effect of phototherapy, a gap of 7 days after the last phototherapy exposure (Groups III and X) in certain study groups was applied until the start of IMQ application. It was observed that IMQ treatment led to development of strong inflammation with erythema and swelling on the dorsal skin within 24 h after topical administration of its first dose at day 14. This was increased further in the following days with repetitive treatment for the period of 3 days (Fig. 2.4.5 A and 2.4.6 A). This study has shown that both phototherapy pretreatment regimes significantly reduced the susceptibility of the skin to mount IMQ-induced inflammation. However, PUVA pretreatment was superior to UVB pretreatment in reducing this susceptibility, as depicted in Fig. 2.4.5 A and 2.4.6 A and Table 2.5.1. The overall mean

suppression of IMQ-induced psoriatic skin swelling was 62.9% for PUVA pretreatment and 22.6% for UVB (Table 2.5.1).

But this therapeutic effect of PUVA was partially sustained in comparison to the effect of UVB, which was entirely lost after the prolonged gap of 7 days between last PUVA/UVB exposure at day 11 and start of IMQ at day 18. This led to the overall mean suppression of 22.6% in psoriatic skin swelling for PUVA, while there was deteriorating of macroscopic skin swelling for UVB with an overall negative value of 21.6% suppression (Table 2.5.1).

2.2.3 Histopathological assessment of psoriatic phenotype development

Complementary to the assessment of macroscopic skin swelling, the microscopic histological analysis was performed. The skin swelling observations were consistent with the results of histological examination of the skin samples taken 24 h after the last IMQ administration (Fig. 2.4.5 B and C and Fig. 2.4.6 B and C and Table 2.5.1). IMQ application led to epidermal hyperplasia with strong epidermal thickening, hyperkeratosis along with the formation of elongated rete ridges and parakeratosis and cellular infiltration in the dermis. The average epidermal thickness was 18.4 μm in control mice (data not shown) vs up to 78.56 μm and 86.68 μm in IMQ-treated mice in the experiment depicted in Fig. 2.4.5 C and 2.4.6 C, respectively.

The average number of epidermal layers was 1.3 in control mice (data not shown) vs up to 7.2 and 7.8 layers in IMQ-treated mice in the experiment depicted in Fig. 2C and 3C, respectively. The overall mean suppression of IMQ-increased epidermal hyperplasia was 58.1% and 48.5% for PUVA and UVB (reduction of skin thickness to 46.94 μm and 49.4 μm, respectively), as measured by epidermal thickness, and 45.3% and 25.3%, as measured by epidermal layers (Table 2.5.1). Similar to the macroscopic skin swelling, the effect of PUVA in reducing epidermal hyperplasia was partially sustained, whereas the effect of UVB was entirely lost after the prolonged gap of 7 days between last PUVA/UVB exposure and start of IMQ. After the 7-day gap, the overall mean suppression of epidermal hyperplasia was 15.6% for epidermal thickness and 16.2% for the increase in epidermal layers for PUVA, whereas there was worsening in epidermal hyperplasia for UVB (with

overall negative values of 5.1% and 15.9%) (Table 2.5.1). Pretreatment with a single dose of PUVA (Group VII) did also diminish IMQ-induced inflammation but its effect was smaller than that after repetitive PUVA exposure (data not shown). Thus, this observation strongly indicated that PUVA was much more effective to maintain long term disease free condition along with longer remission time compare to UVB treatment.

2.2.4 PUVA pretreatment influences Th1/Th2/Th17 cytokine and chemokines profile in IMQ-treated mice

Another important question was to check whether antipsoriatic effect of PUVA pretreatment observed in skin was linked to any alterations of serum levels of cytokines and chemokines or not. There was a down regulatory effect of PUVA pretreatment on the serum levels of cytokines of the Th1 and IL-23/Th17 axis, including IFN-gamma, IL-1 beta, TNF-α, IL-17A, IL-22, IL-23 (Group I) as well as chemokines like GRO alpha, IP-10, MCP-1, MCP-3, MIP-1 alpha, MIP-1 beta, MIP-2, RANTES and eotaxin (Fig. 2.4.7). In contrast, there was ambivalent response of Th2 cytokines with a trend of upregulation of IL-4 ($p=0.057$) and downregulation of IL-5 ($p=0.05$) after PUVA treatment. However, for most cytokines, except for IL-23 and GRO-alpha, the effects of PUVA vanished when they were measured at the end of the experiment after a gap of 7 days between last PUVA and first IMQ exposure. IL-2, IL-6, IL-10, IL-27 and GM-CSF levels were below the detection limit of the immunobead assay in all samples. IL-6 is known to be an important factor in recruiting myelomonocytic cells (Flutter and Nestle, 2013) like neutrophils, monocytes and macrophages specifically in psoriatic skin lesions (Grossman et al., 1989, Fielding et al., 2008); but in present study it was not detected. Though IL-6 association has been described recently in context of IMQ-driven inflammation (van der Fits et al., 2009), it can be hypothesized from the current cytokine data that in absence of IL-6 an alternative pathway through GRO-aplha (CXCL1) and macrophage inflammatory protein (MIP) chemokine family might regulate inflammation (El Malki et al., 2013). As depicted in Fig.2.4.8 PUVA pretreatment did reduce the responsiveness of the

neutrophils from Group II and Group III, toward GRO-alpha which has shown a significant reduced migration against the highest concentration of GRO-alpha. Notably, this systemic effect of PUVA on cytokine levels and unresponsiveness of neutrophils was equivalent with its effect on spleen size (Fig. 2.4.5 D).

The cytokine and chemokine levels after PUVA treatment and before start of IMQ treatment were monitored which have shown significant downregulation of IFN-gamma, IL-17A, IL-9, along with upregulation of GRO-alpha compared to untreated controls (Group VIII) (Table 2.5.2). This indicated the potential role of pro-inflammatory cytokine IL-9 and its down-stream effector cytokines IFN-gamma, IL-17A in the pathology of IMQ-induced inflammation. Collectively, these results indicated that PUVA pretreatment does downregulates the IL-23/Th17 pathway and Th1 cytokines but upregulates Th2 cytokines in the pretreatment model. The depression of serum protein levels of the important cytokines of the IL-23/Th17 pathway complemented well to the improvement of the macroscopic skin phenotype and the histological alterations.

2.2.5 Microarray for differential expressed genes, biological function and pathway analyses

Further on, as a closer approach to identify the therapeutic effects of pretreatment the alteration of genes and development of transcriptional gene signature was investigated. Microarray analysis helped to highlight the possible treatment-induced changes leading to the therapeutic effect. For the overall gene expression data analysis, 4 mouse arrays were analyzed from Group V and Group VI while for control (Group VIII) only two arrays were analyzed and compared since the remaining two had considerably different gene expression profiles from the other two samples within the group, most likely due to an interfering hair cycle effect. Those samples were therefore considered as outliers and excluded from all further analyses. The cluster analysis highlighted that the Group V clustered separately from the Group VI and Group VIII (Fig 2.4.9) As depicted in Fig. 2.4.9, PUVA pretreatment significantly altered the expression of 30 genes that were identified based on the fold change of >1.5 and a p-value of <0.05 in the array. Those genes

included Col1A1, Col1A2, Col3A1, Col5A1, Col5A2, Col6A3, Col6A2, TIMP1 and MMP13 that were overexpressed compared to controls (Group VIII) and Group VI that had a 7-day gap between last PUVA exposure and collection of skin samples (Fig. 2.4.4). Notably, these genes belong to collagen (Col), matrix metallopeptidase (MMPs) and tissue inhibitor of metalloproteinase (TIMP 1) families which are associated with senescence and apoptosis. In contrast, alkaline ceramidase 2 (Acer2) which mediates cell proliferation, differentiation, apoptosis, adhesion, and migration, belonging to the sphingosine and sphingosine-1-phosphate (S1P) metabolism pathway (Xu et al., 2006), and miRNA-29a, that is a negative regulator of TIMP 1, were down-regulated (Huang et al., 2015). The fold-change bar diagram in the lower part of Fig. 2.4.9 B highlights the differences in the expression of the 30 genes (normalized to control) 3 days after the last PUVA treatment (Group V) compared to Group VI that had a 7-day gap between last PUVA exposure and collection of skin samples. This helped to identify and understand the mechanism taking place in the skin of PUVA-pretreated mice before IMQ application, leading to reduced response.

To confirm the activation of the key up-steam components of senescence pathway, the expression of p21 and p16 was quantified in the dorsal skin of the mice using immunohistochemistry. The presence of p21 in the basal layer of the epidermis in all treatment groups (Fig. 2.4.10) was strongly evident. PUVA treatment amplified the expression of p21 in the entire epidermis and in the dermis mainly in epithelial cells of hair follicles. Similarly, PUVA treatment also increased the expression of p16 in the epidermis but not. In contrast, UVB pretreatment did not significantly affect the expression of either of these proteins in the skin (data not shown). As outlined in the graphic panel of Fig. 2.4.10, the increase of senescence after PUVA was lost in the mice that had a 7-day gap between last PUVA exposure and collection of tissue samples.

Moreover, the ultimate senescence marker senescence-associated (SA) ß-galactosidase (ß-Gal) was also stained in the tissues. The ß-Gal positive senescent cells were observed predominantly and specifically in the hair follicles and inconsistently in the epidermis and dermis (data not shown). A low expression of p16 is known to be associated with absence of late and irreversible senescence while high expression of p21 is the read-out of onset of early senescence (Vogt et

al., 1998, Coppe et al., 2010). The latter is known to be independent of expression of ß-Gal positive cells and reversible in nature (Childs et al., 2015). However, the staining pattern of these investigations was inconclusive.

Microarray data (Fig. 2.4.9) also indicated that PUVA pretreatment at sub-phototoxic level upregulated Fscn1, a gene that belongs to the dendritic cell maturation markers (Bros et al., 2011). PUVA is known to cause significant induction leading to higher expression of MHC class II expression displayed by DCs leading to a tolerogenic effect. Thus, to validate this finding multiplex immunohistochemical staining using Opal™ 6-Color Fluorescent IHC Kit (Perkin Elmer) was performed to quantify dendritic cell maturation using MHC-II expression as the marker of the skin samples taken after PUVA pretreatment. Opal allows staining of multiple IHC targets using unlabeled primary antibodies to detect up to 6 biomarkers in one tissue section. To gain an understanding in of how these cells populating pretreated skin are modulated, the Vectra 3 automated quantitative pathology imaging system together with inForm® software was employed that accurately detects and measures even weakly expressing and overlapping biomarkers within a single H&E, IHC or IF tissue section.

2.3 DISCUSSION

Knowing the fact that the skin of different strains of mice does exhibit different level of susceptibility to environmental stimuli including UV radiation (Hart et al., 1998, Gyongyosi et al., 2016), the MPD in the BALB/c mice was determined first (Fig. 2.4.1) and subsequently sub-inflammatory doses (i.e. 50% of the MPD) were administered in the study for repetitive use. The MPD was 0.5 J/cm^2 for PUVA and 0.4 J/cm^2 for UVB in this study. The PUVA MPD was identical to that determined in a previous study for wild type controls with ICR (CD-1R) background of the K5.hTGF-β1 psoriasis model (Singh et al., 2010). In those studies, the lower PUVA dose of 0.25 J/cm^2 (as used in the present study) was found to be more effective than the higher dose of 0.5 J/cm^2 in clearing psoriatic lesions in the K5.hTGF-β1 mice (Singh et al., 2010).

Herein the data indicated the fact that the IMQ model can be useful to study both the therapeutic effects of PUVA and UVB. PUVA to a greater degree than UVB radiation was able to suppress established IMQ-induced psoriatic inflammation (Fig 2.4.2) but also pretreatment (before imiquimod administration) with PUVA was able to suppress the susceptibility of murine skin to mount a psoriatic inflammation again to a greater degree than UVB radiation (Fig. 2.4.5 and Fig. 2.4.6). Moreover, the influence of phototherapy was dropping when a gap of 7 days was allowed to elapse between the last phototherapeutic exposure of PUVA and the start of IMQ treatment or was totally lacking in case of UVB after a gap of 7 days.

In the present work, the therapeutic effect of PUVA on IMQ-induced macroscopic psoriatic skin changes (Fig. 2.4.5 A) was paired with a reduction of histologic psoriatic alterations of epidermal hyperplasia and inflammation (Fig. 2.4.5 B and C) and downregulation of psoriatic cytokines of the Th1 and Th17 axis including IFN-gamma, TNF-α, IL-17, IL-23 and IL-22 (Fig. 2.4.7) (Singh et al., 2010). Moreover, repetitive PUVA treatment also downregulated pro-psoriatic cytokine levels of IFN-gamma, IL-9 and IL-17 at baseline before start of IMQ treatment (Table 2.5.2). The effect of PUVA on IL-23 and GRO-alpha was sustained as measured in Group III after the last PUVA exposure and 24 h after the last IMQ exposure (Fig. 2.4.7). As IL-23 is crucial for driving the IL-23/Th17 axis and GRO-alpha which is also known as IL-8, is essential for growth promotion of

keratinocytes (Lemster et al., 1995) and chemoattracting neutrophils (De Filippo et al., 2008, Schlager et al., 2015). The inhibition of these cytokines was consistent with the partially sustained effect of PUVA in reducing macroscopic and microscopic skin inflammation and epidermal hyperplasia (Fig. 2.4.5 B and C).

Further on, the observation that PUVA induced downregulation of IL-9 before start of IMQ treatment (Table 2.5.2) was fascinating since IL-9 is known to be produced transiently and prior to the activation-induced up-regulation of other downstream inflammatory pro-psoriatic cytokines (Schlapbach et al., 2014). Also, IL-9 is known to operate indirectly by regulating the induction of downstream effector Th1/Th2/Th17 cytokines such as IFN-gamma, IL-5, IL-13, and IL-17 (Schlapbach et al., 2014). Moreover, in the past the dermal injection of IL-9 had shown to enhanced Th17-related psoriasiform inflammation in K5.hTGF-b1 transgenic mice where as its blockade by anti-IL-9 antibody treatment did suppressed the psoriatic inflammation and the expression of IL-17A (Singh et al., 2013). In the same study, PUVA was also effective in diminishing psoriatic inflammation, in parallel with strong downregulation of IL-9 (Singh et al., 2010). Additionally, IL-9 and its receptor have been found to be expressed in the infiltrating cells of lesioned skin in psoriasis patients (Singh et al., 2013, Schlapbach et al., 2014), which indicated its potential role in psoriatic pathophysiology.

At molecular level, using high through-put genome microarray analysis, enrichment of senescence-related pathway genes after PUVA pretreatment was detected. The trend of normalization in the expression of senescence-related genes after the gap of 7 days between last PUVA exposure and start of IMQ indicated that PUVA-induced senescence may indeed be crucial for its anti-psoriatic activity, as seen in Group V. This was further supported by staining of two upstream cyclin CDKIs, p21 and p16, (Fig. 2.4.10) which play a pivotal role in the cell cycle arrest leading to development of senescence (Waldman et al., 1995).

Further on, functional activation of p53 and pRB family proteins that regulates growth signalling is required for the initiation and regulation of cellular senescence. In contrast, its downstream effector CDKI p21 that belongs to the CIP/KIP family of CDKIs is best known as an inhibitor of cell proliferation. Also, p21 plays a complex role in regulating apoptosis and differentiation. *In vitro* studies have shown that

PUVA treatment does cause cellular senescence, leading to growth arrest of fibroblasts, with enlarged cytoplasm and an increased synthesis of MMPs (Briganti et al., 2008). These responses are mainly regulated by the two potent CDKIs p21 and p16, where the former is a direct target of p53 transactivation, while the latter is known to be induced by stress without DNA damage (Sherr and DePinho, 2000, Bringold and Serrano, 2000). Senescence phenotype development is also known to stimulate cytokines and chemokines cocktail, termed as senescence-associated secretory phenotype (SASP). This phenotype can affect surrounding cells by activating cell-surface receptors and corresponding signal transduction pathways that lead to irreversible senescence induced by soluble signaling interleukins and chemokines (Campisi and d'Adda di Fagagna, 2007), including IL-1, IL-5, IL-6, IL-13, GRO-alpha, GM-CSF, MIP-1 (alpha & beta) and MIP-2 (Coppe et al., 2010). In the current study while the levels of GRO-alpha were seen to be significantly stimulated after PUVA pretreatment, SASP related cytokines were insignificantly modulated or remained undetectable (IL-6 and GM-CSF) (Table 2.5.2).

MMPs and TIMPs are other products of genes associated with senescence and apoptosis (Mannello et al., 2005). Elevated concentrations of MMPs have been found in the scales from the mild form of psoriatic lesions, while their levels were shown to be decreased in patients with more severe form of the disease, consistent with inverse PASI correlation (Flisiak et al., 2006). Similarly, TIMP-1 and TIMP-2 serum levels also decreased with severity of psoriasis. In the present study, PUVA-induced MMP gene expression pattern (Fig. 2.4.9) was equivalent by improvement of psoriatic skin phenotype due to PUVA pretreatment (Fig. 2.4.5). In addition, the microarray data also indicated that PUVA did downregulate miR-27a and miR-29a, uncovering its correlation in the regulatory networks of PUVA. The miRs are known as essential controllers of cell fate decisions in immune responses. They act by coordination that leads to overpowering of multiple target genes. Lately, miR-27a has been recognized as inhibitor of Th2 cell differentiation and function, which thereby limits the IL-4 production in T cells along with the network that regulates IL-4 production (Pua et al., 2016). Knocking down of this miR has reportedly down regulated expression of TNF- α and IL-6 significantly via reducing the phosphorylation level of NF-κB p65. Moreover, miR-27a neutralization with anti-miR-27a hairpin had been shown to down regulate TNF- α

expression, which is consistent with the cytokine results seen in the current study (Fig. 2.4.7) (Wang et al., 2014). Additionally, miR-29a´s role in association with extracellular matrix (ECM) induction is well documented (Huang et al., 2015). miR-29a overexpression in murine hepatic stellate cells resulted in a downregulation of collagen expression thereby directly targeting the mRNA expression of ECM genes (Roderburg et al., 2011). These collective facts correlated well with the observation of collagen-associated genes which were significantly expressed in the Group V, possibly due to downregulation of miR-29a. Likewise, PUVA also downregulated the Acer2 gene that is involve in regulating sphingolipid metabolism and the S1P signaling pathway (Xu et al., 2010). Recently, S1P has attracted attention for its effects in promoting cell proliferation and survival in psoriasis (Obinata and Hla, 2012, Xu et al., 2006, Checa et al., 2015).

Taken together, the current data not only shows that phototherapy and in particular with PUVA was able to suppress established psoriatic inflammation but also proves that pretreatment with phototherapy (before IMQ administration) was able to suppress the susceptibility of murine skin to mount a psoriatic inflammation. Together, this indicates that PUVA-induced senescence may make cells more unsusceptible to stimulation by IMQ, resulting in less psoriatic inflammation and hyperplasia. Consistent to all the previous comparative studies of PUVA with UVB to treat psoriasis (Gordon et al., 1999, Van Weelden et al., 1990, Dawe et al., 2003, Snellman et al., 2004, Salem et al., 2010, Yones et al., 2006), the current study not only shows that PUVA gives better remission but additionally unveils the molecular events and signature set that leads to priming the skin to be less responsive to IMQ.

2.4 FIGURES

A.

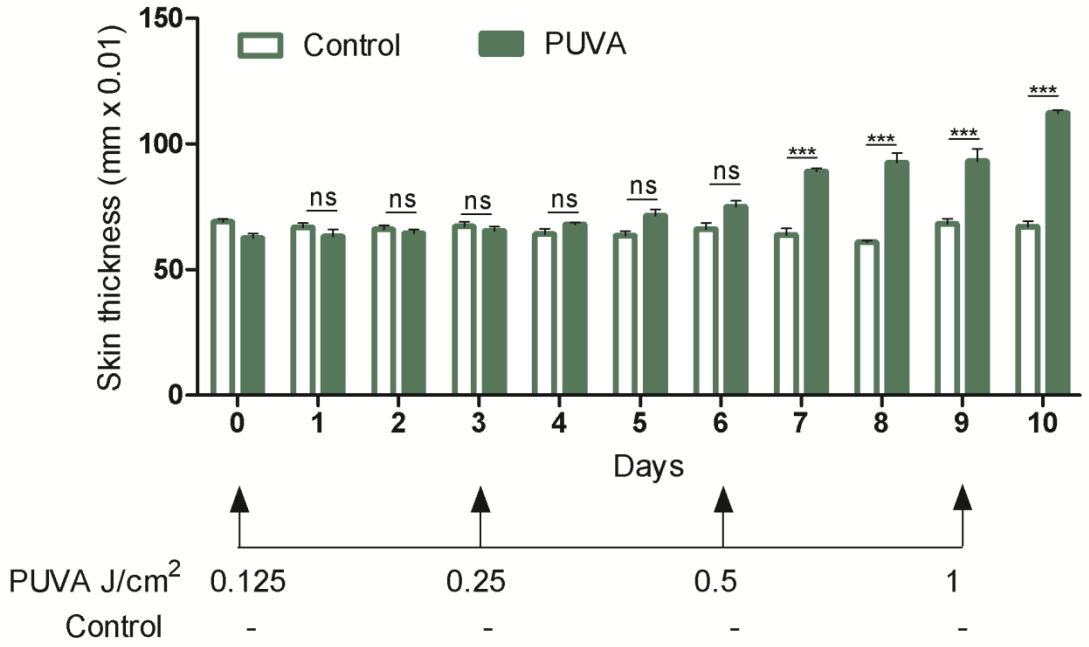

B.

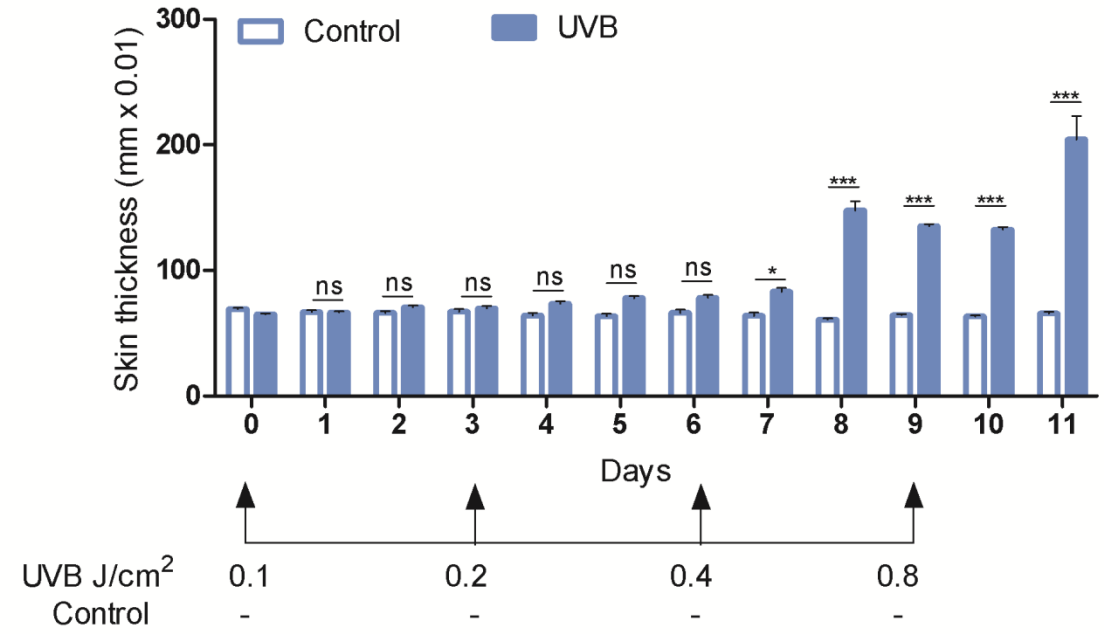

Figure 2.4.1 Determination of the minimal phototoxic dose (MPD) of PUVA and UVB treatment in BALB/c mice skin by measuring the double skin fold thickness (DSFT) on the dorsal skin. A. Mice were treated topically with increasing dose starting from 0.125 J/cm^2 to maximum of 1 J/cm^2 for PUVA therapy and B. 0.1 J/cm^2 to maximum of 0.8 J/cm^2 for UVB therapy. Data shown are from one representative experiment, with n = 5 per treatment group. Statistical differences were determined by Two-way ANOVA using Bonferroni post-test (*$p \leq 0.05$; **$p \leq 0.01$; ***$p \leq 0.001$).

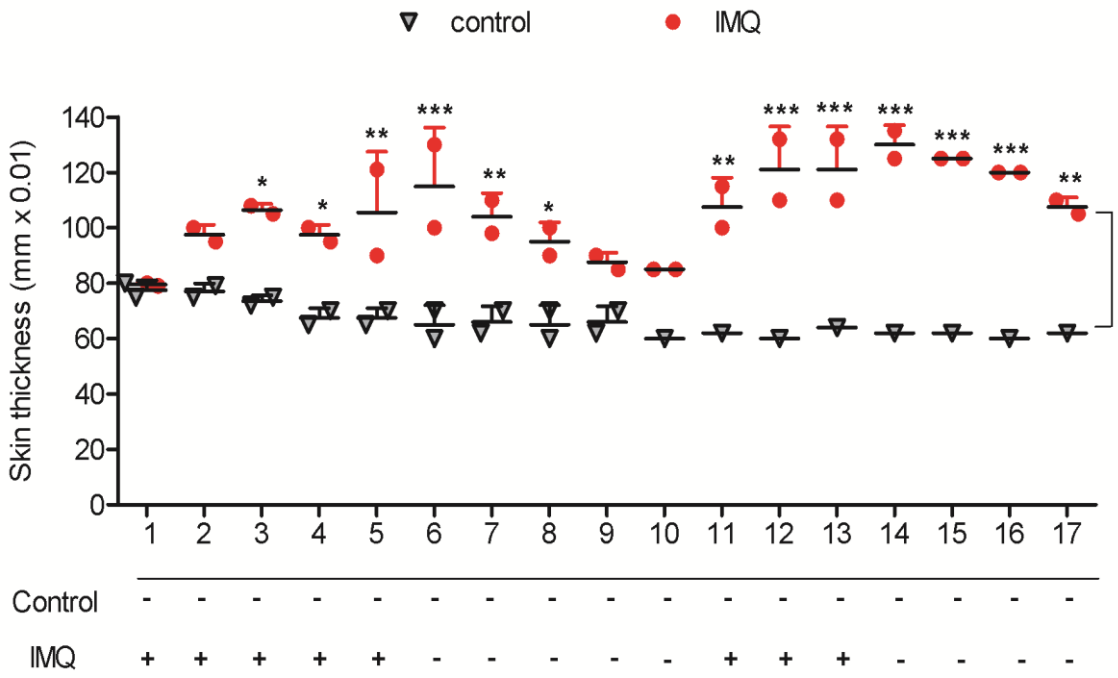

Figure 2.4.2 Identification of the duration of imiquimod (IMQ)-induced psoriatic phenotype development and inflammation. DSFT on the dorsal skin of the BLB/c mice was measured as a read-out to quantify IMQ-induced inflammation for over the period of 17 days.

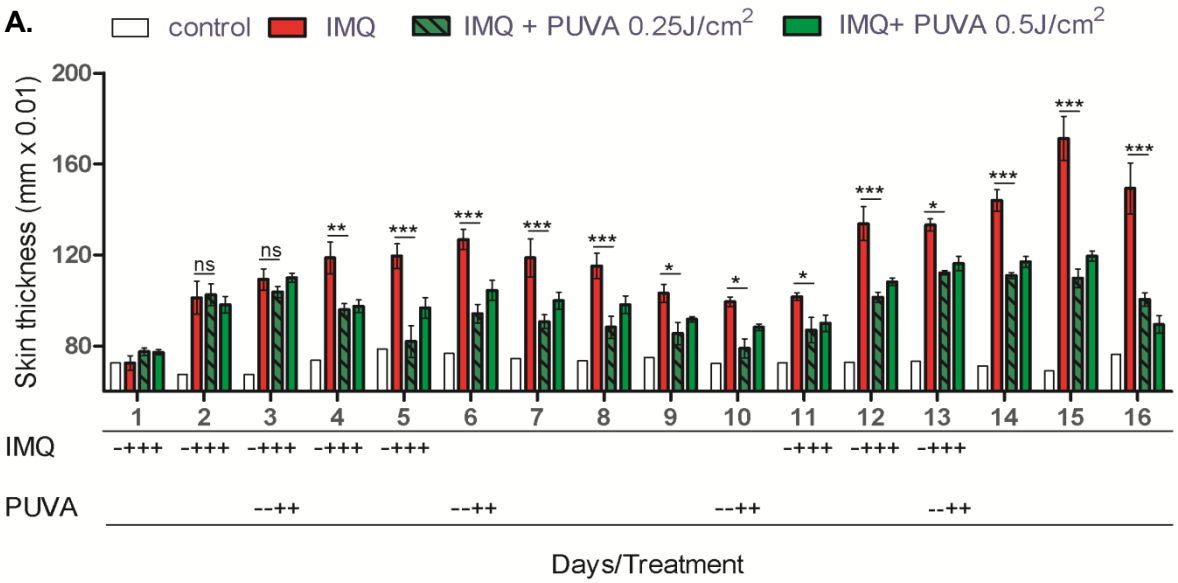
A.
control
IMQ
IMQ + PUVA 0.25J/cm2
IMQ+ PUVA 0.5J/cm2
Skin thickness (mm x 0.01)
200
160
120
80
ns
ns
**
***
***
***
***
*
*
*
***
*
***
***
***
1 2 3 4 5 6 7 8 9 10 11 12 13 14 15 16
IMQ
-+++ -+++ -+++ -+++ -+++ -+++ -+++ -+++
PUVA
--++ --++ --++ --++
Days/Treatment

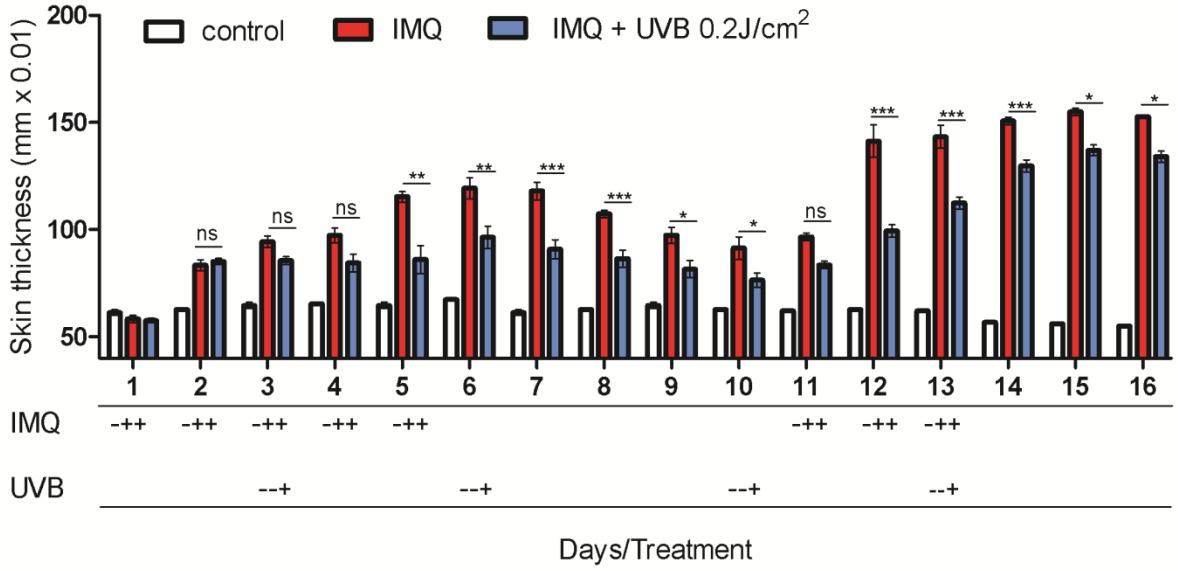
B.
control
IMQ
IMQ + UVB 0.2J/cm2
Skin thickness (mm x 0.01)
200
150
100
50
ns
ns
ns
**
**
***
***
*
*
ns
***
***
***
*
*
1 2 3 4 5 6 7 8 9 10 11 12 13 14 15 16
IMQ
-++ -++ -++ -++ -++ -++ -++ -++
UVB
--+ --+ --+ --+
Days/Treatment

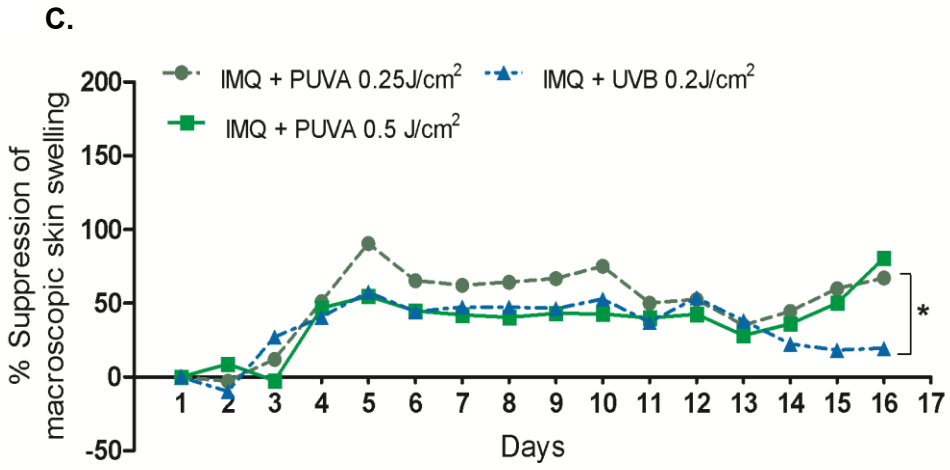
C.
IMQ + PUVA 0.25J/cm2
IMQ + UVB 0.2J/cm2
IMQ + PUVA 0.5 J/cm2
% Suppression of macroscopic skin swelling
200
150
100
50
0
-50
*
1 2 3 4 5 6 7 8 9 10 11 12 13 14 15 16 17
Days

Figure 2.4.3 DSFT on the back of the mice was measured to quantify IMQ-induced thickening of the skin after (A) PUVA and (B) UVB treatment over the period of 16 days. (C) Percent suppression of IMQ-induced skin swelling by PUVA and UVB. Data shown are from one representative experiment, with n=5 mice per group/experiment. Statistical differences were determined by Two-way ANOVA using Bonferroni post-test (*P < 0.05; **p ≤ 0.01; ***p ≤ 0.001; ns= Not Significant).

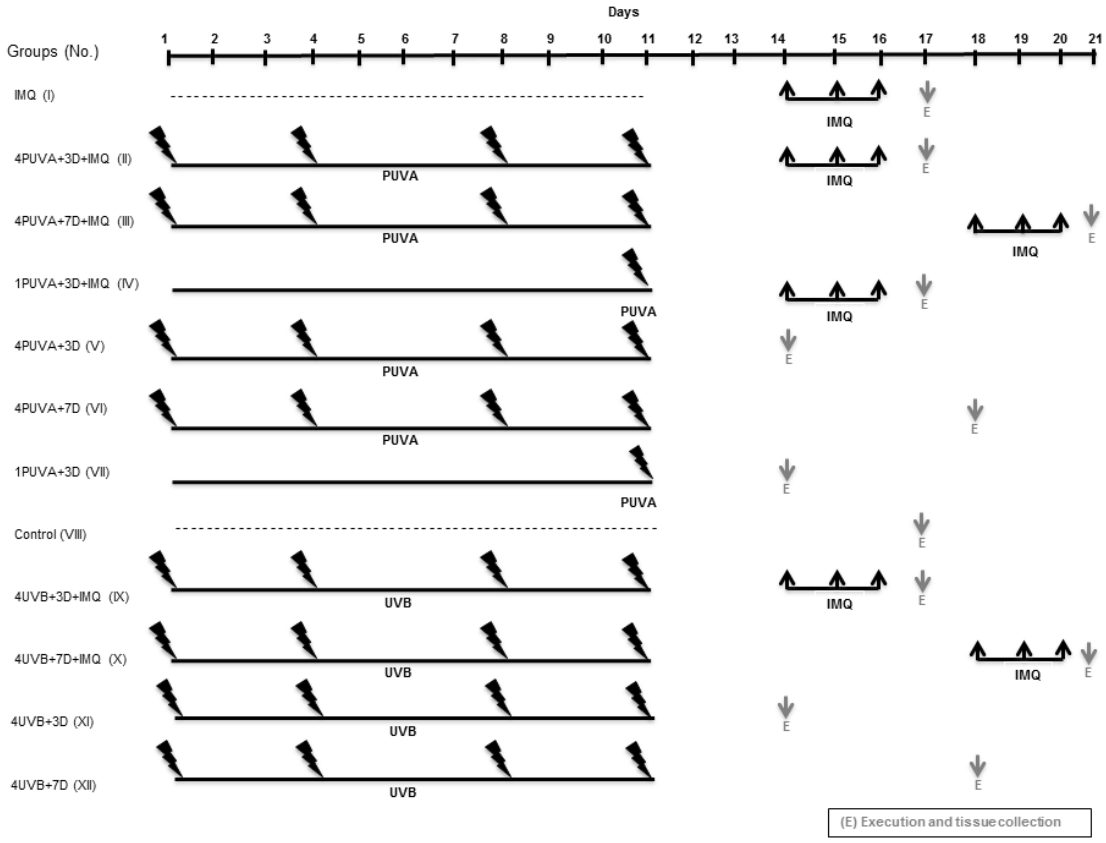

Figure 2.4.4 Schematic representation of the irradiation regime and overall experimental design. PUVA and UVB was given at a sub-phototoxic dose level of 0.25 J/cm^2 and 0.2 J/cm^2, respectively. Imiquimod (IMQ) was applied topically for 3 days at a quantity of 62.5 mg/day per mouse at the indicated timepoints. The execution (E) and tissue collection for each group is indicated with arrows at the respective time point. Each study group consisted of n=5 mice.

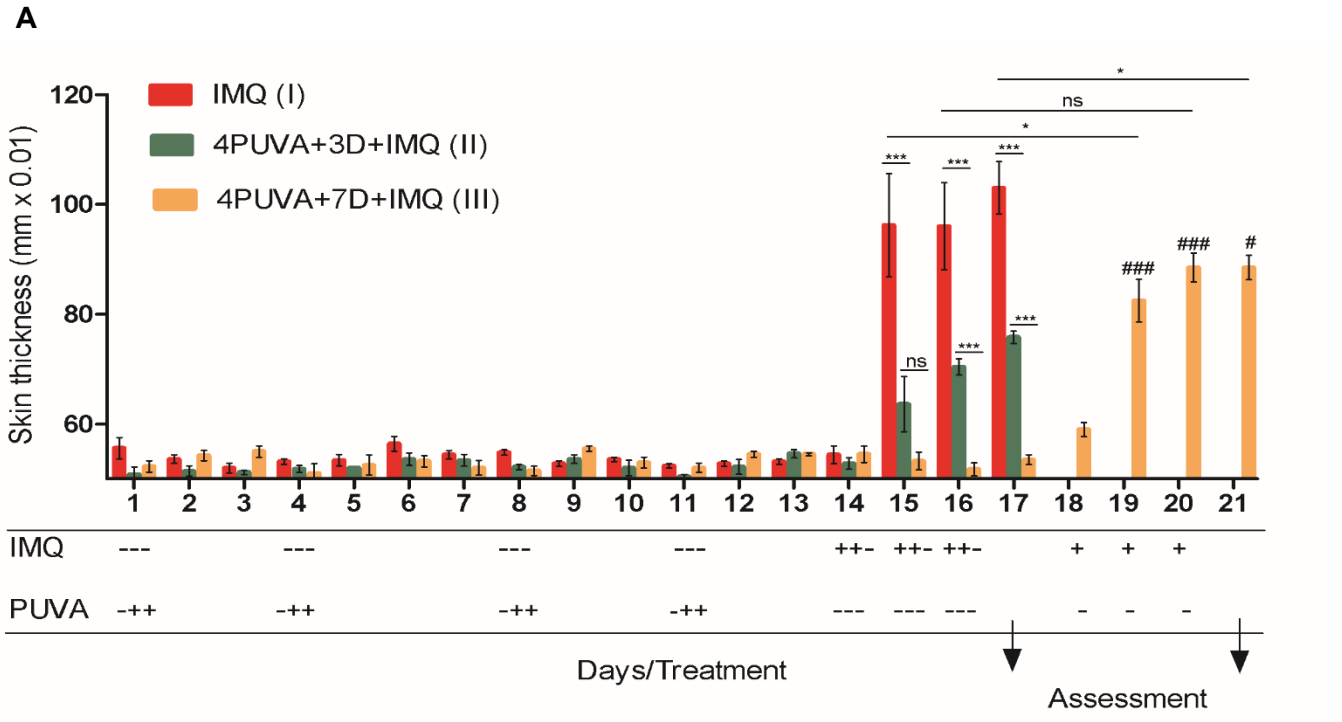
A
IMQ (I)
4PUVA+3D+IMQ (II)
4PUVA+7D+IMQ (III)
Skin thickness (mm x 0.01)
120
100
80
60
1 2 3 4 5 6 7 8 9 10 11 12 13 14 15 16 17 18 19 20 21
IMQ --- --- --- --- ++- ++- ++- + + +
PUVA -++ -++ -++ -++ --- --- --- - - -
Days/Treatment
Assessment
ns
*
***
###
#

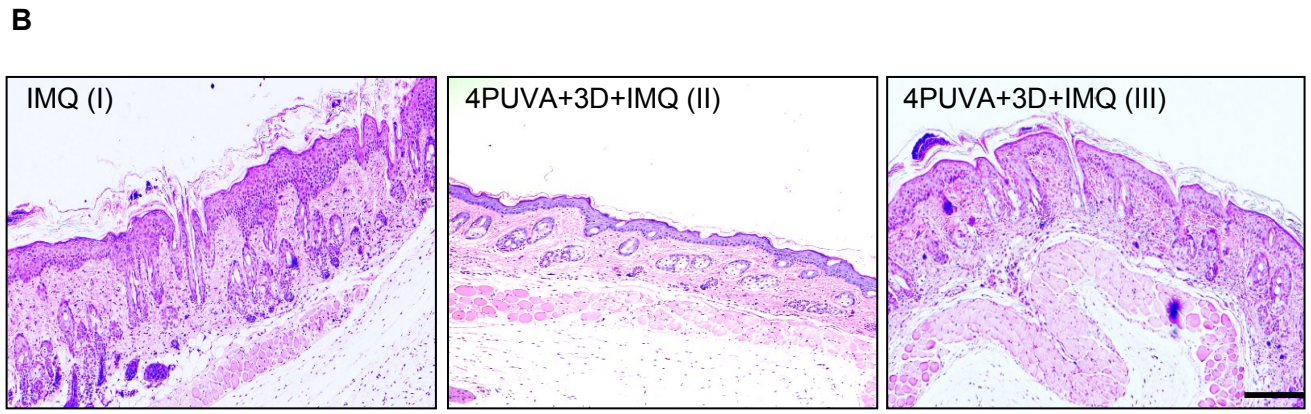
B
IMQ (I)
4PUVA+3D+IMQ (II)
4PUVA+3D+IMQ (III)

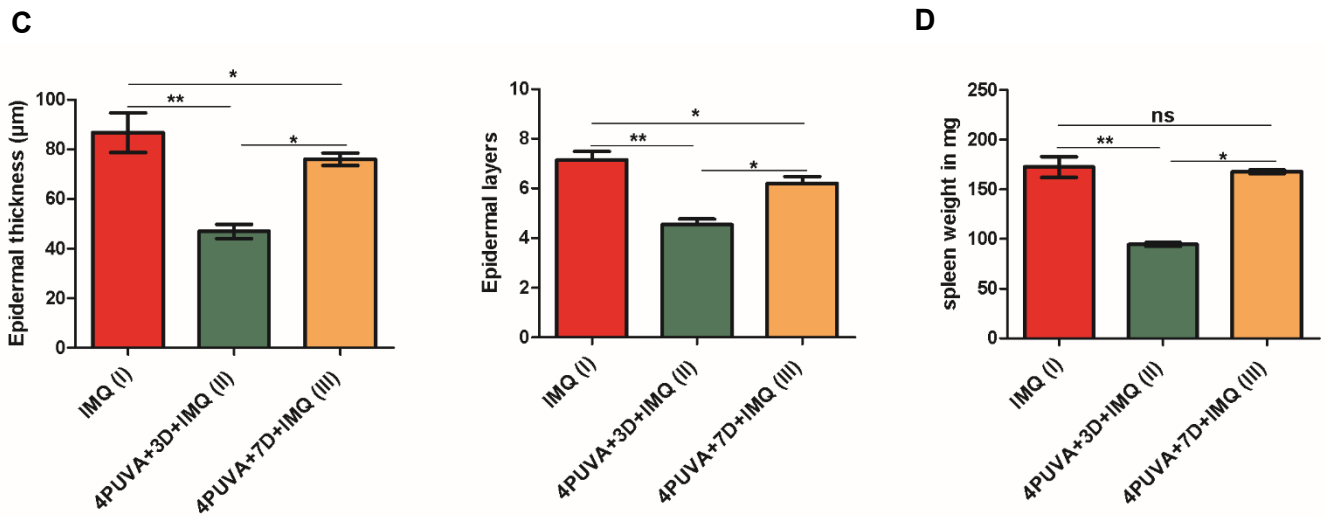
C
Epidermal thickness (µm)
Epidermal layers
D
spleen weight in mg
ns
*
**
IMQ (I)
4PUVA+3D+IMQ (II)
4PUVA+7D+IMQ (III)

Figure 2.4.5 PUVA pretreatment suppressed IMQ-induced inflammation and hyperplasia. (A) DSFT on the back of the mice was measured to quantify the change in IMQ-induced thickening of the skin after PUVA pretreatment. (B,C) Representative image of H&E-stained section from dorsal skin of a mouse from each group (scale bar, 200 μm) along with evaluation of histological features such as epidermal thickness (μM) and epidermal layers. (D) Sign of systemic treatment effect was measured by spleen weight. Data shown are from one representative experiment, with n=5 mice. Statistical differences were determined by Two-way ANOVA using Bonferroni post-test (*p <0.05; **p ≤ 0.01; ***p ≤ 0.001 for Group I vs Group II or Group III and # p < 0.05; ### p ≤ 0.001 for Group III vs Group II).

A.

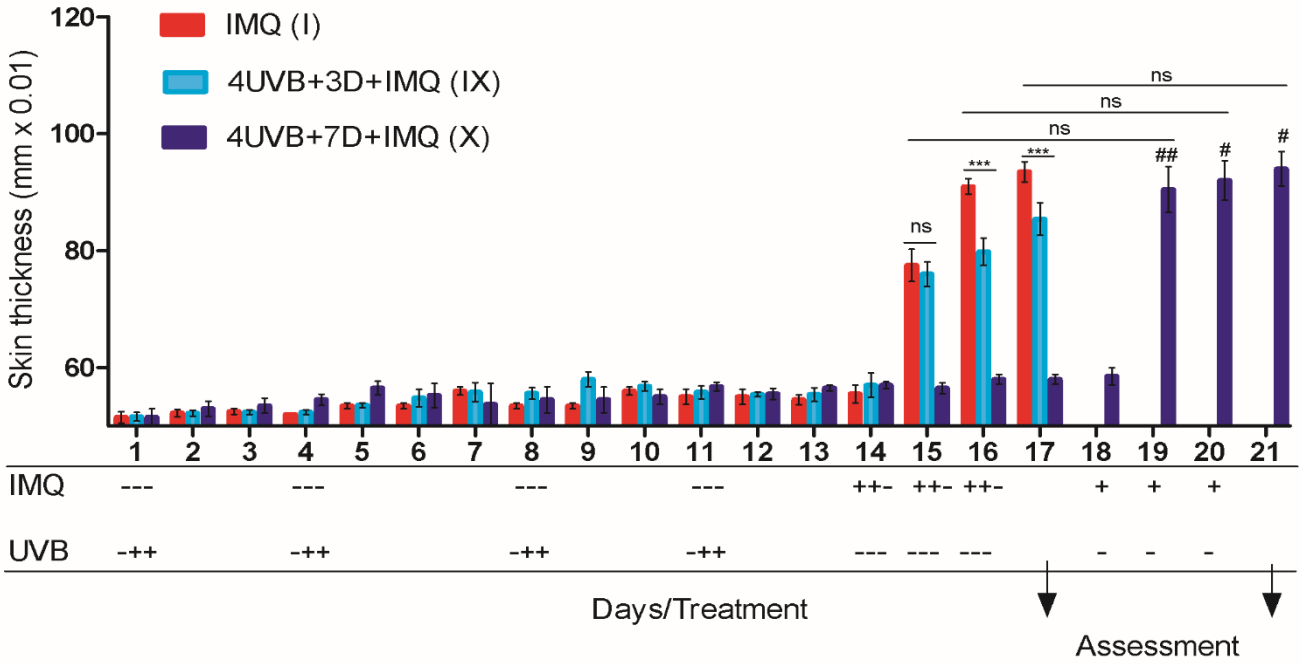
IMQ (I)
4UVB+3D+IMQ (IX)
4UVB+7D+IMQ (X)
Skin thickness (mm x 0.01)
120
100
80
60
ns
ns
ns
***
***
##
#
#
ns
1 2 3 4 5 6 7 8 9 10 11 12 13 14 15 16 17 18 19 20 21
IMQ --- --- --- --- ++- ++- ++- + + +
UVB -++ -++ -++ -++ --- --- --- - - -
Days/Treatment
Assessment

B.

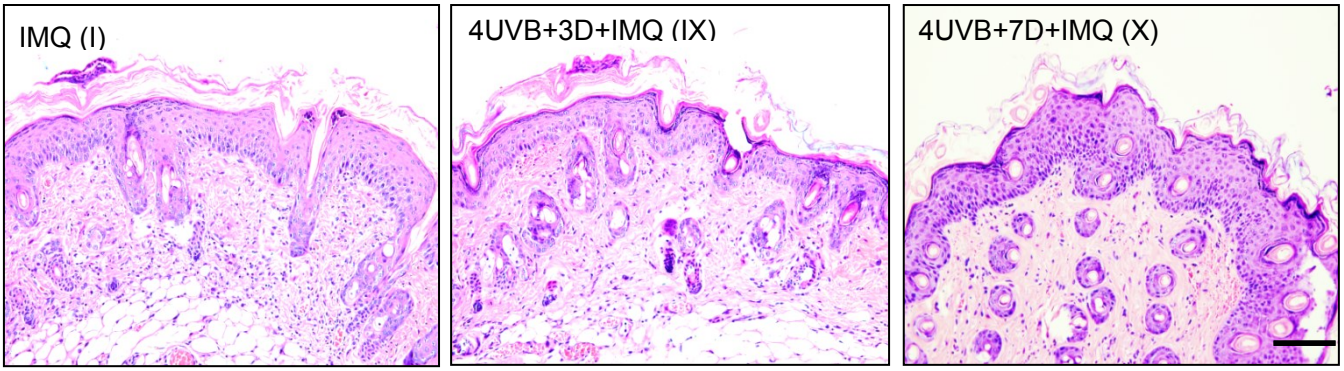
IMQ (I)
4UVB+3D+IMQ (IX)
4UVB+7D+IMQ (X)

C.

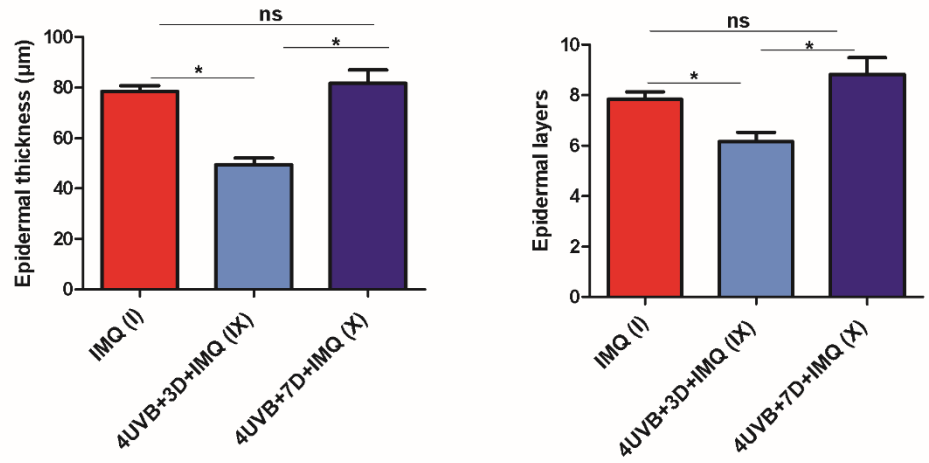
Epidermal thickness (µm)
100
80
60
40
20
0
ns
*
*
IMQ (I)
4UVB+3D+IMQ (IX)
4UVB+7D+IMQ (X)
Epidermal layers
10
8
6
4
2
0
ns
*
*
IMQ (I)
4UVB+3D+IMQ (IX)
4UVB+7D+IMQ (X)

Figure 2.4.6 UVB pretreatment suppressed IMQ-induced inflammation and hyperplasia A) DSFT on the back of the mice was measured to quantify the change in IMQ-induced thickening of the skin after UVB pretreatment. (B, C) Representative image of H&E-stained section from dorsal skin of a mouse from each group (scale bar 200 μm) along with evaluation of histological features such as epidermal thickness (μM) and epidermal layers. Data shown are from one representative experiment, with n=5 mice. Statistical differences were determined by Two-way ANOVA using Bonferroni post-test (*$p < 0.05$; ***$p \leq 0.001$ and # $p < 0.05$ for Group I vs Group IX or Group X; ## $p \leq 0.01$ for Group X vs Group IX).

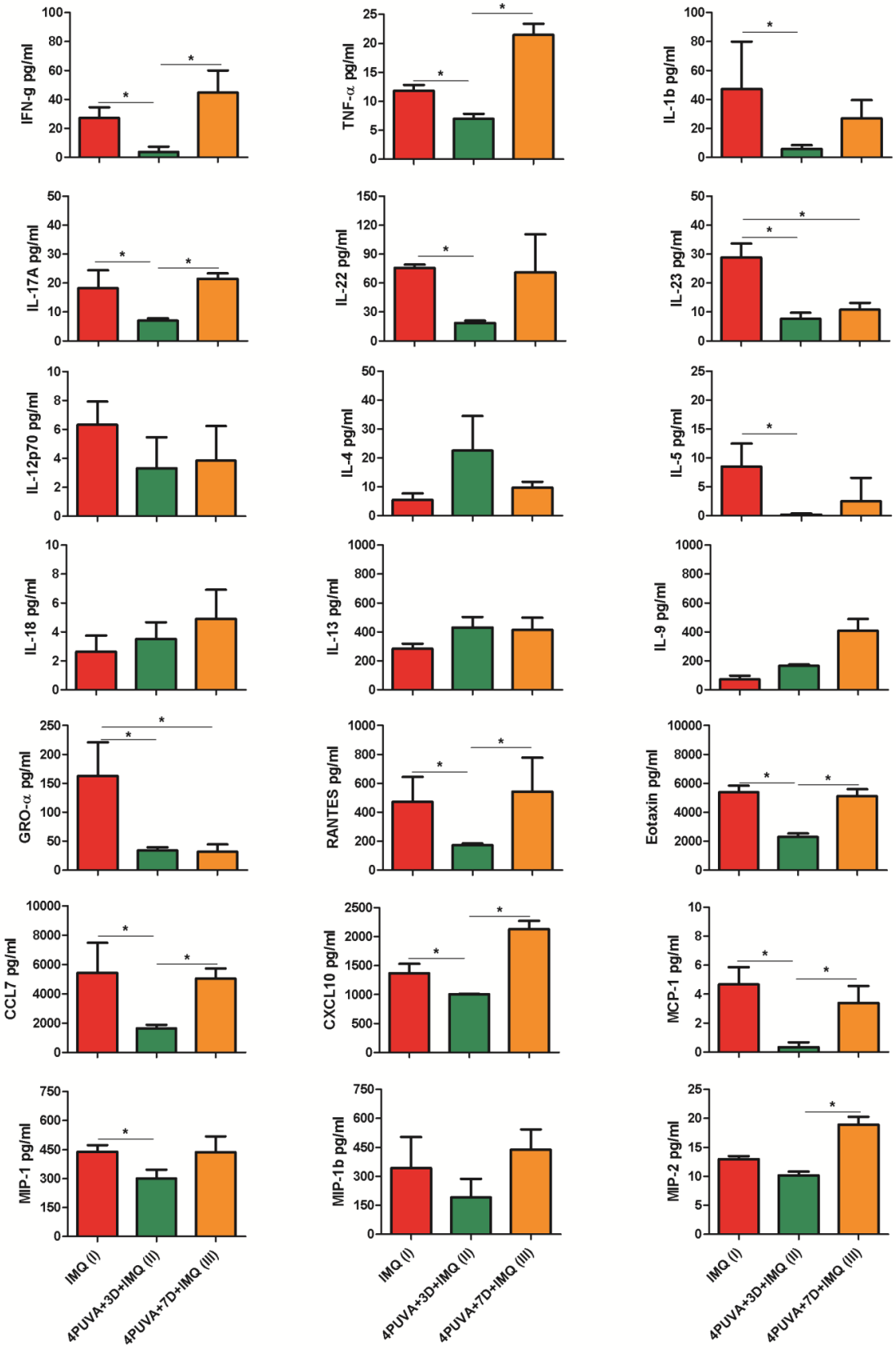
IFN-g pg/ml
TNF-α pg/ml
IL-1b pg/ml
IL-17A pg/ml
IL-22 pg/ml
IL-23 pg/ml
IL-12p70 pg/ml
IL-4 pg/ml
IL-5 pg/ml
IL-18 pg/ml
IL-13 pg/ml
IL-9 pg/ml
GRO-α pg/ml
RANTES pg/ml
Eotaxin pg/ml
CCL7 pg/ml
CXCL10 pg/ml
MCP-1 pg/ml
MIP-1 pg/ml
MIP-1b pg/ml
MIP-2 pg/ml
IMQ (I)
4PUVA+3D+IMQ (II)
4PUVA+7D+IMQ (III)

Figure 2.4.7 PUVA pretreatment influenced chemokine and Th1/Th2/Th17 cytokine profile expression in IMQ-treated mice. BALB/c mice were treated, as described in M&M. 24 hrs after the last IMQ treatment, serum samples were collected and analyzed by 26-plex bead immunoassay. Data shown are from one representative experiment, with n=5 mice. Statistical analysis was performed using unpaired t-test (*$p < 0.05$).

A.

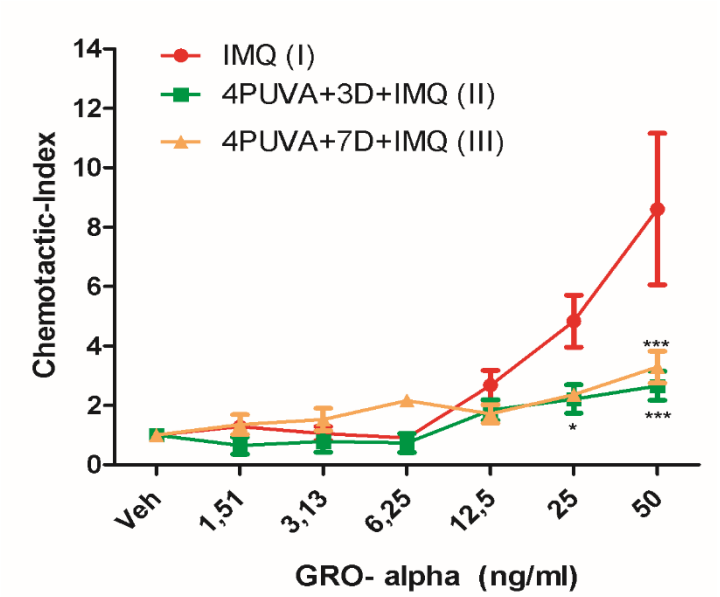

B.

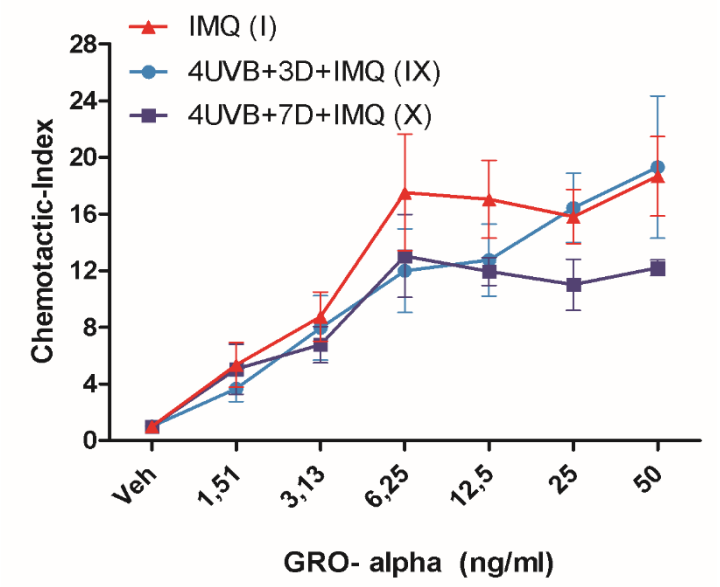

Figure 2.4.8 PUVA pretreatment and the responsiveness of bone marrow-derived neutrophils towards GRO-alpha chemoattractant in comparison with UVB. Respective PUVA and UVB pretreated mice´s bone marrow-derived neutrophils sensitivity was enumerated by flow cytometric counting where n= 5 per group. Statistical differences were determined by Two-way ANOVA using Bonferroni post-test (*$p < 0.05$ and ***$p \leq 0.001$)

A.

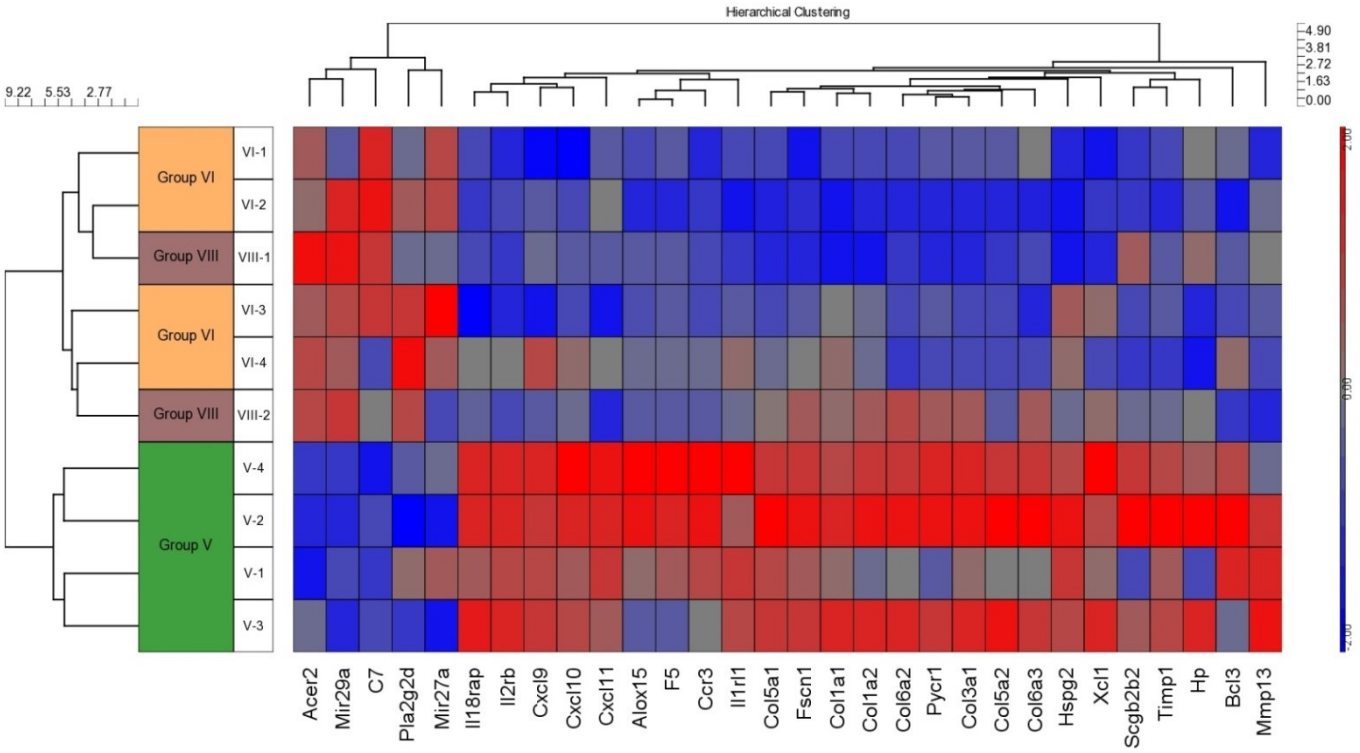
Hierarchical Clustering
9.22 5.53 2.77
4.90
3.81
2.72
1.63
0.00
Group VI
Group VIII
Group VI
Group VIII
Group V
VI-1
VI-2
VIII-1
VI-3
VI-4
VIII-2
V-4
V-2
V-1
V-3
Acer2
Mir29a
C7
Pla2g2d
Mir27a
Il18rap
Il2rb
Cxcl9
Cxcl10
Cxcl11
Alox15
F5
Ccr3
Il1rl1
Col5a1
Fscn1
Col1a1
Col1a2
Col6a2
Pycr1
Col3a1
Col5a2
Col6a3
Hspg2
Xcl1
Scgb2b2
Timp1
Hp
Bcl3
Mmp13

B.

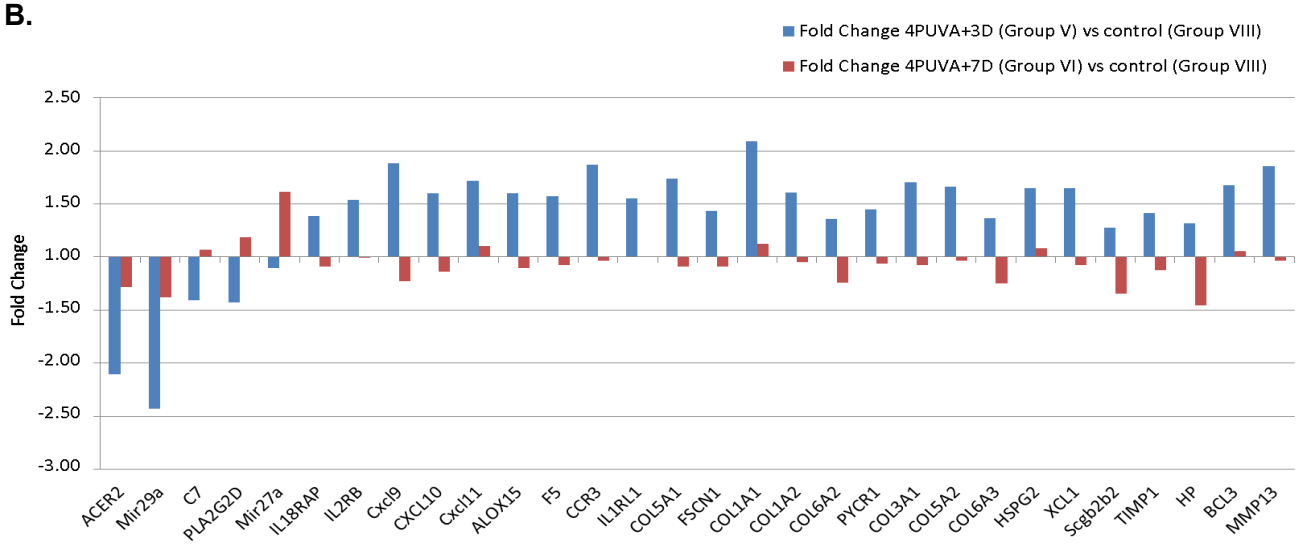
Fold Change 4PUVA+3D (Group V) vs control (Group VIII)
Fold Change 4PUVA+7D (Group VI) vs control (Group VIII)
Fold Change
2.50
2.00
1.50
1.00
-1.50
-2.00
-2.50
-3.00
ACER2
Mir29a
C7
PLA2G2D
Mir27a
IL18RAP
IL2RB
Cxcl9
CXCL10
Cxcl11
ALOX15
F5
CCR3
IL1RL1
COL5A1
FSCN1
COL1A1
COL1A2
COL6A2
PYCR1
COL3A1
COL5A2
COL6A3
HSPG2
XCL1
Scgb2b2
TIMP1
HP
BCL3
MMP13

Figure 2.4.9 Heat map of gene array expression with changes in molecular signature due to PUVA pretreatment. (A) Genes identified on the basis of the fold change of >1.5 and a p-value of <0.05 are plotted. Heat map of expression values for 30 genes is shown by two-way clustering of expression levels for Group V (4PUVA+3D) compared to Group VI (4PUVA+7D) and Group VIII (Control) (2 outlier samples from Group VIII had to be excluded due to hair cycling) (n=4 per group). Red denotes increased relative gene expression levels for the indicated genes per mouse and group, while blue denotes decreased expression levels. (B) Bar diagram indicates the fold changes in gene expression after PUVA pretreatment in comparison to controls (Group VIII). Statistical analysis for this data set was performed using the Partek Software v.6.6, as outlined in the M&M section.

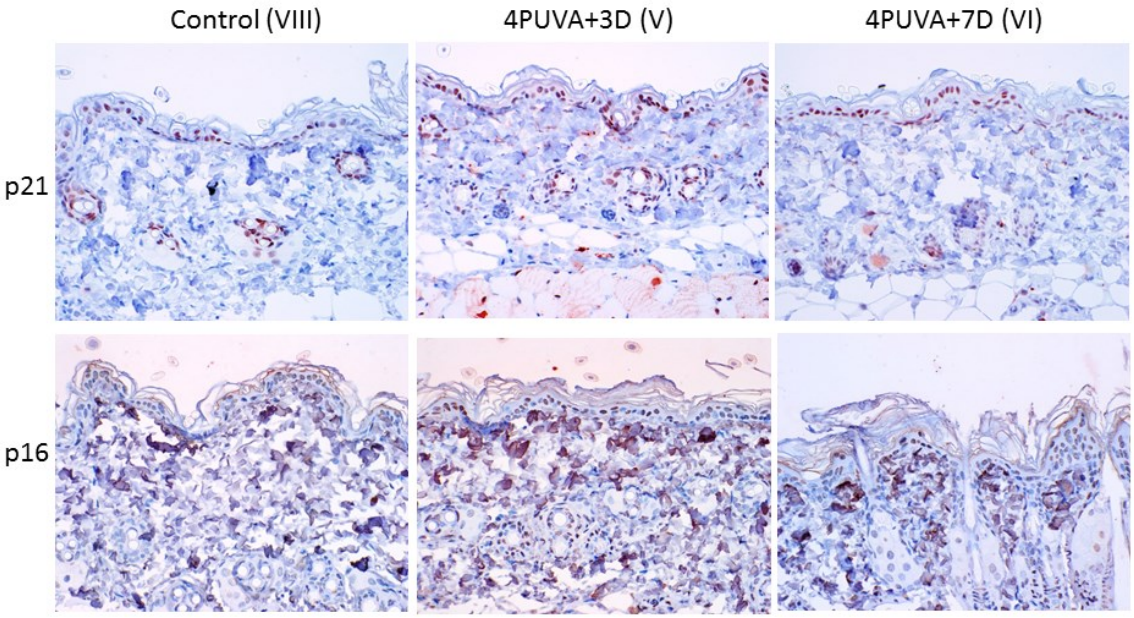
Control (VIII)
4PUVA+3D (V)
4PUVA+7D (VI)
p21
p16

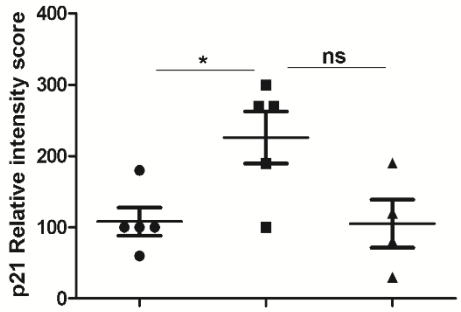
p21 Relative intensity score
400
300
200
100
0
*
ns

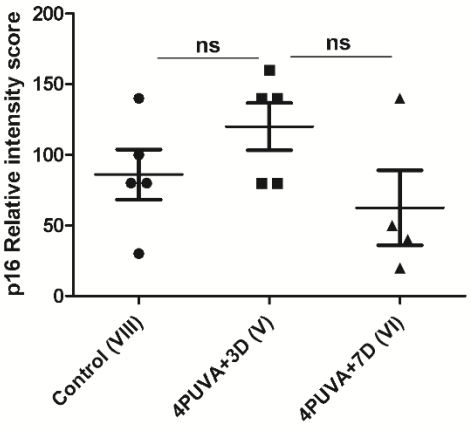
p16 Relative intensity score
200
150
100
50
0
ns
ns
Control (VIII)
4PUVA+3D (V)
4PUVA+7D (VI)

Figure 2.4.10 Expression of p21/p16 associated with cellular senescence in PUVA-pretreated skin. Representative skin sections for p21 and p16 staining in 4PUVA+3D (Group V) and 4PUVA+7D (Group VI) is shown in comparison to untreated control (Group VIII) with n=4-5 per group. Magnification 20X, scale bar 100 μm. Semi-quantitative scoring for p21 and p16 expression was done, as outlined in M&M. Statistical analysis was performed using unpaired t-test (*$p < 0.05$).

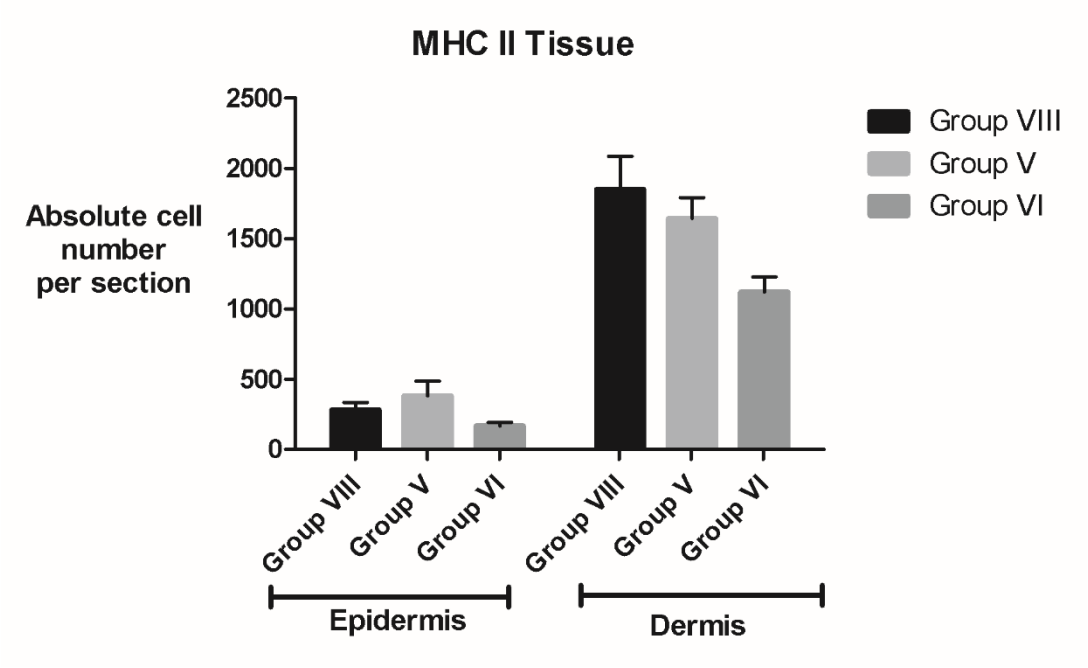

Figure 2.4.11 PUVA pretreatment and its effect on the induction of the MC-II expression in epidermis and dermis of dorsal mouse skin. Multiplex immunohistochemistry (IHC) staining with antibodies specific for MHC-II was performed. Data are mean values ± standard error of the mean (SEM) from 1 experiment, with *n*=3-4 per treatment group.

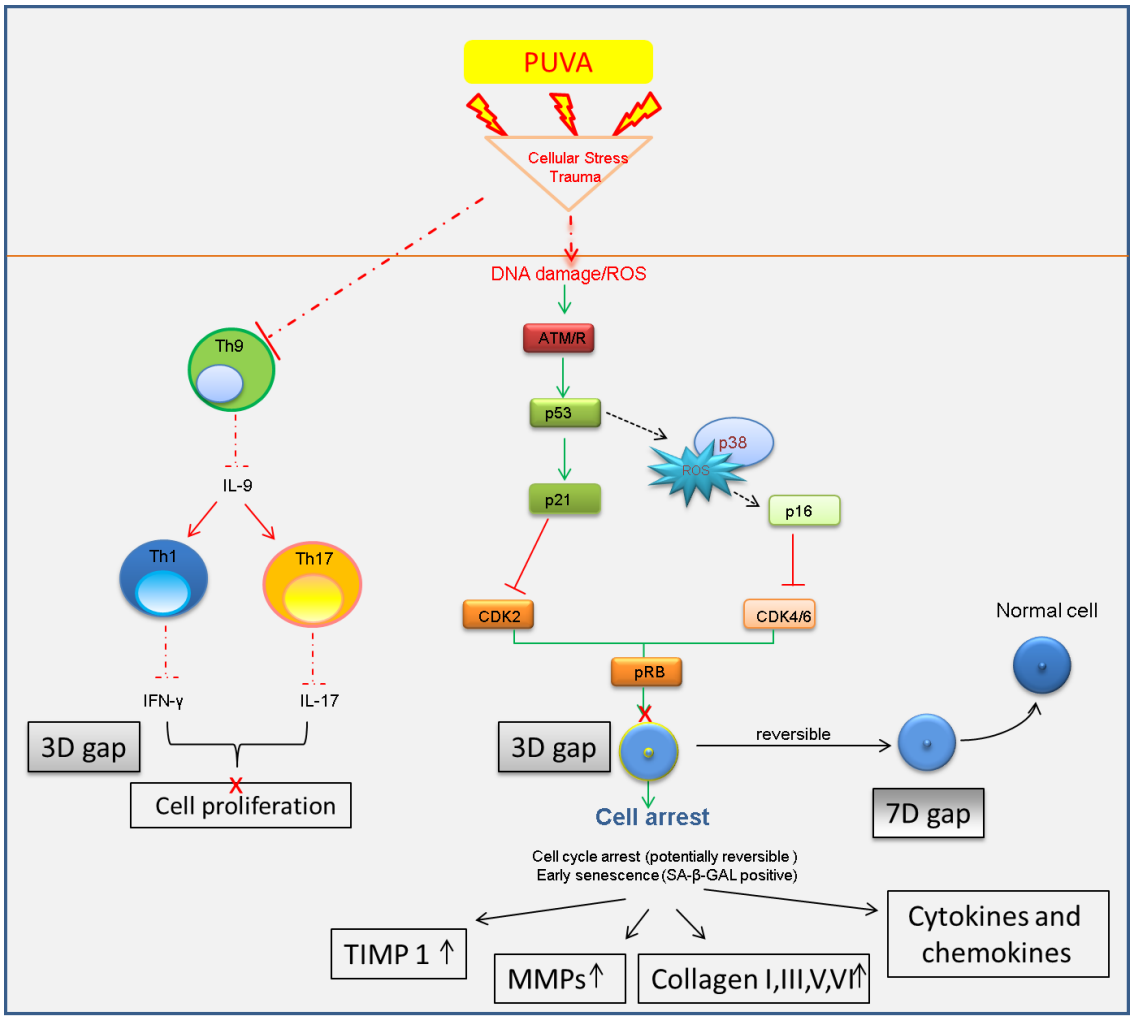

Figure 2.4.12 Schematic representation of the study hypothesis/results to understand the effects of phototherapy pretreatment which leads to inhibition of the Th9/Th1/Th17 axis along with p53/p21 induced senescence phenotype that modulates the proinflammatory cytokines and extracellular matrix-related gene expression, thereby priming the skin to be more tolerant to IMQ stimulation.

2.5 TABLES

Table 2.5.1 Percent suppression in IMQ-induced skin swelling and hyperplasia by pretreatment of PUVA or UVB

Groups	Treatment type and days	Percent suppression by PUVA/UVB		
	PUVA	Macroscopic skin swelling	Increase in epidermal layers	Increase in epidermal thickness
4PUVA+3D+IMQ (II)	day 15	74.4		
	day 16	59.1		
	day 17	55.1		
	Days 15-18 (mean)	62.9*	45.3	58.1
4PUVA+7D+IMQ (III)	day 19	32.6		
	day 20	18.2		
	day 21	30.6		
	Days 19-21 (mean)	27.1*	16.2	15.6
	UVB			
4UVB+3D+IMQ (IX)	day 15	9.5		
	day 16	33.3		
	day 17	25		
	Days 15-18 (mean)	22.6	25.3	48.5
4UVB+7D+IMQ (X)	day 19	-61.9		
	day 20	-3		
	day 21	0		
	Days 19-21 (mean)	-21.6	-15.9	-5.1

Effectiveness of PUVA vs UVB therapy was determined by calculating % suppression observed in macroscopic (skin swelling) and microscopic (epidermal thickness/layers) parameters, as outlined in M&M. For *p-values of comparisons among individual groups and days, see Fig. 2.

Table 2.5.2 Change in levels of cytokines and chemokines in serum due to PUVA pretreatment before IMQ exposure

Cytokines/chemokines	Serum levels in pg/ml		p-Value
	Control (VIII)	4PUVA+3D (V)	
IFN-gamma	8.9 ± 1.1	1.2 ± 4.2	0.03
IL-17A	26.2 ± 14	0 ± 1	0.05
IL-9	63.3 ± 18	0 ± 0	0.05
GRO-alpha	12.3 ± 10.7	34 ± 9.6	0.05
eotaxin	3620 ± 1219	6067 ± 1373	0.11
IL-23	0.17 ± 0.29	0.83 ± 0.76	0.13
IL-13	13.4 ± 20.6	32 ± 16.8	0.20
IL-27	219 ± 74.4	95 ± 139	0.20
IP-10	978 ± 324	618 ± 113	0.23
MCP-3	2886 ± 1805	1248 ± 755	0.23
IL-18	7.9 ± 5.9	4.2 ± 3.1	0.24
MCP-1	13.3 ± 10.7	4.7 ± 2.1	0.27
IL-22	10.1 ± 5.6	7.2 ± 6.3	0.31
MIP-2	29.1 ± 8	36.8 ± 5.5	0.40
IL-4	8.3 ± 6.	5.3 ± 1.5	0.43
IL-5	11.3 ± 8.2	43.8 ± 41.6	0.50
IL-1 beta	1.8 ± 1.3	2.8 ± 2.1	0.59
MIP-1 beta	25 ± 8.2	29 ± 3.3	0.70
RANTES	285.2 ± 177	378 ± 55.8	0.70
IL-12p70	3.8 ± 1.5	3 ± 1.8	0.82
TNF-alpha	11.7 ± 7.5	8 ± 4.5	0.86
MIP-1 alpha	214.6 ± 58.3	226.8 ± 37.3	0.86

Control (VIII) vs 4PUVA+3D (V) samples were analyzed using multiplex bead immunoassay. Entries represent values of detected cytokines and chemokines while IL-2, IL-6, IL-10 and GM-CSF were not detected by the assay. Data shown are expressed as mean ± SEM of cytokine and chemokine levels in pg/ ml^{-1}. P-values were determined by using Mann–Whitney U test.

Table 2.5.3 Top enriched interaction networks in PUVA pretreatment (comparison of Group V vs Group VI).

Top Diseases and Functions	Score	Focus Molecules
Connective Tissue Disorders, Organismal Injury and Abnormalities, Dermatological Diseases and Conditions	55	28
Cellular Development, Cellular Growth and Proliferation, Organ Development	25	16
Cell Death and Survival, Cellular Development, Cellular Growth and Proliferation	19	13
Cellular Movement, Cardiovascular System Development and Function, Cell-To-Cell Signaling and Interaction	17	12
Skeletal and Muscular System Development and Function, Tissue Development, Tissue Morphology	17	12
Inflammatory Response, Organismal Injury and Abnormalities, Inflammatory Disease	11	9
Gastrointestinal Disease, Hepatic System Disease, Lipid Metabolism	2	1
Cellular Development, Cellular Growth and Proliferation, Developmental Disorder	2	1

These enriched interaction networks ranks each network based on p-value, with higher score indicating a greater number of network eligible molecules. Focus molecules indicates the number of network eligible molecules per network.

3. STUDY PART 2: REGULATION AND FUNCTIONAL IMPORTANCE OF MAMMALIAN TARGET OF RAPAMYCIN IN PSORIATIC SKIN LESIONS

Aims

Research in psoriasis has highlighted the activation status of PI3-K/mTOR cascade that is influenced by cytokines in keratinocytes biology (Buerger et al., 2013, Raychaudhuri and Raychaudhuri, 2014). Since dysregulated cytokine secretion in auto-inflammatory diseases is known to activate mTOR signaling, the aim of this thesis part was to determine the mTOR pathway activation status using archived samples of K5.hTGF-b1 transgenic mice. Further on, to investigate in detail the exact immunological mechanisms and functional importance of mTOR signalling in the pathogenesis of psoriasis by using an mTOR agonist to understand if it can induce psoriatic phenotype. The efficacy of topical rapamycin was tested using the IMQ psoriasis mouse model.

Parts of this work shown in the dissertation were published in the Experimental Dermatology, PLOS One and Acta-Dermatology-Venereology, as listed below:

- SHIRSATH, N., MAYER, G., SINGH, T. P. & WOLF, P. 2015. 8-methoxypsoralen plus UVA (PUVA) therapy normalizes signalling of phosphorylated component of mTOR pathway in psoriatic skin of K5.hTGFbeta1 transgenic mice. *Exp Dermatol,* 24**,** 889-91.

- BURGER, C., SHIRSATH, N., LANG, V., DIEHL, S., KAUFMANN, R., WEIGERT, A., HAN, Y. Y., RINGEL, C. & WOLF, P. 2017. Blocking mTOR signalling with rapamycin ameliorates imiquimod-induced psoriasis in mice. *Acta Derm Venereol*.

- BUERGER, C., SHIRSATH, N., LANG, V., BERARD, A., DIEHL, S., KAUFMANN, R., BOEHNCKE, W. H. & WOLF, P. 2017. Inflammation dependent mTORC1 signaling interferes with the switch from keratinocyte proliferation to differentiation. *PLoS One,* 12**,** e0180853.

The permission for reprinting the content (text and figures) of the published manuscript for incorporation in my PhD thesis was obtained by the copywrite holder or Copyright Clearance Center RightsLink® Service partnered by Wiley and Sons and Acta Dermato-Venereologica.

3.1 MATERIALS AND METHODS

3.1.1 Mice and Treatment

BALB/c mice were purchased from Charles-River and housed in the animal facility of the Center for Medical Research, Medical University of Graz, Austria. All procedures to which the mice were subjected were approved by the Austrian Government, Federal Ministry for Science and Research, through protocol no. BMWF-66-010/0032-11/3b/2013. For K5.hTGF-b1 transgenic mice study (Fig. 3.4.1-3.4.3) which express wild-type (latent) TGF-b1, all experiments were conducted using archived paraffin sections of murine tissues of wild type control (WT) and untreated and PUVA-treated K5.hTGF-β1 transgenic (TG) skin from previously reported research by Singh TP et. al (Singh et al., 2010, Singh et al., 2011). The tissue isolation and processing was done as indicated by Singh et al (Singh et al., 2010) and these archived samples were used to perform immunohistochemistry stainings for the downstream markers of mTOR pathway.

To study the effect of mTOR agonist MHY 1485 (Fig. 3.4.7 and 3.4.8), mice of 8–10 weeks received MHY1485 dissolved in ethanol/propylene glycol in a ratio of 3:7 while control received vehicle alone topically once daily to the dorsal skin in a cumulative manner with increasing doses every third day (0.1 mg/ml, 0.3, 10 mg/ml, 1 mg/ml, 3 mg/ml, 10 mg/ml). For rapamycin study (Fig. 3.4.10-3.4.15), female mice at the age of 7–8 weeks were shaved on the back skin 48 h before the start of experiment. Experimental groups included three regimes: vehicle + no IMQ (control), vehicle + IMQ (IMQ) and 1% Rapamycin + IMQ (RAPA+IMQ). 50 mg of freshly made 1% Rapamycin ointment or vehicle (petroleum jelly) was applied to the dorsal skin using a flat spatula in the morning and 6 h later 62.5 mg IMQ cream was applied. Both rapamycin and IMQ treatments were given for 4 days, while rapamycin alone was applied for one additional day.

To measure the severity of inflammation on the back, a scoring system similar to the human PASI (Psoriasis Area and Severity Index) score was used as previously described (Singh et al., 2010, Singh et al., 2013). In brief, to describe the severity of psoriasis, erythema, infiltration and scaling of the skin were scored “blindly” on a scale from 0 to 3, as follows: 0: none; 1: slight; 2: moderate; 3: severe. These single scores were summed up, resulting in a theoretical maximal total score of 9

(Fig. 3.4.11). Also, skin thickness was assessed by measuring the double skin-fold thickness (DSFT) of dorsal skin of the mice with a spring-loaded engineer's micrometer (Mitutoyo, Japan) throughout the experiment. Percent reduction of specific skin swelling (S) was determined using the following formula: (1-(SRapa+IMQ –S control / SIMQ –S control)) X100 (Burger et al., 2017). Mice were euthanized with an overdose of isoflurane and all efforts were made to minimize suffering. All the mice were sacrificed 24 hours after the last application of respective study drug and blood serum, skin, spleen and lymph nodes samples were collected for further analysis. Mice were euthanized with an overdose of isoflurane and all efforts were made to minimize suffering.

3.1.2 Chemicals and reagents

5% Aldara imiquimod (IMQ) was purchased from MEDA Pharmaceuticals. 1% Rapamycin (Merck Calbiochem) ointment was made by mixing 50 mg petroleum jelly with 10 µl of the corresponding rapamycin stock of 50 mg/ml. For the the K5.hTGF-b1 transgenic mouse study following primary rabbit monoclonal anti-murine antibodies were applied: anti-S6 ribosomal protein (clone 5G10), anti-phospho S6 ribosomal protein (Ser235/236) (clone D57.2.2E), anti-mTOR (7C10), anti-phospho mTOR antibody (Ser2448) (clone 49F9) (Cell Signaling, US) and Multilink System (biotinylated polyclonal swine anti-goat, -mouse, -rabbit IgG, code E 0453) at a concentration of 1/50. For MHY1485 mouse study, involucrin (Poly19244) was from Biolegend. In the rapamycin study, P-mTOR S2448 #2976 and P-S6 S235/6 #2211 antibodies were from Cell Signaling Technology. Keratin6 antibody (Ks6.KA12) from Thermo Scientific and caspase 14 antibody (NB100-56126) was from Novus Biologicals. Fluorescein Isothiocyanate (FITC)-conjugated anti-CD3, Phycoerythrin (PE)-conjugated anti-CD4, PE-conjugated anti-CD11c, Allophycocyanin (APC)-conjugated anti-CD11b, FITC-conjugated anti-F4/80, APC-conjugated anti-B220, PE-conjugated anti-Langerin, APC-conjugated anti-EpCAM all were from eBioscience while Peridinin Chlorophyll Protein Complex (PerCP/Cy5)-conjugated anti-Siglec-H was from Biolegend and PerCP-conjugated anti-CD8 was purchased from BD Bioscience (Buerger et al., 2017, Burger et al., 2017).

3.1.3 Immunohistology examination and staining

Approximately 1 cm^2 of central dorsal skin per mouse was excised was fixed in 4% PFA, paraffin embedded and stained with haematoxylin and eosin. The thickness of epidermis was measured and number of layers was determined in five microscopic fields using the fluorescent basic microscope at 20x magnification per mouse. All measurements were made blinded. Results were first averaged per mouse and then averaged per treatment group for statistical analysis. For immunohistochemistry, paraffin sections were processed routinely. Primary antibody was applied overnight after antigen retrieval with citrate solution pH 6. For K5.hTGF-b1 transgenic mice study Dako REAL Detection System with Peroxidase/AEC, Rabbit/ Mouse (code K5003) (Dako, Carpinteria, CA, US) was used for antibody detection, according to the manufacturer's instructions. Images were acquired by using a DP71 digital camera (Olympus) and an Olympus BX51 microscope. For rapamycin study Histofine Simple Stain AP Multi (Medac Diagnostika) was used for detection, according to the manufacturer's instructions. Images were acquired by using a Nikon Eclipse slide scanning microscope (Buerger et al., 2017, Burger et al., 2017).

3.1.4 Quantification of macroscopic vascularization

For quantifying the vascularization, the dorsal skin and the adjacent soft tissue of the mice was prepared for taking photographs from the reverse site in order to quantify the presence of blood vessels, similarly as previously described (Singh et al., 2010). The number of vascular bifurcations per dorsal skin sample was counted.

3.1.5 Multiplex immunfluorescent analysis

The OpalTM 6-Color Fluorescent IHC Kit (Perkin-Elmer, Waltham, USA) was used according to the manufacturer's instructions. Slides were stained with primary antibodies targeting Ki67, Krt10 (both from Abcam, Cambridge (UK)), Krt14,

Loricrin and Involucrin (Biolegend, London, UK). The Vectra® 3 automated quantitative pathology imaging system (Perkin-Elmer) was used for image acquisition and InForm software was used to score the relative abundance of cells expressing a certain marker protein in the epidermis upon tissue segmentation.

3.1.6 Flow Cytometry

Isolated lymph nodes were filtered through sterile sieve (40µm) to obtain single cell suspension. Cells were washed twice, and $1.5x10^7$ cells were stained for 20 min in the dark at RT with fluorescent-labelled antibodies diluted in PBS/0.3% BSA. Stained cells were washed with washing buffer and resuspended in 300µl PBS with 30µl of Sytox (Life Technologies, USA). Labelled cells were quantified on a flow cytometer (FACScan or FACSCalibur; BD Biosciences) and analyzed using CellQuest software (BD Biosciences). Viability of the cells was checked by staining with Sytox (Burger et al., 2017).

3.1.7 Complete blood count

Blood of the mice were collected in EDTA coated vails and stored at 4^0C and were processed and analysed next day using the Cell counter analyser-MELET SCHLOESING LABORATORIES.

3.1.8 Bead immunoassay

Mouse serum cytokine and chemokine levels were measured with Mouse Cytokine/Chemokine bead immunoassay kit, ProcartaPlex, 26Plex from Affymetrix eBioscience according to the manufacturer's specifications using the Bio-Plex 200 (Bio-Rad) and analysed with five parametric curve fitting.

3.1.9 Statistical analysis

All macroscopic readings and scorings of microscopic slides were conducted in a blinded fashion. All data is presented as mean ± SEM. Statistical differences

among experimental groups were determined by use of ANOVA or Mann Whitney U test after testing for normality, whatever appropriate. All analyses were performed with Prism 5.0; statistical significance was set at $p< 0.05$ and levels of significance were given as $*p < 0.05$; $**p < 0.01$; $***p < 0.001$.

3.2 RESULTS

3.2.1 Activation status of mTOR signaling components in psoriatic skin of K5.hTGFb1 transgenic mice

The hyperactivation status of the mTOR signalling cascade in K5.hTGF-b1 transgenic mice psoriatic skin was identified by the phosphorylation of mTOR at Ser2448, a site representative for mTOR activation, in lesional and nonlesional skin of the mice (Fig. 3.4.1 and 3.4.2). To provide further evidence that mTOR signalling is activated in psoriasis, the activation pattern of signalling molecules downstream of the mTOR complex was checked. As indicated in Fig 3.4.1, phosphor S6 levels were strongly upregulated in the TG psoriatic skin samples compared with WT skin. Also the mTOR and its downstream signaling components were strongly activated particularly in epidermis (Fig. 3.4.2). The phosphorylated levels of the S6 ribosomal protein were highly intense from stratum corneum to basal layer in diseased mice while mTOR expression was in both normal and diseased skin. Moreover, the phospho-S6 ribosomal protein was significantly reduced while phosphor mTOR expression was unaffected in the PUVA-treated group. This altered spatial activation pattern emphasized on the diverse function of mTOR in the manifestation of the disease. Besides, the expression pattern of EGFR (Fig. 3.4.3), subfamily receptor of tyrosine kinases that function upstream of PI3-K/mTOR cascade, was detected. This have shown high expression in the diseased skin of TG mice, probably due to dysregulated cytokines network in this model which thereby contributed to the pathogenesis of psoriasis (Yoshida et al., 2008, Wang et al., 2009). Thus this data identified that mTOR signalling is activated in the lesional skin of K5.hTGFb1 transgenic mice (Shirsath et al., 2015).

3.2.2 Deactivation of mTOR signalling promotes keratinocyte differentiation while cytokine-mediated induction leads to inhibition

Though there were several studies reported the activation status of mTOR (Buerger et al., 2013, Shirsath et al., 2015, Chamcheu et al., 2016), the evidence

of mechanistic significance of mTOR in navigating psoriatic phenotype development was still missing. To shed light in this direction, Buerger et al (Buerger et al., 2017) recently identifed the contribution of mTOR signaling to keratinocyte maturation using an in vitro differentiation model of HaCaT cells. These cells were driven into differentiation by post-confluent growth with increasing cell numbers (0.3 up to $6x10^5$ cells / 12 well). And the differentiation was confirmed and measured by the expression of involucrin and filaggrin. This observation was comparable with mTOR pathway as it was shut off, measured by the phosphorylation levels of the mTOR kinase itself, PRAS40, 4E-BP1 and the ribosomal protein S6 (Fig 3.4.5 A). However, other proliferative pathways such as Akt or Erk1 were turned off concomitant with p38MAPK activation (Fig. 3.4.5 A). To verify whether the shutdown of mTOR signaling is part of the differentiation process, the normal epidermis, keratinocyte stem cells (KSC), transient amplifying (TA) and post-mitotic (PM) cells were separated from primary human keratinocytes. Briefly, early passage keratinocytes were divided in KSCs, TA and PM cells on the basis of their ability to adhere to type IV collagen, as described before (Tiberio et al., 2002). Then the cells were allowed to adhere to type IV collagen dishes for 5 min which identify the KSC and non-adherent cells were transferred to fresh collagen-coated dishes and allowed to attach overnight, which was the TA cell. Remaining non-adherent cells was belonging to the PM cell population. These cells were verified by the expression of β1 integrin and keratin 6. While KSCs of the basal epidermal layer expressed low amounts of the differentiation marker involucrin, paired with high mTOR activity as measured by S6 phosphorylation. TA cells that leave the basal layer for differentiation, started to downregulate PI3-K signaling as measured by reduced Akt phosphorylation. In contrast, PM cells that are above to terminal differentiate completely shut down their mTOR signaling and only little S6 phosphorylation could be detected in these cells (Fig. 3.4.5 B). This study highlighted that deactivation of mTOR signaling is important phenomenon for the progression of keratinocyte differentiation.

As low mTORC1 signaling was inversely-proportional to the proper differentiation process favouring its expression, a question was raised whether aberrant activation of mTORC1 by pro-inflammatory cytokines involved in psoriasis is the cause for the differentiation defect in the epidermis. To answer this, differentiating HaCaT cells were treated with IL-17, IL-1β, TNF-α alone and with the mixture of

these three which led to repressed the protein expression of involucrin and mRNA level of keratin1, involucrin, loricrin and filaggrin (Fig. 3.4.6). This was parallel with their capacity to activate mTOR signaling. Interestingly, IL-17A and IL-22 have shown mild activation of mTORC1 with no effect on involucrin. To confirm this effect the Raptor, which specifically blocks mTORC1 signaling, was knocked-out using siRNA. This not only upregulated involucrin expression but also significantly rescued cytokine-induced repression of differentiation when comparing Raptor knockdown cells with control cells ($p \leq 0.05$). The relative density further verified that there was indeed a trend of regularisation of involucrin expression in raptor knockdown cells. In contrast when both mTOR complexes were inhibited through knockdown of the mTOR kinase itself, the effect was same on differentiation as seen before but with no efforts of rescuing the cytokine induced differentiation repression was detected (Fig. 3.4.6). Thus, it indicated that psoriatic cytokines do play a role in inducing mTORC1 activity in the epidermis, which inhibits correct epidermal stratification (Buerger et al., 2017).

3.2.3 Hyperactivation of mTORC1 signaling by agonist, MHY1485, inhibits differentiation leading to psoriasis-like skin morphology

For further verification of the findings of Buerger et al study (Buerger et al., 2017) in in vivo settings, the chemically synthesized mTOR agonist compound (Choi et al., 2012), MHY1485, was used. It is the mTOR agonist that is designed to specifically activate downstream components of mTOR signaling. This study exhibited that MHY1485 induced mTORC1 signaling, as shown by the phosphorylation of S6 or 4E-BP1 (Fig. 3.4.7 A and B), was mediated by mTORC1 as pretreatment with rapamycin completely blocked the effect (Fig. 3.4.7 A). Moreover, the mTORC2 signaling was not influenced as the levels of phosphorylation of Akt at S473 remained unchanged (Fig. 3.4.7 A and B). In HaCaT differentiation model MHY1485 maintained continuous mTORC1 signaling activation, while in untreated control cells the mTOR activity faded as differentiation was progressing. Further on, continuous mTORC1 activation by the agonist did hampered differentiation which was measured by reduced involucrin expression. However, this effect of the agonist was not strong enough to maintain

S6 phosphorylation under fully differentiated conditions, which resulted in flimsy expression of involucrin at the highest cell density (Fig. 3.4.7 C). Likewise in vivo, when MHY1485 was applied to the dorsal skin of mice with increasing doses, the skin dispayed macroscopically normal phenotype, while the dorsal skin fold thickness (DSFT) was increased in MHY1485 treated animals (Fig. 3.4.7 D). Additionally, histological analysis revealed a psoriasis-like morphology (Fig. 3.4.7 E) that was characterized by more epidermal layers and a small but not significant acanthosis (Fig. 3.4.7 F). At the same time, proper differentiation of the epidermal differentiation marker was disturbed as involucrin was also expressed in the spinous and granular layer, while in control mice it was exclusively detected in the upper granular and corneal layer (Fig. 3.4.7 G). Nevertheless, topical application of MHY1485 did not lead to a systemic effect that resembled the situation in psoriasis as no induction of chemokines and Th1/Th17 cytokines could be detected (Fig. 3.4.8). In summary, this invivo study strongly validated and complimented the invitro findings of Buerger et al (Buerger et al., 2017) that in healthy skin, deactivation of mTORC1 signaling seems to be required for basal keratinocytes to enter the epidermal maturation process and with activation leads to disturbed differentiation pattern. While, in psoriasis overexpression of Th1/Th17 cytokines encourages strong stimulation of mTOR signalling this prevents the proper differentiation of the keratinocytes that leads to stratified epidermis. Thus, this study recognised that hyperactivation of mTORC1 signaling by MHY1485 results in induction of psoriasis-like skin morphology (Fig. 3.4.9) (Buerger et al., 2017). This finding strongly supported the notion that psoriasis patients would be rather benefited from the topical use of mTOR inhibitors on the affected skin then systemic administration, which had shown encouraging results in a small trial (Ormerod et al., 2005). This local application would not only help to inhibit the proliferation of psoriatic keratinocytes but will also contribute in restoring the epidermal differentiation defect (Chamcheu et al., 2016) thereby restoring the barrier integrity.

3.2.4 Topical mTOR inhibition ameliorates skin and systemic symptoms of imiquimod-induced psoriasis

With this study base, the efficiency of topical rapamycin treatment in IMQ induced psoriasis-like skin lesions was evaluated as shown in the study plan (Fig. 3.4.10 A) (Burger et al., 2017). Rapamycin cream or vehicle was applied in the morning for 5 days followed by IMQ cream, after a 6h gap, on the shaved back skin of BALB/c mice for the first four consecutive days. Two days after the start of IMQ application, the back skin of the mice started to display signs of swelling. In comparison to the IMQ only treated group, the rapamycin treated group had shown statistically significant reduced specific skin swelling of 24% from day 2 and this difference further was increased on day 3 to 49% ($p<0.01$), reaching a peak difference of 64% at day 4 and 61% at day 5 ($p<0.001$) (Fig. 3.4.10 B). Meanwhile, the typical features of IMQ-induced skin inflammation (erythema, infiltration and scaling) was scored on daily basis during the investigation. The individual (Fig. 3.4.11) as well as the cumulative scores have displayed significant reduction by topical rapamycin compared to the IMQ only group (Fig. 3.4.10 C and D). While IMQ treated mice had shown high induction of neovascularization in the dorsal skin compared to the control group, topical rapamycin prominently led to reduced neovascularization formation (Fig. 3.4.10 E and F). Also there was significant spleen enlargement observed in disease mice by IMQ-induced inflammation that was rescued by topical rapamycin treatment (Fig. 3.4.10 G). In summary, the macroscopic observations highlighted efficacy of the rapamycin treatment with significant improvement of the psoriasis-like skin phenotype induced by IMQ. Following to this, the paraffin sections were stained to study the histological parameters. This analysis of H&E-stained sections had shown a strong epidermal thickening, hyperkeratosis and elongated rete ridges in IMQ treated mice (Fig. 3.4.12 A), while rapamycin treatment led to a significant reduction in epidermal thickness and keratinocyte layers paired with complete reduction in neutrophil rich micro-abscess formation on the surface of epidermis (Fig. 3.4.12 A-D).

3.2.5 Rapamycin reduces inflammation induced by dermal mTOR signalling

To check whether this approach of topically targeting the disease skin by rapamycin was able to interfere with inflammation dependent mTOR signaling activation in this model, the skin tissues were stained and checked for the

activation of mTOR kinase itself namely phosphorylation of S2448 and its downstream target, the ribosomal protein S6 (Burger et al., 2017). While in the control group hardly any phosphorylation was detected (Fig. 3.4.12 E), IMQ treated skin had shown an increase of p-mTOR at S2448 (Fig. 3.4.12 F), especially in the basal layer compartment of epidermis, as observed in human psoriatic skin. Here, rapamycin treatment strongly diminished mTOR activation (Fig. 3.4.12 G). A similar pattern was seen for the ribosomal protein S6, with strong phosphorylation in supra-basal layers after the strong stimulation of dermal inflammation by IMQ (Fig. 3.4.12 I), that was noticeably reduced through rapamycin treatment (Fig. 3.4.12 J). Keratin 6 upregulation in the supra-basal layers of psoriatic plaque is a hallmark of hyper proliferative cells whereas Caspase-14 is crucial element of an intact skin barrier that contributes to the proper terminal differentiation by processing filaggrin (Hoste et al., 2011) and who's expression are reduced in psoriatic skin (Hvid et al., 2011). In the present study the keratin 6 expression was induced in supra-basal layers after the induction of inflammation (Fig. 3.4.12 L) and was effectively reduced if mTOR was inhibited by topical rapamycin (Fig. 3.4.12 M). Similarly, the expression of caspase-14 was reduced which was rescued by rapamycin treatment (Fig. 3.4.12 N-P). This outcome of reinstating expression patters and normalization of the skin phenotype after rapamycin treatment strongly advocated the topical approach.

3.2.6 Topical rapamycin treatment normalizes the epidermal differentiation pattern and extravasation of immune cells

To further examine the impact of abnormal mTOR signaling activation and its inhibition on restoring normal epidermal maturation and barrier functions, multiplex IHC staining was performed (Burger et al., 2017). Here markers from the different stages of keratinocytes development were identified along with their expression patters, such as Keratin 10 as a marker of early differentiation and Loricrin as a marker of late expression. Ki-67 was used as a read-out for detecting the proliferation patter. Keratinocytes in the epidermis were recognized using keratin 14 as a marker of mature keratinocytes that was quantified by co-staining with selected markers for the different epidermal layers, as indicated in Fig. 3.4.13 A.

Where IMQ increased the number of proliferating cells treatment with rapamycin had clearly reduced the number of Ki-67 positive cells to normal levels. (Fig. 3.4.13 B). Keratin10 was significantly reduced from 33% to 13% and 10% of positive cells respectively, under inflammatory condition. Interestingly, the reduced expression of keratin 10 was not able to rescue by rapamycin treatment (Fig. 3.4.13 C). However, the number of involucrin positive cells which were doubled by IMQ treatment, was significantly regularized when rapamycin was added (Fig. 3.4.13 D). Loricrin was also diminished by approximately 50% (from 9% to 4% of positive cells) under IMQ induced inflammation, and have shown a not significant increase trend after mTOR inhibition (Fig. 3.4.13 E).

Moreover, the number of innate immune cells infiltration in the epidermis and dermis was determined using the same multiplex IHC approach. IMQ treatment did induce a small but non-significant increase of CD3+ cells in the dermis, which could be normalized by rapamycin (data not shown). MHCII dendritic cells and neutrophils have shown increased extravasation into the skin after IMQ treatment, which could be inhibited by rapamycin. Especially the effect on neutrophils was in line with the reduced number of neutrophil rich micro-abscesses observed in H&E sections after rapamycin treatment (Fig. 3.4.12D). However, none of these developments proofed to be statistically significant, which majorly attributed to the vulnerability of the assay to inter-individual deviation in small number of samples which were analyzed.

3.2.7 Topical rapamycin reverse the shift from lymphoid to myeloid cells in imiquimod model of psoriasis

The systemic effects of topical rapamycin treatment on the secondary lymphoid organ were also scrutinized by counting the influx of cells of innate and adaptive immunity immigrated into lymph nodes (LNs) using flow cytometry (Table 3.5.1). Higher numbers of $F4/80^+$ $CD11b^+$ macrophages, $CD11c^+$ $CD11b^+$ dendritic cells, $CD11c^+$ $120G8^+$ $SiglecH^+$ plasmacytoid dendritic cells and $CD207^+$ $EpCAM^+$ Langerhans cells were present in the LNs of IMQ treated mice compared to untreated controls. Thus a trend of reduction in influx for all these cells in LNs was

observed due to rapamycin treatment, which was most effective and notably seen for pDCs population (Table I).

3.2.8 Topical rapamycin treatment precludes any adverse systemic effects

Complete blood cell count is one of the most commonly performed lab practices to examine the systemic effects of drugs in patients. In this study also, the blood count at the end of the experiment was monitored (Fig. 3.4.14) (Burger et al., 2017). Consistent to the previous findings, here IMQ treatment also causes a shift from lymphoid to myeloid cells (van der Fits et al., 2009). Here, IMQ-induced inflammation have shown an abnormally increased absolute leukocyte number possibly due to increased levels of monocytes and neutrophils observed here. However, a trend for a decrease in the absolute number of lymphocytes was also seen and was consistent to the previous findings indicating a possible transient side effect of rapamycin treatment which is paired with its therapeutic effect (Prevel et al., 2013). Fascinatingly, there was also effective normalization of the IMQ-increased absolute numbers of neutrophils and monocytes by rapamycin. This was reliable with the fact that mTOR complex plays crucial role in regulating and influencing many pivotal immunomodulatory functions of these innate immune cells (Weichhart and Saemann, 2008). Collectively, this data point-out the efficacy of topical use of rapamycin in ameliorating IMQ-induced psoriatic phenotype.

3.3 DISCUSSION

Emerging studies have made it gradually more obvious the fact that constitutive overactivation of Akt/mTOR pathway in psoriatic lesions corresponds to dropped Foxp3 expression (Sauer et al., 2008) along with PTEN mutation (Li et al., 2014) which controls the functions of natural and inducible Treg cells (Powell et al., 2012). This is in agreement with the study of Singh et al. (Singh et al., 2010) that provided the hint that formed the rational to check and correlate the expression of pS6 in the present study. First hint was the induced Foxp3+ Treg cell number in the lymph nodes and skin of K5.hTGF-b1 mice (Singh et al., 2010) due to PUVA therapy. Notably, this induction of Treg function in the skin was paired with downregulation of Th17 that appeared to be crucial for the efficacy of an anti-psoriatic treatment in patients (Keijsers et al., 2015, Keijsers et al., 2014). Second, the increased trafficking of CD62L and CCR7 in lymph nodes in PUVA-exposed animals is known to be inhibited by mTOR pathway (Sinclair et al., 2008). Thus in this part of the thesis, the role of mTOR signalling in psoriasis was scrutinized starting with the detection of activation status of phosphorylated mTOR on Ser2448 and also its downstream signalling molecule S6.

This data suggests a role for mTOR signalling in the pathogenesis of psoriasis, consistent with other recent studies (Huang et al., 2014, Buerger et al., 2013). Although psoriasis is a benign disease, its pathophysiology has similarities with epidermal tumour biology (Leo and Sivamani, 2014) with triggered PI3-K/mTOR cascade, leading to hyperproliferative and differentiation defects (Chen et al., 2009b, Chen et al., 2009a). Therefore the activation of these proteins, which have an important role in protein translation, reflects the need of the diseased keratinocytes to acquire building blocks for cell growth and proliferation (Raychaudhuri and Raychaudhuri, 2014). The present findings are intriguing with regard to the expression pattern of the subfamily receptor of tyrosine kinases, EGFR, which regulates upstream of PI3-K/mTOR cascade (Yoshida et al., 2008). mTOR that was activated in both lesional skin, mainly due to the knock-in effect in mouse (Li et al., 2004), and non-lesional skin while S6 activation was found only in the diseased skin (Fig. 3.4.1-3.4.3). This argues again for diverse functions of mTOR and S6 and projects that pathological activation of mTOR might be an early

event in psoriasis pathogenesis, while S6 activity might contribute to the manifestation of the plaque to sustain psoriasis (Buerger et al., 2013). In summary, this report showcased for the first time that mTOR signaling is downregulated by PUVA therapy analogously to the treatment with rapamycin (Yang et al., 2014). The normalization of psoriatic phenotype was linked to downregulation of Th1-Th17cytokines and growth factors. In addition, many upcoming reports have shown invitro data indicating upstream p53 dependent RIG-1 signaling activation that suppresses Akt/mTOR pathway in keratinocytes (Chowdhari and Saini, 2016) by inhibiting signal transduction in the PI3K pathway by preventing efficient plasma membrane recruitment of crucial effector kinases in ECP treatment for GVHD (Van Aelst et al., 2016). The investigation in this part of the thesis highlighted the fact that study of skin biopsies for site-specific S6 phosphorylation might be a useful criterion in future to evaluate the pharmacodynamics and effectiveness of anti-psoriatic therapies in clinical studies.

Though the hyperactivation causing uncontrolled keratinocyte proliferation with differentiation defects was hypothesized to be regulated by PI3-K/Akt/mTOR cascade by Huang et al (Huang et al., 2014). Buerger et al (Buerger et al., 2017) shed light on the involvement of mTORC1 signaling and its pathogenic role in normal homeostasis and in the psoriatic epidermis. It was found that in healthy keratinocytes the relation between Akt/mTOR signaling and differentiation was inversely proportional where mTOR signaling deactivation occurred when differentiation was progressing. Thus, this emphasises that epidermal loss of mTORC1 signaling is necessary to cause reduced proliferation of epidermal progenitors cells in the basal layer (Ding et al., 2016). This appears to be an indispensable step for proper keratinocyte maturation that is allowed by blockade of mTORC1, leading to progression of differentiation (Huber and Teis, 2016). Indeed, autophagy induction is known to be paralleled by differentiation in keratinocytes which are undergoing a selective form of nucleophagy, where Akt contributes to its nuclear degradation (Aymard et al., 2011, Akinduro et al., 2016). Buerger et. al and others (O'Shaughnessy et al., 2007, Buerger et al., 2012, Sully et al., 2013) proved that functional activation of Akt in the upper granular layer of healthy skin is an important characteristic in the formation of the cornified envelope that thereby contributes to the nuclear degradation process. Further on

the work from Buerger et al. indicates that cytokine- induced aberrant activation of the mTOR cascade occurred. These in vitro findings by Buerger et. al. were modelled and validated further in this part of the thesis using a murine model that proved the aberrant mTOR activation demonstrated by using the synthetic mTOR agonist MHY 1485. The findings indicated that the agonist induced psoriasis-like skin changes associated with dislocalisation of involucrin. This data was consistent with the work Chen J.Q et al. finding (Chen et al., 2013) who have showen that involucrin which is mainly localized in the granular layer in healthy human skin, is overexpressed and mislocalized into the stratum spinosum of psoriatic lesional skin which forms a signal for disturbed differentiation. It can be assumed that mTOR hyperactivation might have a dual effect, first on the cells that still have the capacity to divide mTORC1 signaling enforces proliferation contributing to the acanthosis seen in MHY1485-treated mice and in psoriasis patients, and second in the cells that are already determined for differentiation the regular maturation program is blocked leading to aberrant epidermal maturation such as dislocation of involucrin (Buerger et al., 2017). Thus, mTOR inhibition seems a promising anti-psoriatic strategy. Remarkably, systemic rapamycin or its derivatives have been used for its immunosuppressive properties in anti-psoriatic trials alone or in combination with low doses of cyclosporine (Frigerio et al., 2007, Reitamo et al., 2001, Wei and Lai, 2015). This also supports the notion that psoriasis patients could be benefited from the topical use of mTOR inhibitors on affected skin, which had showen encouraging results in the past in a small trial (Ormerod et al., 2005). Thus this gives rational that local application could not only inhibit the proliferation of psoriatic keratinocytes but may also restore the epidermal differentiation defect (Chamcheu et al., 2016).

The recent study by Swindell et al. who used RNA microarray analysis confirmed the disease signature observed in the IMQ mouse model to reflect the human setting specifically with respect to genes involved in epidermal development (Swindell et al., 2011), thereby validating the use of this model. Moreover, the usefulness of this model to test the topical delivery profiles of anti-psoriatic drugs strongly supports its use as well (Lin et al., 2015). In the current study IMQ-induced epidermal signalling pattern of mTOR was assessed what supported previous findings (Buerger et al., 2013, Chamcheu et al., 2016). Here, topical

rapamycin treatment did ameliorate the severity of erythema and scaling of the psoriasis-like condition along with reduced skin thickness (Fig. 3.4.10-3.4.14). This was supplemented by a noticeable reduction of spleen size, with steady blood count parameters and reduced influx of (innate) immune cells with antigen presenting capacity into secondary lymphoid organ(s). The effect was quite prominent for the cells that express endosomal TLR7 and in which mTOR plays an important role for TLR-mediated activation like pDCs (Liu, 2005, Cao et al., 2008). mTOR pathway is important in regulating interferon production by pDCs and inhibition of which resulted in impaired IFN-alpha/beta production (Cao et al., 2008). Moreover, mTOR is also known to endorse vascular permeability by enhancing VEGF functions (Huang et al., 2014). This leads to increased tissue vascularity thereby enhancing the leucocyte traffic into the skin. This was also effectively targeted by rapamycin (Frost et al., 2013). Thus, the normalized dermal vessel density resulting in a decreased flow of leucocytes to the skin might be also contributing to the reduced influx of APCs into secondary lymphoid organs in rapamycin-treated animals. Together, this data indicated that topical rapamycin treatment worked effectively not only in conditioning APCs causing them to be less responsive to TLR agonist but also preventing its channelizing through inhibition of new blood vessel formation.

All together rapamycin not only diminished some of the systemic effects of IMQ but also had a strong influence on the activation of the mTOR pathway itself and its target proteins such as keratin 6 and caspase 14 (Fig. 3.4.12 E-P). Other than the fact that Keratin 6 is upregulated in the suprabasal layers of psoriatic plaques (Korver et al., 2006) and is an important biomarker of hyperproliferative cells, what is even more interesting is that its mRNA containing putative 5' oligopyrimidine (5´TOP), known to be specifically regulated by mTORC1 are sensitive to rapamycin treatment (Hickerson et al., 2009). Treatment with rapamycin has been shown to cause selective inhibition of the translation of the mRNAs that incorporates terminal 5′ TOP thereby obstructing downstream mTOR pathway components involved in TOP mRNA translation. Thus, it could be hypothesized that inhibition of mTOR might have reduced the aberrant expression of keratin 6 which by this means contributed to the observed normalization of keratinocyte maturation. Similarly, control of caspase 14 expression after rapamycin treatment was observed, what can contribute to epidermal maturation

by the processing filaggrin expression (Hoste et al., 2011). This went in line with the fact that lack of caspase 14 in psoriatic plaques is associated with disturbed epidermal barrier formation (Hoste et al., 2013).

To further investigate the expression of these epidermal differentiation markers in detail, a quantitative multiplex immunostaining approach was used which revealed reduced expression of keratin 10 and loricrin and an increase in expression with aberrant distribution of involucrin by IMQ, resembling the clinical scenario observed in psoriasis (Ishida-Yamamoto and Iizuka, 1995). Here, topical rapamycin was able to reinstate disturbed expression patterns for most of the markers (Fig. 3.4.13), similar to what can be observed in human skin biopsies after treatment with biologics (Donetti et al., 2012). This highlighted rapamycin more as an differentiation-promoting agent, analogous to other naturally occurring compounds that hinders mTOR activity (Chamcheu et al., 2016). In addition, rapamycin also normalized the IMQ dependent increase in Ki-67 positive keratinocytes, which can possibly linked to a direct effect of rapamycin on proliferative control, underlining the role of mTORC1 in keratinocyte stem cell homeostasis (Rho et al., 2014). On the other hand, the failure in proliferative keratinocytes might be a consequence of the onset of the mechanism causing the shift towards keratinocyte differentiation induced by mTOR inhibition itself.

To date, systemic mTOR therapy has shown encouraging outcome in autoimmune diseases but was accompanied from significant side effects (Fogel et al., 2015). Moreover, there is limited data on the efficacy of topical rapamycin and its direct effect on skin structure and barrier integrity. Though recent efforts have highlighted topical rapamycin as an effective approach in a mouse model of tuberous sclerosis complex and allergic dermatitis (Baumer et al., 2005, Rauktys et al., 2008). In a recent clinical study topical rapamycin ointment not only have showen passable skin penetration along with good safety profile, but also significantly inhibited the growth of skin angiofibromas which are characterized by hyperactivation of mTOR signaling (Tanaka et al., 2013). These conclusions together with the present finding strongly advocate the rational that mTOR activation is not only an important biomarker for prognosis of the disease but also has a significant functional importance in balancing keratinocyte proliferation and differentiation balance (Fig.3.4.15). Thus the data in this part of thesis along with other upcoming research (Eline et al., 2017) highlights the fact that a topical approach can be an

effective treatment option for psoriasis that avoids the side effects associated with systemic administration.

Altogether, the findings in this section of thesis corroborate current reports of the dysregulated mTOR pathway in hyperplastic skin diseases and provide further evidence for mTOR as a pathogenic factor also in psoriasis. However, more work is needed to further study the optimal frequency and duration of overall treatment, also with regard to the rate of recurrence after treatment is discontinued (Fogel et al., 2015). Nevertheless, it has to be taken into consideration that inhibition of mTOR may have side effects related to regenerative response capacity of keratinocytes that possibly can be restored by interrupting the therapy from time to time (Ding et al., 2016).

3.4 FIGURES

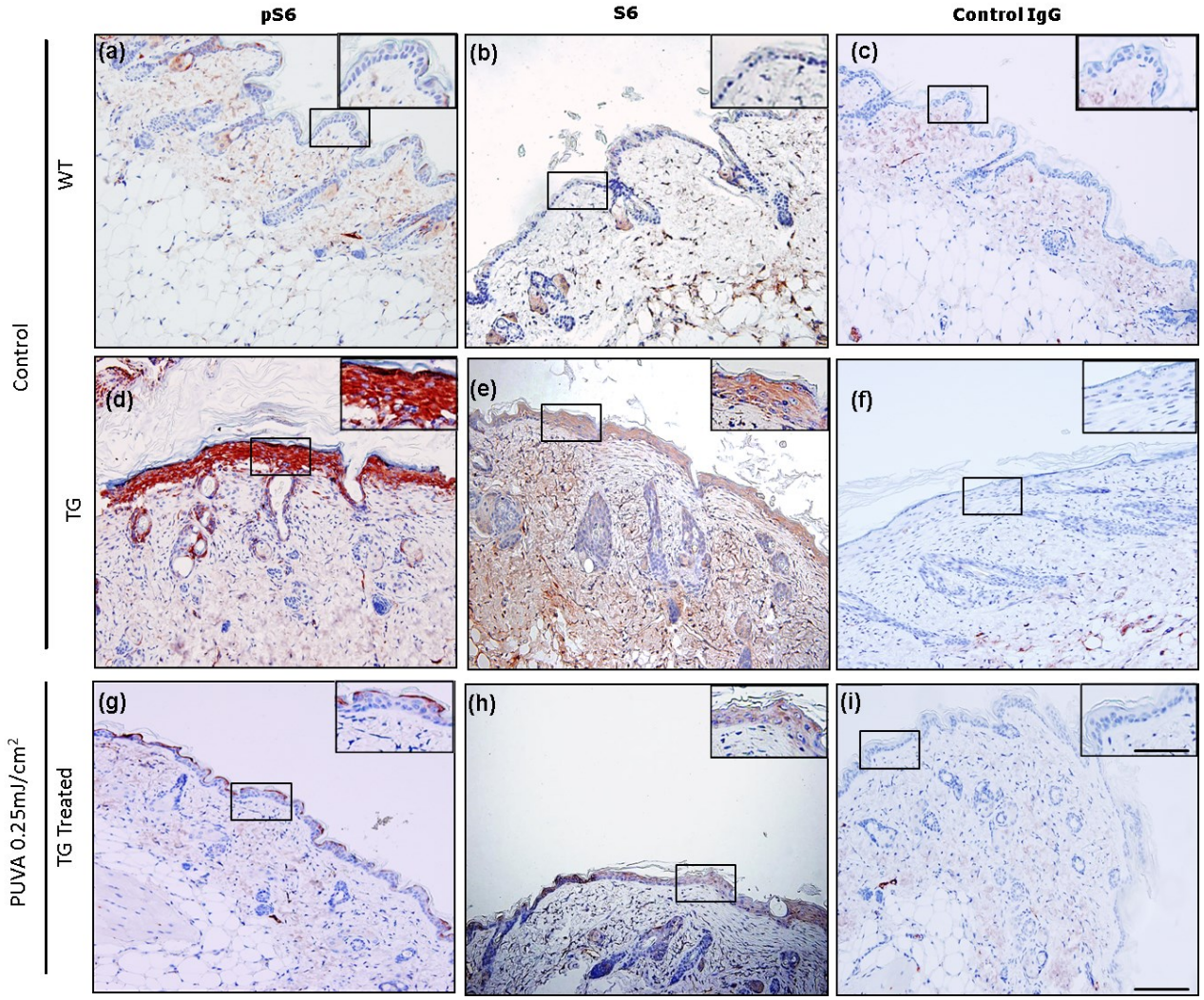
pS6
S6
Control IgG
Control
WT
TG
PUVA 0.25mJ/cm2
TG Treated
(a)
(b)
(c)
(d)
(e)
(f)
(g)
(h)
(i)

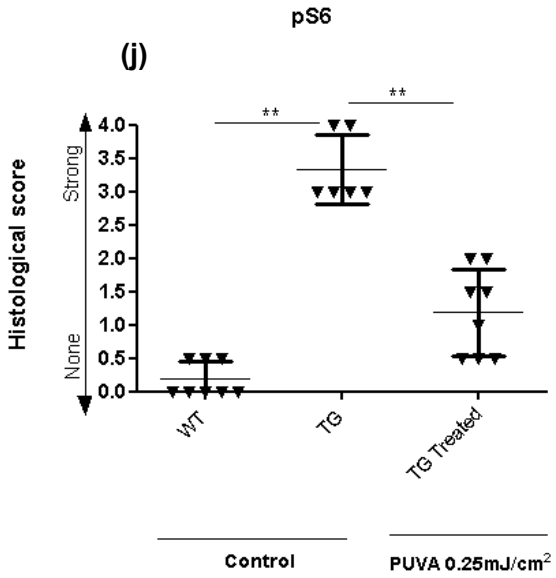
pS6
(j)
Histological score
Strong
None
4.0
3.5
3.0
2.5
2.0
1.5
1.0
0.5
0.0
**
**
WT
TG
TG Treated
Control
PUVA 0.25mJ/cm2

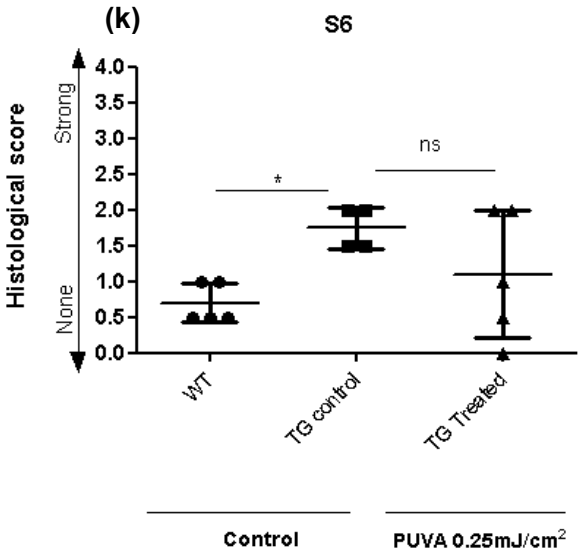
(k)
S6
Histological score
Strong
None
4.0
3.5
3.0
2.5
2.0
1.5
1.0
0.5
0.0
*
ns
WT
TG control
TG Treated
Control
PUVA 0.25mJ/cm2

Figure 3.4.1 The downstream effector of mTOR signaling cascade is functionally active in psoriatic skin of K5.TGFß1 transgenic (TG) mice. The immunohistochemical stainings demonstrate high levels of phospho S6 (pS6) in the skin of TG mice (d) compared to WT controls (a) and its downregulation by treatment with 0.25mJ/cm^2 PUVA (g). Note that activated protein was mainly observed in the cytoplasm of epidermal cells in the untreated TG mice. No significant staining was found for S6 (b,e,h). Control IgG, isotype antibody staining (c,f,i). Scale bar, 100 µm for main image and 50 µm for insert. Histological scoring of immunohistochemical stainings of phosphorylated ribosomal protein S6 (pS6) (j) and S6(k). The data shown represent the individual scores as well as the mean and range of the histological scores for both proteins. Statistical analysis was performed using unpaired Mann-Whitney (*P < 0.05, ** P< 0.005). n, 4 to 8 mice per experimental group. Reused from (Shirsath et al., 2015) with permission of John Wiley and Sons publisher.

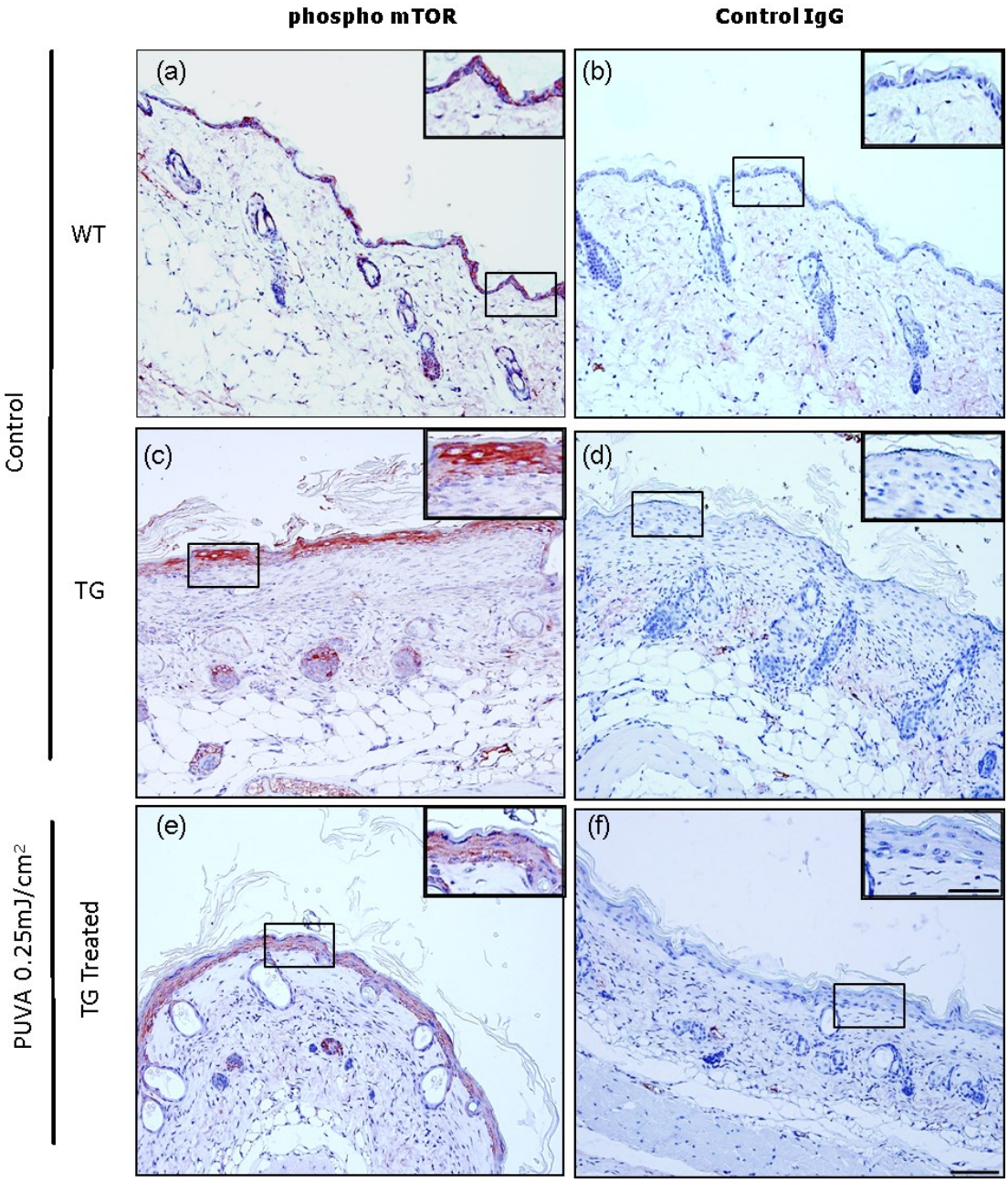

Figure 3.4.2 Activation status of the mammalian target of rapamycin (mTOR) kinase in psoriatic skin of K5.TGFß1 transgenic (TG) mice. Immunohistochemical studies reveal that mTOR is activated in both nonlesional (a) and lesional (c,e) skin. Control IgG, isotype antibody staining (b,d,f). Scale bar, 100 µm for main image and 50 µm for insert. Reused from (Shirsath et al., 2015) with permission of John Wiley and Sons publisher.

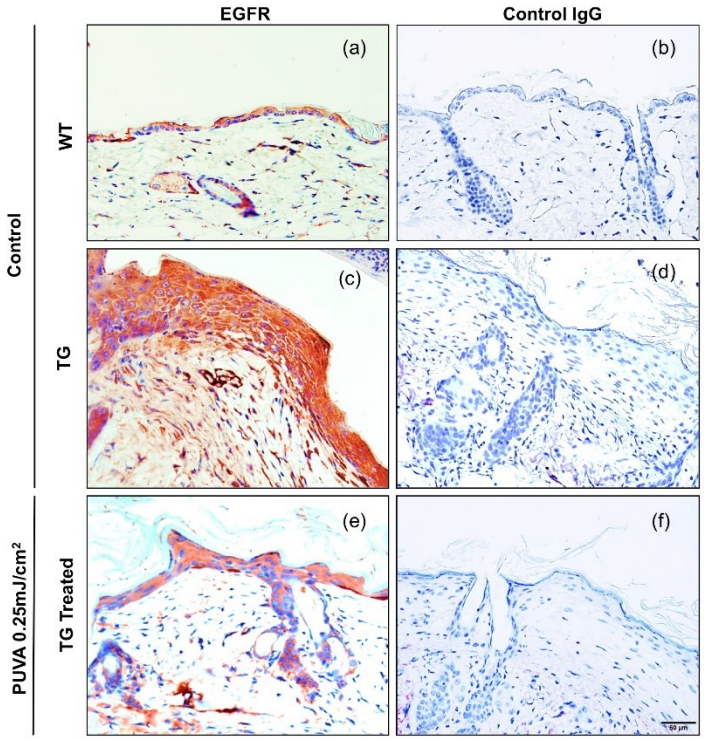

Figure 3.4.3

The staining intensity of EGFR (receptor for members of the epidermal growth factor) is slightly upregulated in psoriatic epidermis of K5.hTGFß1 transgenic (TG) mice (c) compared to wild type mice (WT) (a) and PUVA-treated mice (e). Control IgG, isotype antibody staining (b, d, f). Scale bar, 50 μm. Reused from (Shirsath et al., 2015) with permission of John Wiley and Sons publisher.

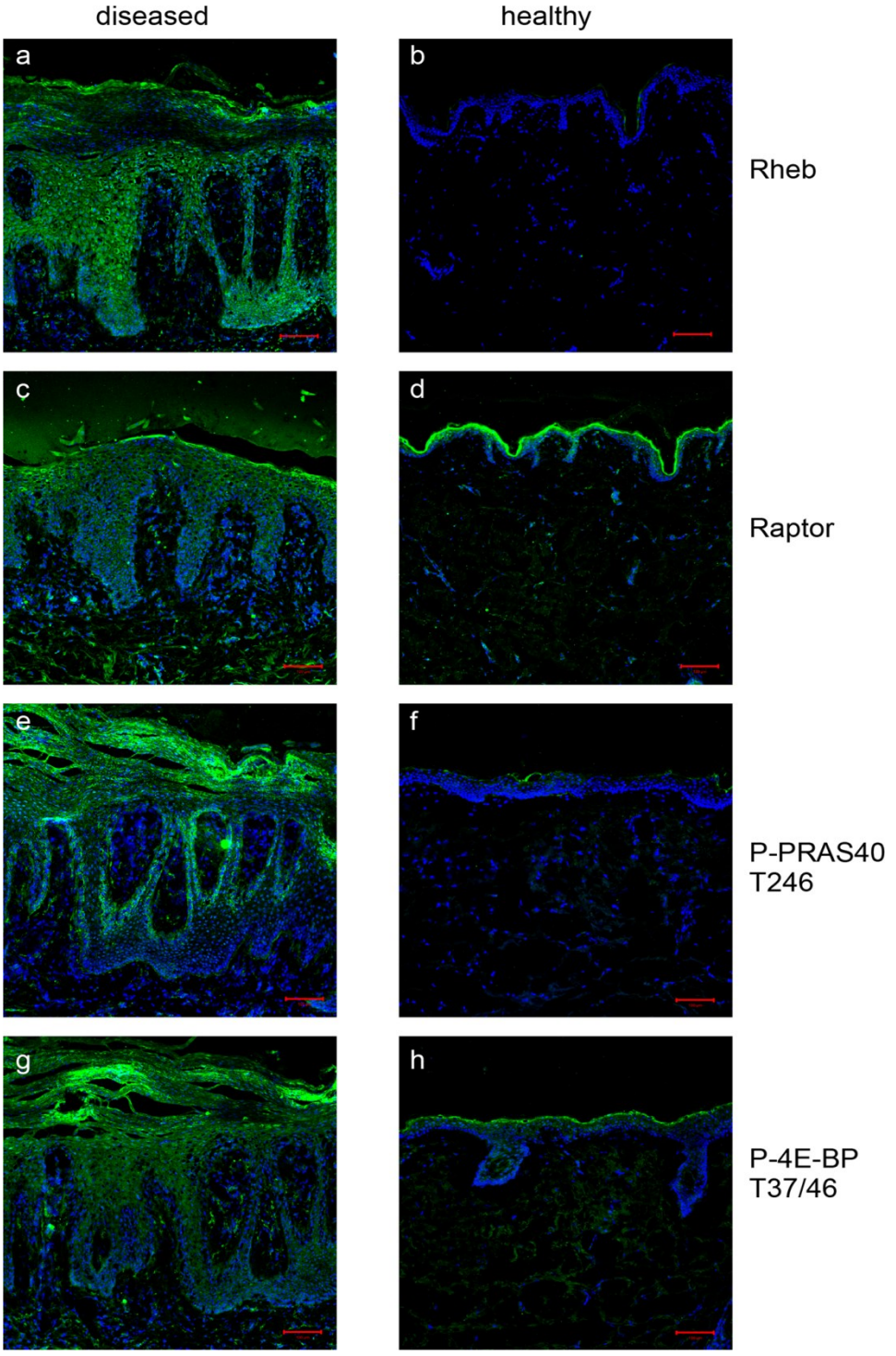

Figure 3.4.4 mTORC1 and its downstream mediator are strongly activated in psoriatic lesions. Punch biopsies from lesional psoriatic skin (a,c,e,g) of 20 patients and five healthy donors (b,d,f,h) were stained with antibodies for specific

for Rheb, Raptor, P-PRAS40 and P-4E-BP. Nuclei were stained with DAPI. Representative overlay images from one patient and one healthy donor are shown. Bars represent 100 µm. Reused from (Buerger et al., 2017) with permission of the copywrites holder.

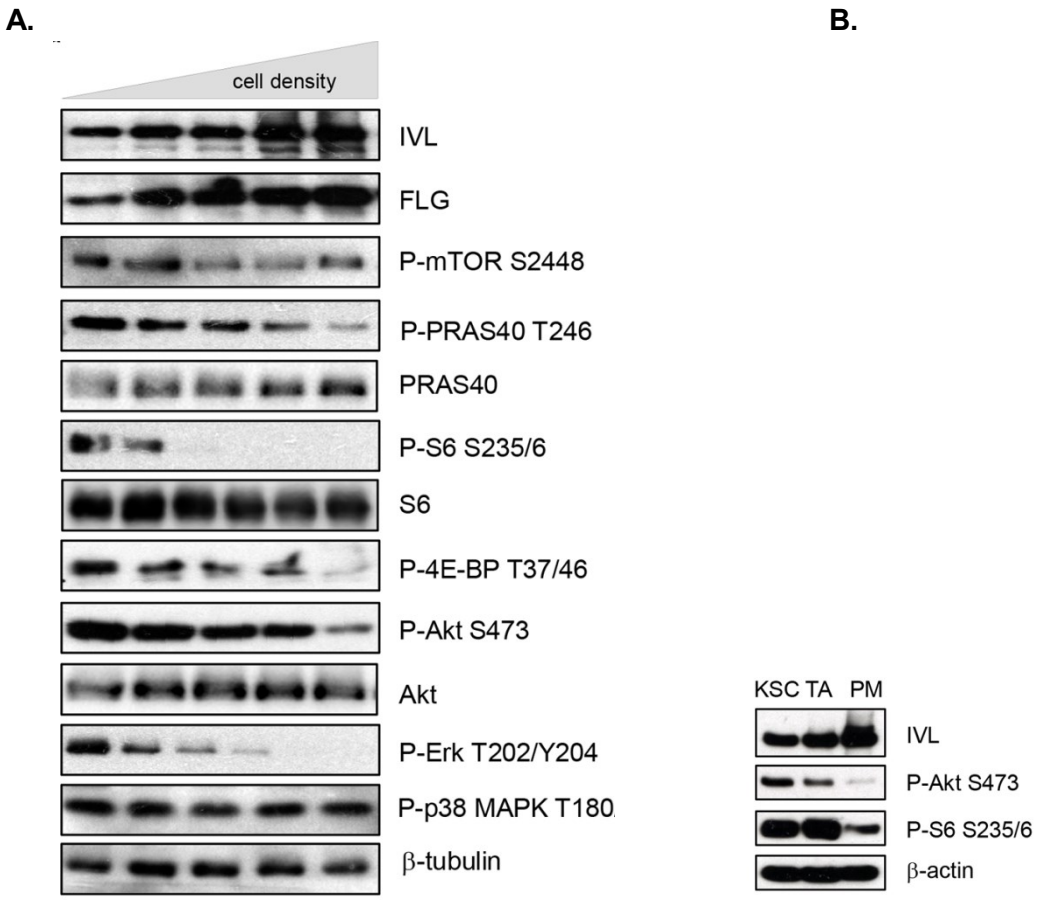

Figure 3.4.5 mTOR signaling is deactivated during differentiation and only partially contributes to the control of proliferation. (A) Increasing densities of HaCaT were seeded to promote differentiation and harvested after 72h. Protein lysates were subjected to SDS-PAGE and Western Blotting with the indicated antibodies. (B) Keratinocytes stem cells (KSC), transient amplifying (TA) and postmitotic (PM) cells were separated according to their ability to adhere to type IV collagen. Protein lysates were subjected to SDS-PAGE and Western blotting with the indicated antibodies, showing that mTORC1 signaling is mainly present in undifferentiated cells. Reuse from (Buerger et al., 2017) with permission of the copywrites holder.

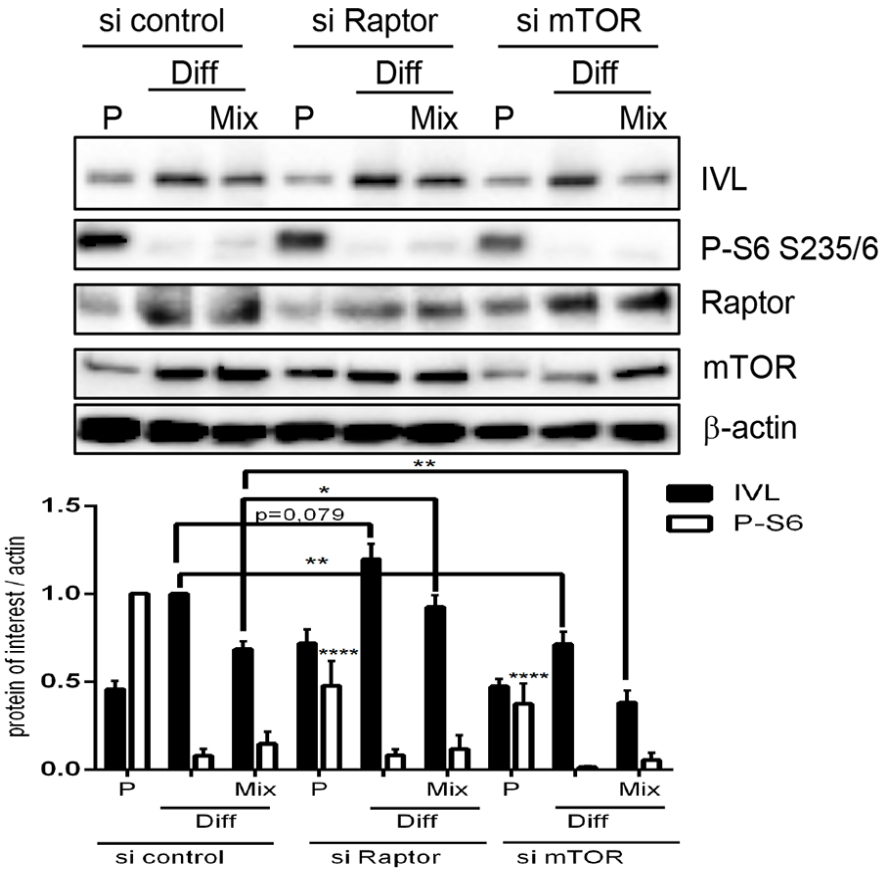

Figure 3.4.6 Cytokine mediated activation of mTOR interferes with differentiation. HaCaT cells were reverse-transfected with siRNA specific for Raptor, mTOR or control siRNA and seeded at 0.6 x10^5 (P) or 6x10^5 (Diff) cells per 12 well. After 24 h cells were treated with 20 ng of IL-1 β, IL-17A and TNF- α (Mix) and harvested after another 72h. Protein lysates were analysed by Western blotting with the indicated antibodies. Below a quantification of 7–9 similar blots is shown. Statistical significance was calculated with two-way ANOVA and Bonferroni multiple comparison. For P-S6 statistical significant difference is shown for proliferating cells of knockdown cells compared to proliferating control cells (*p ≤0.05, **p ≤0.01, **** p ≤0.0001). Reuse from (Buerger et al., 2017) with permission of the copywrites holder. .

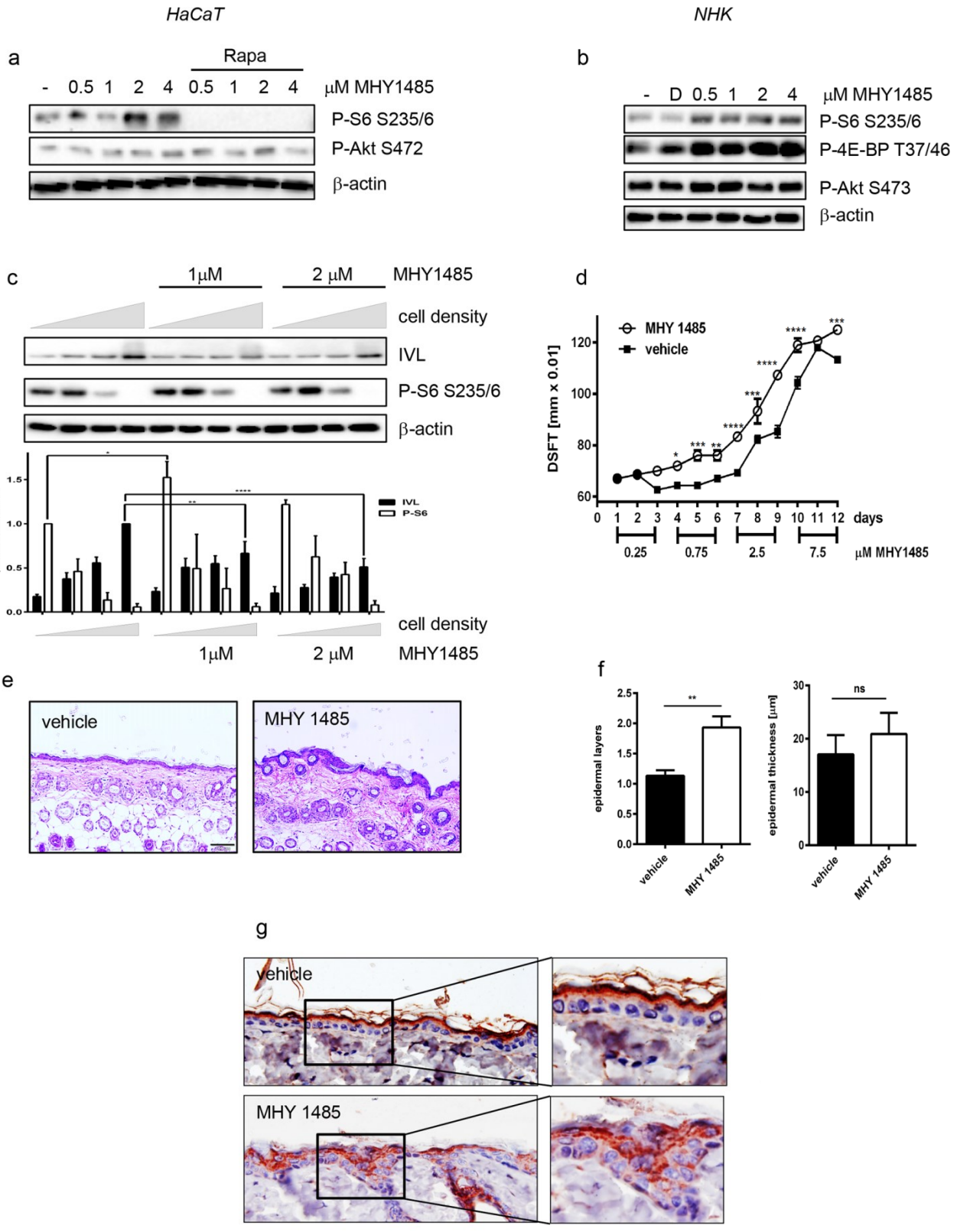
HaCaT
NHK
a
Rapa
- 0.5 1 2 4 0.5 1 2 4 μM MHY1485
P-S6 S235/6
P-Akt S472
β-actin
b
- D 0.5 1 2 4 μM MHY1485
P-S6 S235/6
P-4E-BP T37/46
P-Akt S473
β-actin
c
1μM 2 μM MHY1485
cell density
IVL
P-S6 S235/6
β-actin
protein of interest / actin
IVL
P-S6
cell density
1μM 2 μM MHY1485
d
MHY 1485
vehicle
DSFT [mm x 0.01]
days
0.25 0.75 2.5 7.5 μM MHY1485
e
vehicle
MHY 1485
f
epidermal layers
epidermal thickness [μm]
ns
vehicle
MHY 1485
g
vehicle
MHY 1485

Figure 3.4.7 Activation of mTORC1 signaling inhibits differentiation. HaCaT cells (a) or NHK cells (b) were serum starved overnight and treated with increasing doses of MHY1485 or DMSO for 30 min If indicated cells were pre-treated with 100 nM Rapamycin for 30 min. Cells were harvested and protein lysates were analyzed by Western blotting with the indicated antibodies, 669 showing that mHY1485 induces mTORC1 signaling. (c) Increasing numbers of HaCaT cells were seeded and driven into differentiation by post-confluent growth in the presence of the indicated concentrations of MHY1485. Protein lysates were analyzed by Western blotting with the indicated antibodies. Below a quantification of four similar Western blots is shown. **p ≤0.005 (d-g) MHY1485 or vehicle control was topically applied to the dorsal skin of mice for 12 consecutive days with increasing doses. (d) DSFT (Double Skin Fold Thickness) was measured before the first treatment (day1) and repeated every day. Data shown are mean values from one experiment, with n=3 mice per treatment. *p ≤0.05, **p ≤0.005 (e) Representative images of H&E-stained sections from dorsal skin of a mouse of control and MHY 1485 treated groups (scale bar, 100μM). (f) Evaluation of histological features, including number of epidermal layers and epidermal thickness in μM. Data shown are mean values of five measurements per mouse ± SEM. **p ≤0.05. (g) Involucrin staining of vehicle control or MHY1485 treated mice. Overview images and close-ups are shown. MHY1485 induces in vivo psoriasis like phenotype and interferes with proper differentiation. Reuse from (Buerger et al., 2017) with permission of the copywrites holder. .

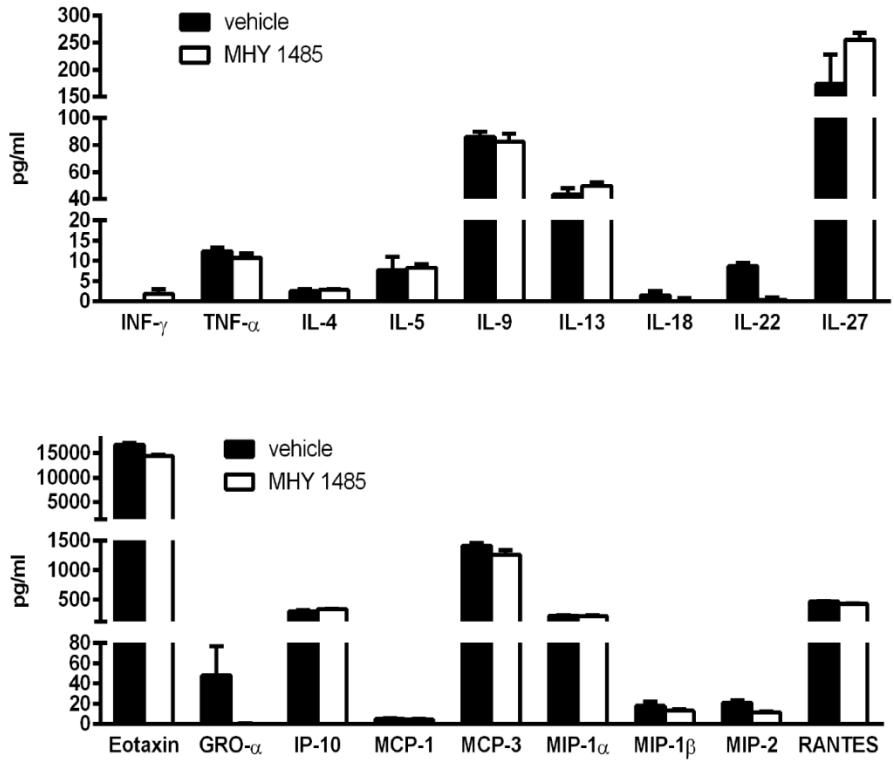

Figure 3.4.8 Effect of topical MHY1485 treated on chemokine and Th1/Th2/Th17 cytokine profile expression. BALB/c mice were treated, as described in M&M (3.1). 24 hrs after the last treatment, serum samples were collected and analysed by 26-plex bead immunoassay. IL-1 β, IL-2, IL-6, IL-10, IL-12, IL-17, IL-23, and GM-CSF levels were below detection level. Data shown are from one experiment, with n = 2–3 mice per treatment group. Reuse from (Buerger et al., 2017) with permission of the copywrites holder. .

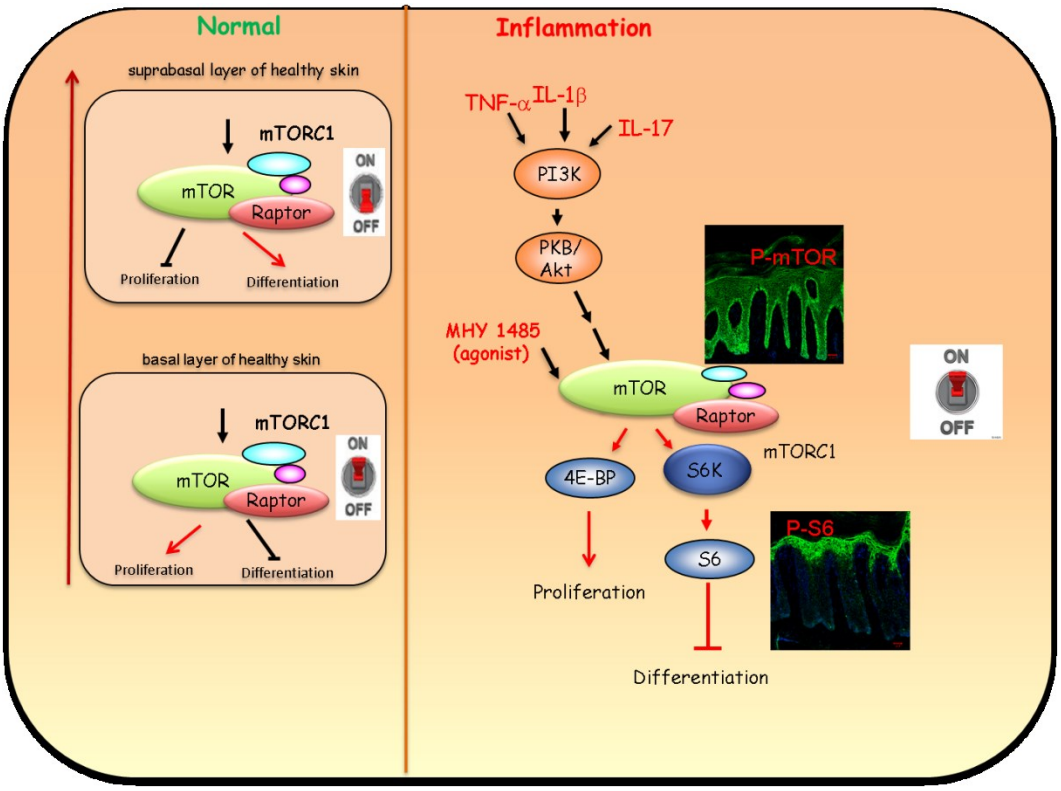

Figure 3.4.9 Schematic representation of the study hypothesis/results to explain functions of mTOR in normal and in diseased skin where it serves as a switch to determine the fate of keratinocytes.

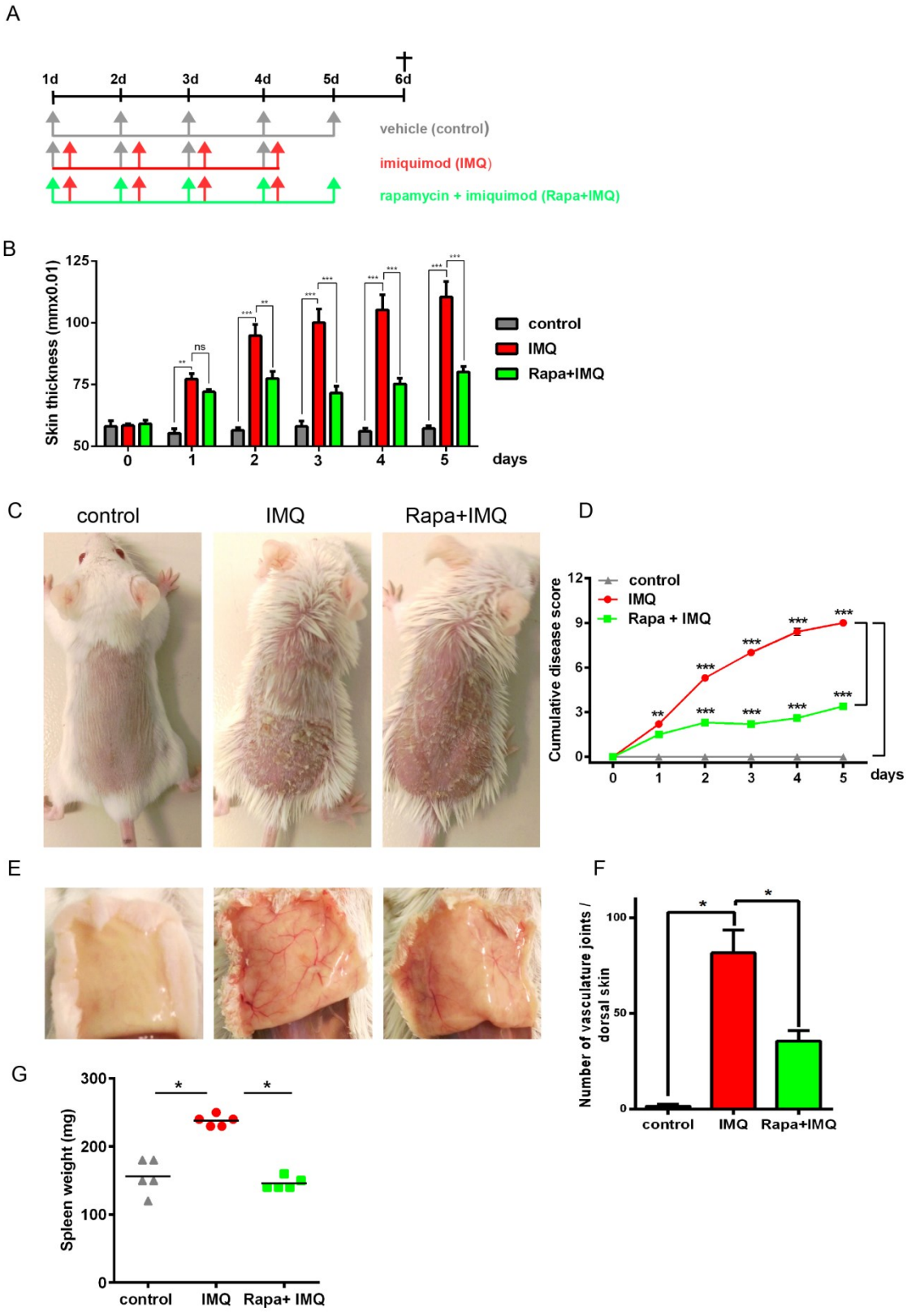
A
1d
2d
3d
4d
5d
6d
vehicle (control)
imiquimod (IMQ)
rapamycin + imiquimod (Rapa+IMQ)
B
Skin thickness (mmx0.01)
125
100
75
50
ns
0
1
2
3
4
5
days
control
IMQ
Rapa+IMQ
C
control
IMQ
Rapa+IMQ
D
Cumulative disease score
12
9
6
3
0
control
IMQ
Rapa + IMQ
days
E
F
Number of vasculature joints / dorsal skin
100
50
0
control
IMQ
Rapa+IMQ
G
Spleen weight (mg)
300
200
100
0
control
IMQ
Rapa+ IMQ

Figure 3.4.10 mTOR inhibition ameliorates skin and systemic symptoms of imiquimod induced psoriasis. (A) Study plan: BALB/c mice were treated on the dorsal skin for 4 to 5 days by three different treatment regimes, as described in materials and methods. (B) Double skin-fold thickness (DSFT) assessment of dorsal skin of the mice measured throughout the experiment. (C) Macroscopic presentation of mice from the three treatment regimens (D) A specific score (composed of a rating from 0 to 3 for erythema, infiltration, and scaling) was used to monitor macroscopic cumulative disease severity in the mice (E) Reduced neoangioenesis formation observed in dorsal skin of rapamycin treated mice compared to IMQ treated ones. (F) Macroscopic bifurcations were counted as a measure of blood vessel formation. (G) Spleens were prepared from each mouse and weighed. All data shown is from one representative experiment, with n = 5 per treatment group and error bars representing SEM. Statistical differences were determined by using one-way ANOVA or Mann-Whitney U test (*$p \leq 0.05$. **$p \leq 0.01$. ***$p \leq 0.001$). As a copywrite holder of the article, the figure was reused from (Burger et al., 2017) with the permission of publisher.

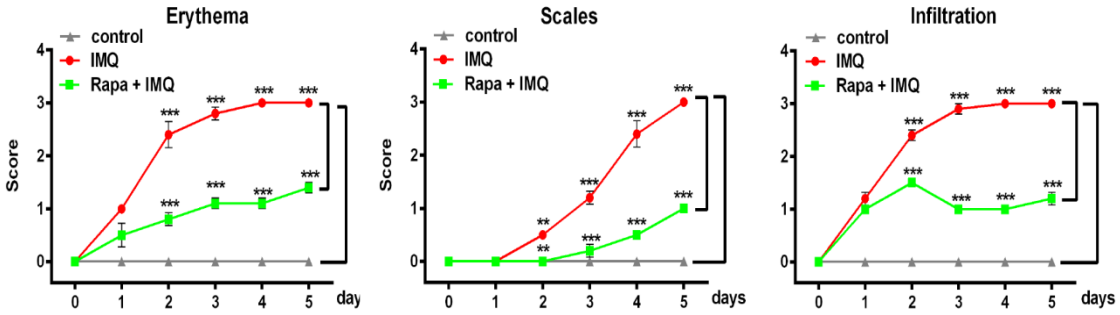

Figure 3.4.11 Detailed clinical disease score. The severity of inflammation on the back was assessed with a scoring system similar to the human Psoriasis Area and Severity Index (PASI) score. Erythema, infiltration and scaling of the skin were scored “blindly” on a scale from 0 to 3, as follows: 0: none; 1: slight; 2: moderate; 3: severe. Statistical differences were determined by 2-way analysis of variance (ANOVA) and Bonferroni multiple comparison (**$p \leq 0.01$; ***$p \leq 0.001$). As a copywrite holder of the article, the figure was reused from (Burger et al., 2017) with the permission of publisher.

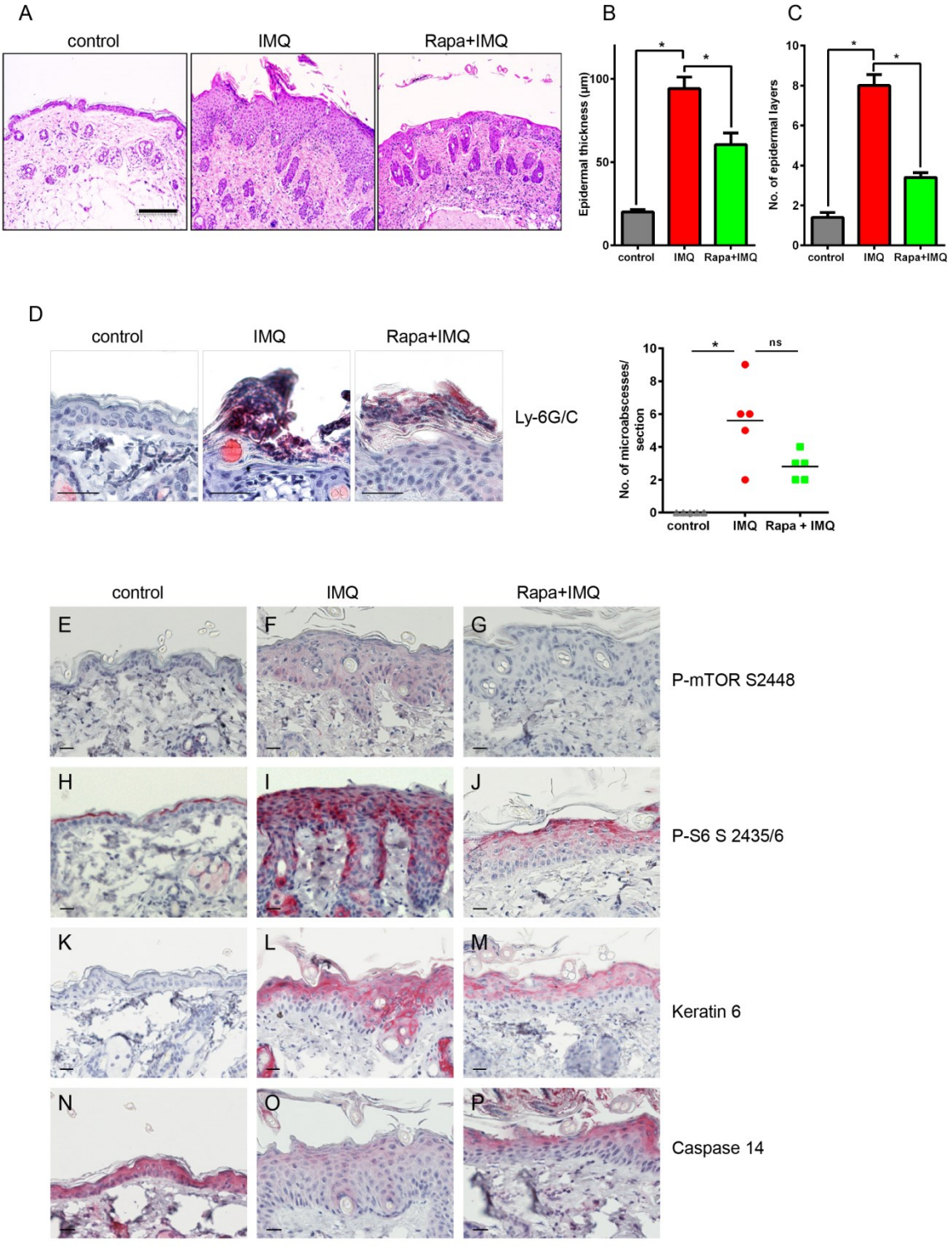
A
control
IMQ
Rapa+IMQ
B
Epidermal thickness (µm)
control
IMQ
Rapa+IMQ
C
No. of epidermal layers
control
IMQ
Rapa+IMQ
D
control
IMQ
Rapa+IMQ
Ly-6G/C
No. of microabscesses/ section
ns
control
IMQ
Rapa + IMQ
control
IMQ
Rapa+IMQ
E
F
G
P-mTOR S2448
H
I
J
P-S6 S 2435/6
K
L
M
Keratin 6
N
O
P
Caspase 14

Figure 3.4.12 Rapamycin reduces inflammation induced by dermal mTOR signaling (A) H&E staining of representative image from each group. (Bar represents 100μm. (B-C) Evaluation of histological features, including epidermal thickness and epidermal layers. (D) The number of neutrophil rich micro abscesses (indicated by arrow) was counted in the whole epidermis sheet. (Bar represents 100μm) Data shown is from one experiment, with n =5 per treatment group and error bars representing SEM. Statistical differences were determined by using one-way ANOVA or Mann-Whitney U test (*p ≤ 0.05. **p ≤ 0.01. ***p ≤ 0.001). (E-P) Immunohistochemistry staining with the indicated antibodies is shown from one representative mouse from each group. Scale bar represent 20 μm. As a copywrite holder of the article, the figure was reused from (Burger et al., 2017) with the permission of publisher.

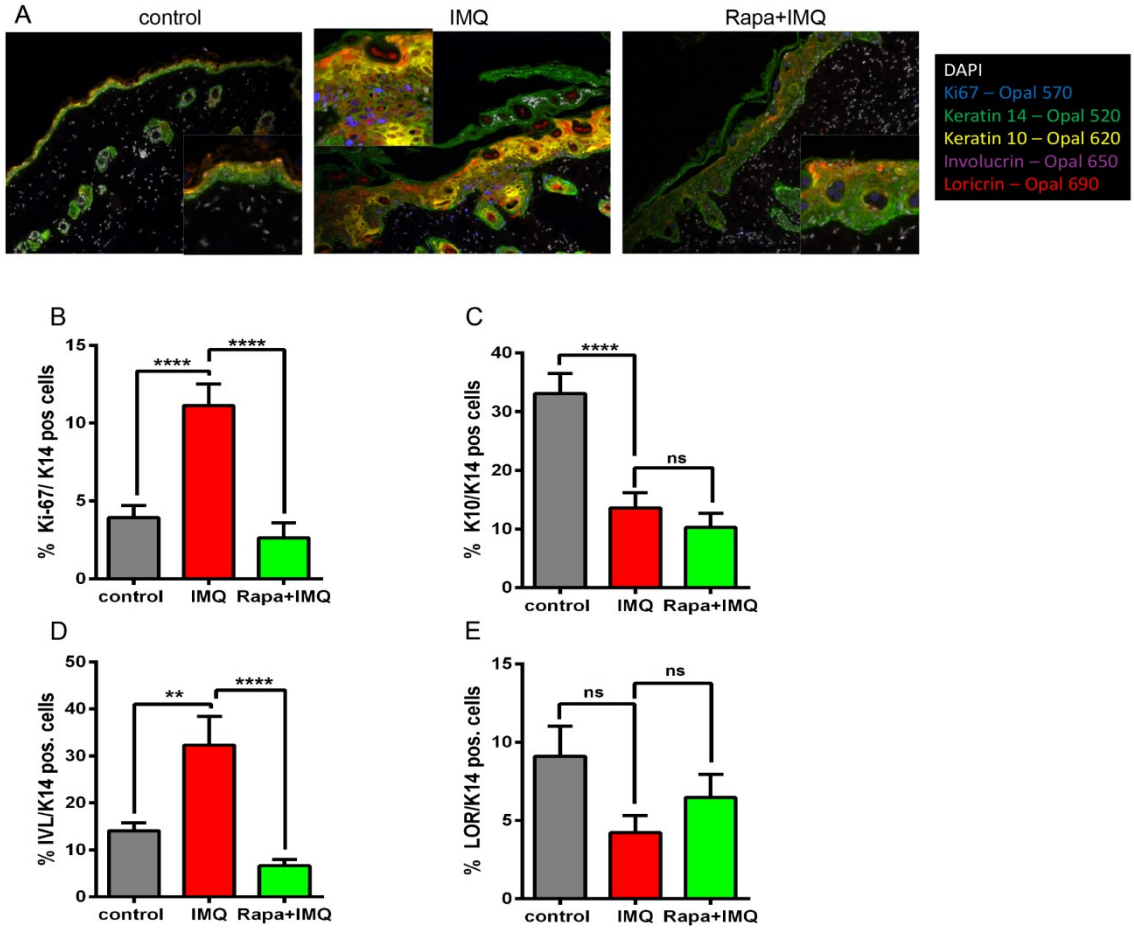

Figure 3.4.13 Rapamycin treatment normalizes the epidermal differentiation pattern. (A) Multiplex IHC staining with antibodies specific for Ki-67, keratin 14, keratin 10(K10), involucrin(IVL) and loricrin(LOR) was performed. Composite images from one representative mouse of each group are shown. Insert present close-up images from the same slides. (B-E) The number of positive cells for the specific marker (Ki-67, K10, IVL or LOR) of all (keratin 14 positive) keratinocytes per mouse sample was quantified in %. Data shown is from one experiment, with n =5 per treatment group and error bars representing SEM Statistical differences were determined by using one-way ANOVA or Mann-Whitney U test (*p ≤ 0.05. **p ≤ 0.01. ***p ≤ 0.001). As a copywrite holder of the article, the figure was reused from (Burger et al., 2017) with the permission of publisher.

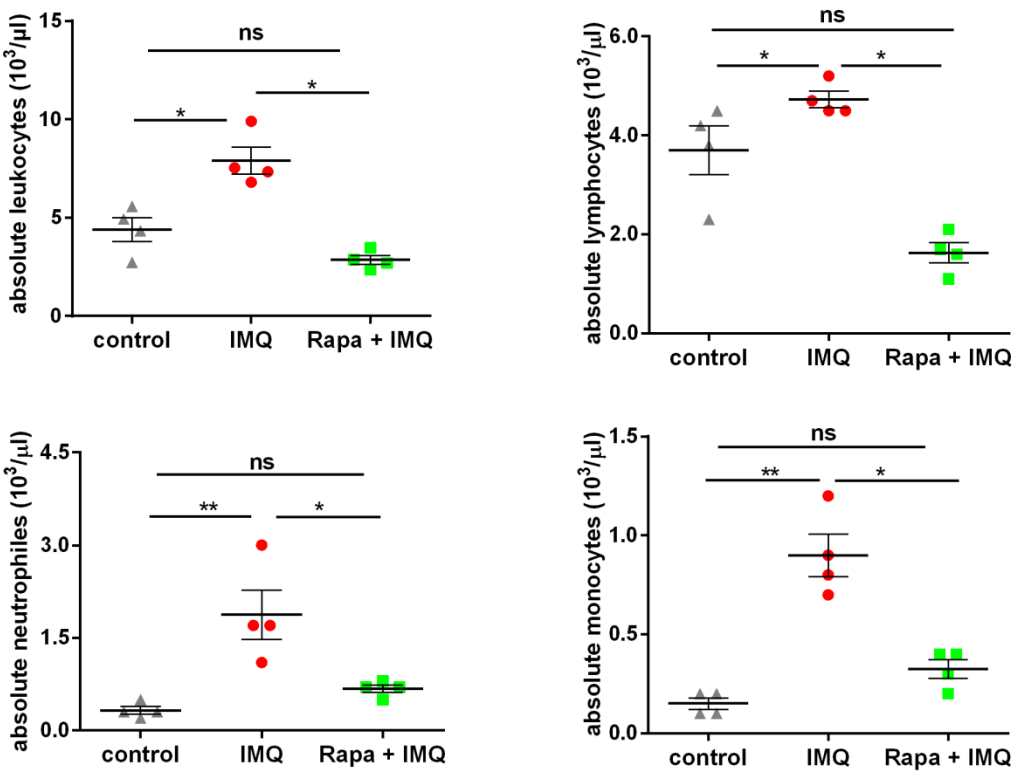

Figure 3.4.14 Systemic effect of topical rapamycin on total and differential leukocyte count. Total leukocytes were counted per 10^3/µL from n = 5 mice per treatment group and the absolute numbers of monocytes, neutrophils and lymphocytes were determined. Statistical differences were determined by using one-way ANOVA or Mann-Whitney U test (*p ≤ 0.05. **p ≤ 0.01. ***p ≤ 0.001). As a copywrite holder of the article, the figure was reused from (Burger et al., 2017) with the permission of publisher.

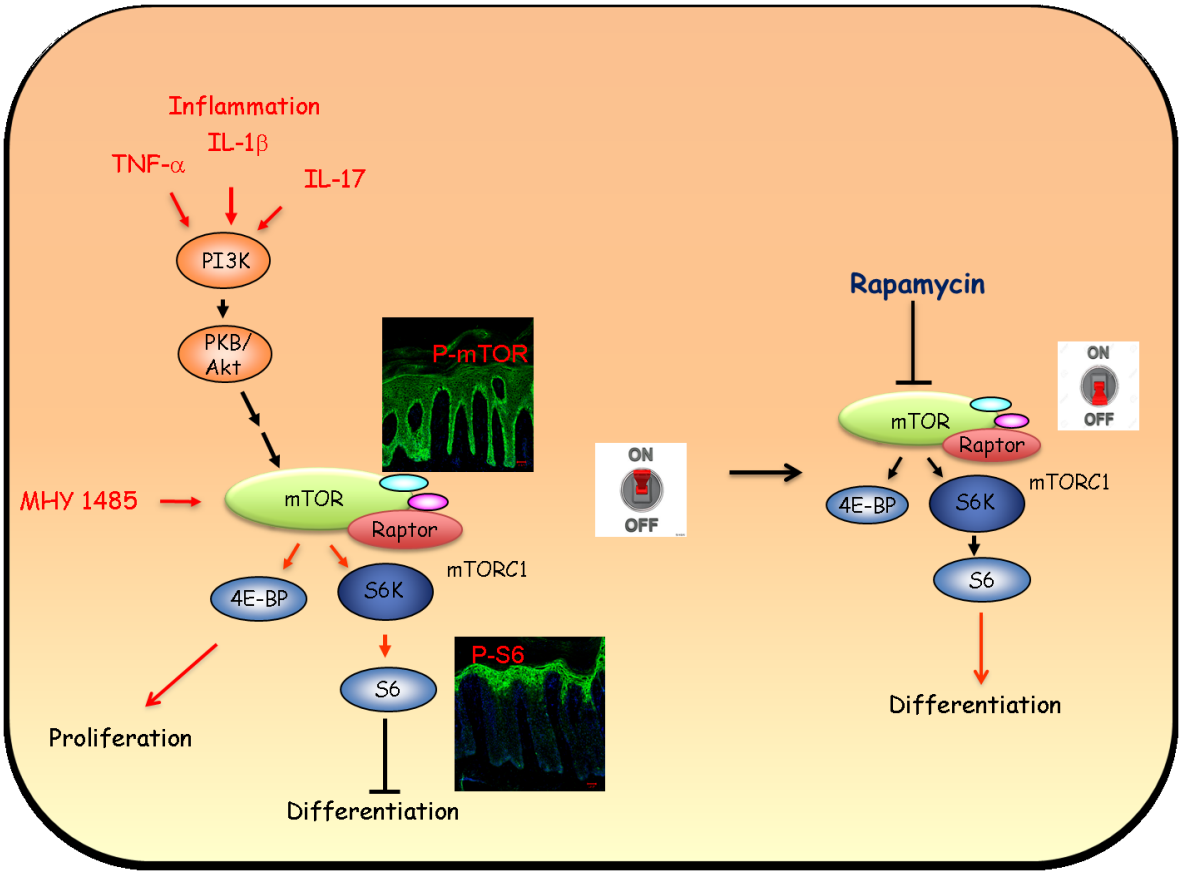

Figure 3.4.15 Schematic representation of targeting mTOR by topical application of rapamycin leading to normalization of inflammation-dependent aberrant activation of mTORC1.

3.5 TABLES

Study Groups	Macrophages(MF)	Dendritic cell (DC)	Plasmacytoid dendritic cells (pDCs)	Langerhans cells (LCs)
	$F4/80^{+}CD11b^{+}$	$CD11c^{+}CD11b^{+}$	$CD11c^{+}120G8^{+}SiglecH^{+}$	$CD207^{+}EpCAM^{+}$
control	0.025 ± 0.005	0.075 ± 0.005	0.195 ± 0.03	0.065 ± 0.055
IMQ	0.550 ± 0.100	0.640 ± 0.110	0.245 ± 0.00	0.160 ± 0.020
Rapa + IMQ	0.465 ± 0.005	0.545 ± 0.015	0.205 ± 0.015	0.125 ± 0.015

Table 3.5.1 Topical rapamycin reverse the shift from lymphoid to myeloid cells in IMQ model of psoriasis. Surface marker staining to quantify innate immune cells influx in lymph nodes was performed for F4/80+CD11b+ Macrophages (MF), CD11c+CD11b+ dendritic cell (DC), CD11c+120G8+SiglecH+ plasmacytoid dendritic cells (pDCs), and CD207+EpCAM+ migratory Langerhans cells (LCs). Sample collected 24 hours after last topical treatment. Average numbers ± SEM from lymph nodes of two samples, each pooled from two mice. As a copywrite holder of the article, the figure was reused from (Burger et al., 2017) with the permission of publisher.

4. THESIS CONTRIBUTIONS

Nitesh Shirsath performed the major part of the experimental work, analysed and interpreted the data and generated figures and tables shown here and wrote the dissertation.

Karin Wagner from Centre for Medical Research, Medical University of Graz, Graz, Austria helped with performing microarray and pathway analysis. Michaela Schlederer from the Department of Pathology, Department of Experimental and Laboratory Animal Pathology, Medical University Vienna performed the immunhistochemical (IHC) stainings of p21 and p16 while Simone Roos from Unit of Laboratory Animal Pathology, University of Veterinary Medicine, Vienna quantified the staining. Christian Ringel and Andreas Weigert from Institute of Biochemistry I, Faculty of Medicine, Goethe-University Frankfurt, Germany performed the multiplex staining for MHC-II marker and epidermal differentiation markers, respectively. Claudia Buerger, Victoria Lang, Alina Berard and Sandra Diehl from Department of Dermatology, Venerology and Allergology, Clinic of the Goethe University, Frankfurt am Main, Germany, performed the vitro tissue cell culture experiment and western blotting along with IHC stainings of patient tissue samples for mTOR pathway markers and for keratin 6 and caspase14. Tej Pratab Singh from Inflammation Biology Section, Laboratory of Molecular Immunology, NIAID, NIH, Bethesda, MD, USA, generated the K5.hTGFβ1 transgenic mouse tissue samples for the mTOR staining. Gerlinde Mayer from Research Unit for Photodermatology, Department of Dermatology and Venereology, Medical University of Graz, Graz, Austria, helped ,in part, in the IHC staining of the the K5.hTGFβ1 transgenic mouse tissue for mTOR pathway markers. Peter Wolf from the Research Unit for Photodermatology, Department of Dermatology and Venereology, Medical University of Graz, Graz, Austria, Lukas Kenner from Ludwig Boltzmann Institute for Cancer Research, Vienna, Austria and Claudia Buerger guided and helped to analyze and interpret the data.

5. ACKNOWLEDGEMENTS

Firstly, I would like to express my sincere gratitude to my PI and mentor Prof. Peter Wolf for the continuous support of my PhD study, for his patience, motivation, and immense knowledge. Thank you for giving me the creative freedom to conduct the research of my interest. His guidance and critical reviewing of my hypothesis helped me in all aspects of my research and writing of this thesis. I could not have imagined having a better advisor and mentor for my PhD study.

Thank you to the FWF Austrian Science Funding agency (Fund number W1241) and my PhD program, Doctoral college of Molecular Fundamentals of Inflammation (DK-MOLIN) of the Medical University of Graz, Austria for funding and supporting my research.

Besides this, my sincere thanks to Dr. Claudia Buerger for her collaboration. Prof.Lukas Kenner, for giving the opportunity to join his team for a limited period of time, and having access to the laboratory and research facilities in Vienna. And I am grateful to my former mentor, Dr. Kalpana Joshi for enlightening me with the first glance of research.

I would also like to express my thanks to the lab technician Mrs Gerlinde Mayer and Mrs Isabella Bambach for their kind support and extended help during my work. My lab mates Nina Schweintzger, Pablo Vieyra-Garcia and Vijaykumar Patra for their stimulating discussions, suggestions and help, along with Theresa and Saptaswa for all the fun we have had over the years.

Very special thank you to my wife, Rajni Shirsath for choosing a path which was not hers, for her unconditional love, encouragement, and tolerance. My son Chiku (Rudra) who's smile and hug at the end of the day made me forgot all the worries, you made all the difference in my life my son. To my parents whom I can't thank enough for allowing me to pursue my dreams. I am forever indebted to them for giving me the opportunities and experiences that have made me who I am. Last but not least, to my siblings Tai and Rahul and my in-laws for their constant support and encouragement.

6. REFERENCES

AKINDURO, O., SULLY, K., PATEL, A., ROBINSON, D. J., CHIKH, A., MCPHAIL, G., BRAUN, K. M., PHILPOTT, M. P., HARWOOD, C. A., BYRNE, C., O'SHAUGHNESSY, R. F. & BERGAMASCHI, D. 2016. Constitutive Autophagy and Nucleophagy during Epidermal Differentiation. *J Invest Dermatol,* 136**,** 1460-70.

ALCORTA, D. A., XIONG, Y., PHELPS, D., HANNON, G., BEACH, D. & BARRETT, J. C. 1996. Involvement of the cyclin-dependent kinase inhibitor p16 (INK4a) in replicative senescence of normal human fibroblasts. *Proc Natl Acad Sci U S A,* 93**,** 13742-7.

AYMARD, E., BARRUCHE, V., NAVES, T., BORDES, S., CLOSS, B., VERDIER, M. & RATINAUD, M. H. 2011. Autophagy in human keratinocytes: an early step of the differentiation? *Exp Dermatol,* 20**,** 263-8.

BAUMER, W., SULZLE, B., WEIGT, H., DE VRIES, V. C., HECHT, M., TSCHERNIG, T. & KIETZMANN, M. 2005. Cilomilast, tacrolimus and rapamycin modulate dendritic cell function in the elicitation phase of allergic contact dermatitis. *Br J Dermatol,* 153**,** 136-44.

BEUTNER, K. R., GEISSE, J. K., HELMAN, D., FOX, T. L., GINKEL, A. & OWENS, M. L. 1999. Therapeutic response of basal cell carcinoma to the immune response modifier imiquimod 5% cream. *J Am Acad Dermatol,* 41**,** 1002-7.

BOEHNCKE, W. H. & SCHON, M. P. 2015. Psoriasis. *Lancet,* 386**,** 983-94.

BRIGANTI, S., WLASCHEK, M., HINRICHS, C., BELLEI, B., FLORI, E., TREIBER, N., IBEN, S., PICARDO, M. & SCHARFFETTER-KOCHANEK, K. 2008. Small molecular antioxidants effectively protect from PUVA-induced oxidative stress responses underlying fibroblast senescence and photoaging. *Free Radic Biol Med,* 45**,** 636-44.

BRINGOLD, F. & SERRANO, M. 2000. Tumor suppressors and oncogenes in cellular senescence. *Exp Gerontol,* 35**,** 317-29.

BROGNARD, J., SIERECKI, E., GAO, T. & NEWTON, A. C. 2007. PHLPP and a second isoform, PHLPP2, differentially attenuate the amplitude of Akt signaling by regulating distinct Akt isoforms. *Mol Cell,* 25**,** 917-31.

BROS, M., DEXHEIMER, N., ROSS, R., TROJANDT, S., HOHN, Y., TAMPE, J., SUTTER, A., JAHRLING, F., GRABBE, S. & RESKE-KUNZ, A. B. 2011. Differential gene expression analysis identifies murine Cacnb3 as strongly upregulated in distinct dendritic cell populations upon stimulation. *Gene,* 472**,** 18-27.

BUERGER, C., MALISIEWICZ, B., EISER, A., HARDT, K. & BOEHNCKE, W. H. 2013. Mammalian target of rapamycin and its downstream signalling components are activated in psoriatic skin. *Br J Dermatol,* 169**,** 156-9.

BUERGER, C., RICHTER, B., WOTH, K., SALGO, R., MALISIEWICZ, B., DIEHL, S., HARDT, K., BOEHNCKE, S. & BOEHNCKE, W. H. 2012. Interleukin-1beta interferes with epidermal homeostasis through induction of insulin resistance: implications for psoriasis pathogenesis. *J Invest Dermatol,* 132**,** 2206-14.

BUERGER, C., SHIRSATH, N., LANG, V., BERARD, A., DIEHL, S., KAUFMANN, R., BOEHNCKE, W. H. & WOLF, P. 2017. Inflammation dependent mTORC1 signaling interferes with the switch from keratinocyte proliferation to differentiation. *PLoS One,* 12**,** e0180853.

BULAT, V., SITUM, M., DEDIOL, I., LJUBICIC, I. & BRADIC, L. 2011. The mechanisms of action of phototherapy in the treatment of the most common dermatoses. *Coll Antropol,* 35 Suppl 2**,** 147-51.

BURGER, C., SHIRSATH, N., LANG, V., DIEHL, S., KAUFMANN, R., WEIGERT, A., HAN, Y. Y., RINGEL, C. & WOLF, P. 2017. Blocking mTOR signalling with rapamycin ameliorates imiquimod-induced psoriasis in mice. *Acta Derm Venereol*.

BYRNE, S. N., BEAUGIE, C., O'SULLIVAN, C., LEIGHTON, S. & HALLIDAY, G. M. 2011. The immune-modulating cytokine and endogenous Alarmin interleukin-33 is upregulated in skin exposed to inflammatory UVB radiation. *Am J Pathol,* 179**,** 211-22.

BYRNE, S. N. & HALLIDAY, G. M. 2005. B cells activated in lymph nodes in response to ultraviolet irradiation or by interleukin-10 inhibit dendritic cell induction of immunity. *J Invest Dermatol,* 124**,** 570-8.

CAMPISI, J. & D'ADDA DI FAGAGNA, F. 2007. Cellular senescence: when bad things happen to good cells. *Nat Rev Mol Cell Biol,* 8**,** 729-40.

CAO, W., MANICASSAMY, S., TANG, H., KASTURI, S. P., PIRANI, A., MURTHY, N. & PULENDRAN, B. 2008. Toll-like receptor-mediated induction of type I interferon in plasmacytoid dendritic cells requires the rapamycin-sensitive PI(3)K-mTOR-p70S6K pathway. *Nat Immunol,* 9**,** 1157-64.

CHAMCHEU, J. C., CHAVES-RODRIQUEZ, M. I., ADHAMI, V. M., SIDDIQUI, I. A., WOOD, G. S., LONGLEY, B. J. & MUKHTAR, H. 2016. Upregulation of PI3K/AKT/mTOR, FABP5 and PPARbeta/delta in Human Psoriasis and Imiquimod-induced Murine Psoriasiform Dermatitis Model. *Acta Derm Venereol,* 96**,** 854-6.

CHAMIAN, F., LOWES, M. A., LIN, S. L., LEE, E., KIKUCHI, T., GILLEAUDEAU, P., SULLIVAN-WHALEN, M., CARDINALE, I., KHATCHERIAN, A., NOVITSKAYA, I., WITTKOWSKI, K. M. & KRUEGER, J. G. 2005. Alefacept reduces infiltrating T cells, activated dendritic cells, and inflammatory genes in psoriasis vulgaris. *Proc Natl Acad Sci U S A,* 102**,** 2075-80.

CHANDRAN, V. & RAYCHAUDHURI, S. P. 2010. Geoepidemiology and environmental factors of psoriasis and psoriatic arthritis. *J Autoimmun,* 34**,** J314-21.

CHECA, A., XU, N., SAR, D. G., HAEGGSTROM, J. Z., STAHLE, M. & WHEELOCK, C. E. 2015. Circulating levels of sphingosine-1-phosphate are elevated in severe, but not mild psoriasis and are unresponsive to anti-TNF-alpha treatment. *Sci Rep,* 5**,** 12017.

CHEN, J. Q., MAN, X. Y., LI, W., ZHOU, J., LANDECK, L., CAI, S. Q. & ZHENG, M. 2013. Regulation of involucrin in psoriatic epidermal keratinocytes: the roles of ERK1/2 and GSK-3beta. *Cell Biochem Biophys,* 66**,** 523-8.

CHEN, S., NAKAHARA, T., UCHI, H., TAKEUCHI, S., TAKAHARA, M., KIDO, M., DUGU, L., TU, Y., MOROI, Y. & FURUE, M. 2009a. Immunohistochemical analysis of the mammalian target of rapamycin signalling pathway in extramammary Paget's disease. *Br J Dermatol,* 161**,** 357-63.

CHEN, S. J., NAKAHARA, T., TAKAHARA, M., KIDO, M., DUGU, L., UCHI, H., TAKEUCHI, S., TU, Y. T., MOROI, Y. & FURUE, M. 2009b. Activation of the mammalian target of rapamycin signalling pathway in epidermal tumours and its correlation with cyclin-dependent kinase 2. *Br J Dermatol,* 160**,** 442-5.

CHI, H., LI, C., ZHAO, F. S., ZHANG, L., NG, T. B., JIN, G. & SHA, O. 2017. Anti-tumor Activity of Toll-Like Receptor 7 Agonists. *Front Pharmacol,* 8**,** 304.

CHIARINI, F., EVANGELISTI, C., MCCUBREY, J. A. & MARTELLI, A. M. 2015. Current treatment strategies for inhibiting mTOR in cancer. *Trends Pharmacol Sci,* 36**,** 124-35.

CHILDS, B. G., DURIK, M., BAKER, D. J. & VAN DEURSEN, J. M. 2015. Cellular senescence in aging and age-related disease: from mechanisms to therapy. *Nat Med,* 21**,** 1424-35.

CHOI, Y. J., PARK, Y. J., PARK, J. Y., JEONG, H. O., KIM, D. H., HA, Y. M., KIM, J. M., SONG, Y. M., HEO, H. S., YU, B. P., CHUN, P., MOON, H. R. & CHUNG, H. Y. 2012. Inhibitory effect of mTOR activator MHY1485 on autophagy: suppression of lysosomal fusion. *PLoS One,* 7**,** e43418.

CHOLLET, J. L., JOZWIAKOWSKI, M. J., PHARES, K. R., REITER, M. J., RODDY, P. J., SCHULTZ, H. J., TA, Q. V. & TOMAI, M. A. 1999. Development of a topically active imiquimod formulation. *Pharm Dev Technol,* 4**,** 35-43.

CHOWDHARI, S. & SAINI, N. 2016. Gene expression profiling reveals the role of RIG1 like receptor signaling in p53 dependent apoptosis induced by PUVA in keratinocytes. *Cell Signal,* 28**,** 25-33.

COATES, P. J. 2013. In brief: cell senescence. *J Pathol,* 230**,** 239-40.

COIMBRA, S., OLIVEIRA, H., REIS, F., BELO, L., ROCHA, S., QUINTANILHA, A., FIGUEIREDO, A., TEIXEIRA, F., CASTRO, E., ROCHA-PEREIRA, P. & SANTOS-SILVA, A. 2010. Interleukin (IL)-

22, IL-17, IL-23, IL-8, vascular endothelial growth factor and tumour necrosis factor-alpha levels in patients with psoriasis before, during and after psoralen-ultraviolet A and narrowband ultraviolet B therapy. *Br J Dermatol,* 163**,** 1282-90.

COOPER, K. D., OBERHELMAN, L., HAMILTON, T. A., BAADSGAARD, O., TERHUNE, M., LEVEE, G., ANDERSON, T. & KOREN, H. 1992. UV exposure reduces immunization rates and promotes tolerance to epicutaneous antigens in humans: relationship to dose, CD1a-DR+ epidermal macrophage induction, and Langerhans cell depletion. *Proc Natl Acad Sci U S A,* 89**,** 8497-501.

COPPE, J. P., DESPREZ, P. Y., KRTOLICA, A. & CAMPISI, J. 2010. The senescence-associated secretory phenotype: the dark side of tumor suppression. *Annu Rev Pathol,* 5**,** 99-118.

CROW, J. M. 2012. Psoriasis uncovered. *Nature,* 492**,** S50-1.

DAWE, R. S., CAMERON, H., YULE, S., MAN, I., WAINWRIGHT, N. J., IBBOTSON, S. H. & FERGUSON, J. 2003. A randomized controlled trial of narrowband ultraviolet B vs bath-psoralen plus ultraviolet A photochemotherapy for psoriasis. *Br J Dermatol,* 148**,** 1194-204.

DE FABO, E. C. & NOONAN, F. P. 1983. Mechanism of immune suppression by ultraviolet irradiation in vivo. I. Evidence for the existence of a unique photoreceptor in skin and its role in photoimmunology. *J Exp Med,* 158**,** 84-98.

DE FILIPPO, K., HENDERSON, R. B., LASCHINGER, M. & HOGG, N. 2008. Neutrophil chemokines KC and macrophage-inflammatory protein-2 are newly synthesized by tissue macrophages using distinct TLR signaling pathways. *J Immunol,* 180**,** 4308-15.

DEANE, J. A. & FRUMAN, D. A. 2004. Phosphoinositide 3-kinase: diverse roles in immune cell activation. *Annu Rev Immunol,* 22**,** 563-98.

DI MEGLIO, P., VILLANOVA, F. & NESTLE, F. O. 2014. Psoriasis. *Cold Spring Harb Perspect Med,* 4.

DING, X., BLOCH, W., IDEN, S., RÜEGG, M. A., HALL, M. N., LEPTIN, M., PARTRIDGE, L. & EMING, S. A. 2016. mTORC1 and mTORC2 regulate skin morphogenesis and epidermal barrier formation. *Nature Communications,* 7**,** 13226.

DONETTI, E., GUALERZI, A., RICCERI, F., PESCITELLI, L., BEDONI, M. & PRIGNANO, F. 2012. Etanercept restores a differentiated keratinocyte phenotype in psoriatic human skin: a morphological study. *Exp Dermatol,* 21**,** 549-51.

DROBITS, B., HOLCMANN, M., AMBERG, N., SWIECKI, M., GRUNDTNER, R., HAMMER, M., COLONNA, M. & SIBILIA, M. 2012. Imiquimod clears tumors in mice independent of adaptive immunity by converting pDCs into tumor-killing effector cells. *J Clin Invest,* 122**,** 575-85.

DUTHIE, M. S., KIMBER, I. & NORVAL, M. 1999. The effects of ultraviolet radiation on the human immune system. *Br J Dermatol,* 140**,** 995-1009.

EL MALKI, K., KARBACH, S. H., HUPPERT, J., ZAYOUD, M., REISSIG, S., SCHULER, R., NIKOLAEV, A., KARRAM, K., MUNZEL, T., KUHLMANN, C. R., LUHMANN, H. J., VON STEBUT, E., WORTGE, S., KURSCHUS, F. C. & WAISMAN, A. 2013. An alternative pathway of imiquimod-induced psoriasis-like skin inflammation in the absence of interleukin-17 receptor a signaling. *J Invest Dermatol,* 133**,** 441-51.

ELINE, D., VAN GELE, M., GRINE, L., REMAUT, K. & LAMBERT, J. 2017. Towards the development of a RNAi-based topical treatment for psoriasis: Proof-of-concept in a 3D psoriasis skin model. *Exp Dermatol*.

ELMETS, C. A., BERGSTRESSER, P. R., TIGELAAR, R. E., WOOD, P. J. & STREILEIN, J. W. 1983. Analysis of the mechanism of unresponsiveness produced by haptens painted on skin exposed to low dose ultraviolet radiation. *J Exp Med,* 158**,** 781-94.

FIELDING, C. A., MCLOUGHLIN, R. M., MCLEOD, L., COLMONT, C. S., NAJDOVSKA, M., GRAIL, D., ERNST, M., JONES, S. A., TOPLEY, N. & JENKINS, B. J. 2008. IL-6 regulates neutrophil trafficking during acute inflammation via STAT3. *J Immunol,* 181**,** 2189-95.

FIORINO, G. & OMODEI, P. D. 2015. Psoriasis and Inflammatory Bowel Disease: Two Sides of the Same Coin? *J Crohns Colitis,* 9**,** 697-8.

FITCH, E., HARPER, E., SKORCHEVA, I., KURTZ, S. E. & BLAUVELT, A. 2007. Pathophysiology of psoriasis: recent advances on IL-23 and Th17 cytokines. *Curr Rheumatol Rep,* 9**,** 461-7.

FLISIAK, I., POREBSKI, P. & CHODYNICKA, B. 2006. Effect of psoriasis activity on metalloproteinase-1 and tissue inhibitor of metalloproteinase-1 in plasma and lesional scales. *Acta Derm Venereol,* 86**,** 17-21.

FLUTTER, B. & NESTLE, F. O. 2013. TLRs to cytokines: mechanistic insights from the imiquimod mouse model of psoriasis. *Eur J Immunol,* 43**,** 3138-46.

FOGEL, A. L., HILL, S. & TENG, J. M. 2015. Advances in the therapeutic use of mammalian target of rapamycin (mTOR) inhibitors in dermatology. *J Am Acad Dermatol,* 72**,** 879-89.

FRIGERIO, E., COLOMBO, M. D., FRANCHI, C., ALTOMARE, A., GARUTTI, C. & ALTOMARE, G. F. 2007. Severe psoriasis treated with a new macrolide: everolimus. *Br J Dermatol,* 156**,** 372-4.

FROST, P., BERLANGER, E., MYSORE, V., HOANG, B., SHI, Y., GERA, J. & LICHTENSTEIN, A. 2013. Mammalian target of rapamycin inhibitors induce tumor cell apoptosis in vivo primarily by inhibiting VEGF expression and angiogenesis. *J Oncol,* 2013**,** 897025.

FUNK, J., LANGELAND, T., SCHRUMPF, E. & HANSSEN, L. E. 1991. Psoriasis induced by interferon-alpha. *Br J Dermatol,* 125**,** 463-5.

GORDON, P. M., DIFFEY, B. L., MATTHEWS, J. N. & FARR, P. M. 1999. A randomized comparison of narrow-band TL-01 phototherapy and PUVA photochemotherapy for psoriasis. *J Am Acad Dermatol,* 41**,** 728-32.

GORGOULIS, V. G. & HALAZONETIS, T. D. 2010. Oncogene-induced senescence: the bright and dark side of the response. *Curr Opin Cell Biol,* 22**,** 816-27.

GRIFFITHS, C. E., CHRISTOPHERS, E., BARKER, J. N., CHALMERS, R. J., CHIMENTI, S., KRUEGER, G. G., LEONARDI, C., MENTER, A., ORTONNE, J. P. & FRY, L. 2007. A classification of psoriasis vulgaris according to phenotype. *Br J Dermatol,* 156**,** 258-62.

GROSSMAN, R. M., KRUEGER, J., YOURISH, D., GRANELLI-PIPERNO, A., MURPHY, D. P., MAY, L. T., KUPPER, T. S., SEHGAL, P. B. & GOTTLIEB, A. B. 1989. Interleukin 6 is expressed in high levels in psoriatic skin and stimulates proliferation of cultured human keratinocytes. *Proc Natl Acad Sci U S A,* 86**,** 6367-71.

GUNZL, P. & SCHABBAUER, G. 2008. Recent advances in the genetic analysis of PTEN and PI3K innate immune properties. *Immunobiology,* 213**,** 759-65.

GUPTA, A., AVCI, P., DAI, T., HUANG, Y. Y. & HAMBLIN, M. R. 2013. Ultraviolet Radiation in Wound Care: Sterilization and Stimulation. *Adv Wound Care (New Rochelle),* 2**,** 422-437.

GUTTMAN-YASSKY, E., NOGRALES, K. E. & KRUEGER, J. G. 2011. Contrasting pathogenesis of atopic dermatitis and psoriasis--part I: clinical and pathologic concepts. *J Allergy Clin Immunol,* 127**,** 1110-8.

GYONGYOSI, N., LORINCZ, K., KESZEG, A., HALUSZKA, D., BANVOLGYI, A., TATRAI, E., KARPATI, S. & WIKONKAL, N. M. 2016. Photosensitivity of murine skin greatly depends on the genetic background: clinically relevant dose as a new measure to replace minimal erythema dose in mouse studies. *Exp Dermatol,* 25**,** 519-25.

HAMMAR, H., GU, S. Q., JOHANNESSON, A., SUNDKVIST, K. G. & BIBERFELD, P. 1984. Subpopulations of mononuclear cells in microscopic lesions of psoriatic patients. Selective accumulation of suppressor/cytotoxic T cells in epidermis during the evolution of the lesion. *J Invest Dermatol,* 83**,** 416-20.

HART, P. H., GRIMBALDESTON, M. A. & FINLAY-JONES, J. J. 2001. Sunlight, immunosuppression and skin cancer: role of histamine and mast cells. *Clin Exp Pharmacol Physiol,* 28**,** 1-8.

HART, P. H., GRIMBALDESTON, M. A., SWIFT, G. J., JAKSIC, A., NOONAN, F. P. & FINLAY-JONES, J. J. 1998. Dermal mast cells determine susceptibility to ultraviolet B-induced systemic suppression of contact hypersensitivity responses in mice. *J Exp Med,* 187**,** 2045-53.

HAWKES, J. E., GUDJONSSON, J. E. & WARD, N. L. 2017. The Snowballing Literature on Imiquimod-Induced Skin Inflammation in Mice: A Critical Appraisal. *J Invest Dermatol,* 137**,** 546-549.

HEIB, V., BECKER, M., WARGER, T., RECHTSTEINER, G., TERTILT, C., KLEIN, M., BOPP, T., TAUBE, C., SCHILD, H., SCHMITT, E. & STASSEN, M. 2007. Mast cells are crucial for early inflammation, migration of Langerhans cells, and CTL responses following topical application of TLR7 ligand in mice. *Blood,* 110**,** 946-53.

HEMMI, H., KAISHO, T., TAKEUCHI, O., SATO, S., SANJO, H., HOSHINO, K., HORIUCHI, T., TOMIZAWA, H., TAKEDA, K. & AKIRA, S. 2002. Small anti-viral compounds activate immune cells via the TLR7 MyD88-dependent signaling pathway. *Nat Immunol,* 3**,** 196-200.

HENNESSY, E. J., PARKER, A. E. & O'NEILL, L. A. 2010. Targeting Toll-like receptors: emerging therapeutics? *Nat Rev Drug Discov,* 9**,** 293-307.

HICKERSON, R. P., LEAKE, D., PHO, L. N., LEACHMAN, S. A. & KASPAR, R. L. 2009. Rapamycin selectively inhibits expression of an inducible keratin (K6a) in human keratinocytes and improves symptoms in pachyonychia congenita patients. *J Dermatol Sci,* 56**,** 82-8.

HIJNEN, D., KNOL, E. F., GENT, Y. Y., GIOVANNONE, B., BEIJN, S. J., KUPPER, T. S., BRUIJNZEEL-KOOMEN, C. A. & CLARK, R. A. 2013. CD8(+) T cells in the lesional skin of atopic dermatitis and psoriasis patients are an important source of IFN-gamma, IL-13, IL-17, and IL-22. *J Invest Dermatol,* 133**,** 973-9.

HOCKBERGER, P. E. 2002. A history of ultraviolet photobiology for humans, animals and microorganisms. *Photochem Photobiol,* 76**,** 561-79.

HOSTE, E., DENECKER, G., GILBERT, B., VAN NIEUWERBURGH, F., VAN DER FITS, L., ASSELBERGH, B., DE RYCKE, R., HACHEM, J. P., DEFORCE, D., PRENS, E. P., VANDENABEELE, P. & DECLERCQ, W. 2013. Caspase-14-deficient mice are more prone to the development of parakeratosis. *J Invest Dermatol,* 133**,** 742-50.

HOSTE, E., KEMPERMAN, P., DEVOS, M., DENECKER, G., KEZIC, S., YAU, N., GILBERT, B., LIPPENS, S., DE GROOTE, P., ROELANDT, R., VAN DAMME, P., GEVAERT, K., PRESLAND, R. B., TAKAHARA, H., PUPPELS, G., CASPERS, P., VANDENABEELE, P. & DECLERCQ, W. 2011. Caspase-14 is required for filaggrin degradation to natural moisturizing factors in the skin. *J Invest Dermatol,* 131**,** 2233-41.

HUANG, T., LIN, X., MENG, X. & LIN, M. 2014. Phosphoinositide-3 kinase/protein kinase-b/mammalian target of rapamycin pathway in psoriasis pathogenesis. A potential therapeutic target? *Acta Derm Venereol,* 94**,** 371-9.

HUANG, Y. H., TIAO, M. M., HUANG, L. T., CHUANG, J. H., KUO, K. C., YANG, Y. L. & WANG, F. S. 2015. Activation of Mir-29a in Activated Hepatic Stellate Cells Modulates Its Profibrogenic Phenotype through Inhibition of Histone Deacetylases 4. *PLoS One,* 10**,** e0136453.

HUBER, L. A. & TEIS, D. 2016. Lysosomal signaling in control of degradation pathways. *Curr Opin Cell Biol,* 39**,** 8-14.

HVID, M., JOHANSEN, C., DELEURAN, B., KEMP, K., DELEURAN, M. & VESTERGAARD, C. 2011. Regulation of caspase 14 expression in keratinocytes by inflammatory cytokines--a possible link between reduced skin barrier function and inflammation? *Exp Dermatol,* 20**,** 633-6.

IBBOTSON, S. H. & FARR, P. M. 1999. The time-course of psoralen ultraviolet A (PUVA) erythema. *J Invest Dermatol,* 113**,** 346-50.

ISHIDA-YAMAMOTO, A. & IIZUKA, H. 1995. Differences in involucrin immunolabeling within cornified cell envelopes in normal and psoriatic epidermis. *J Invest Dermatol,* 104**,** 391-5.

JAMPEL, R. M., FARMER, E. R., VOGELSANG, G. B., WINGARD, J., SANTOS, G. W. & MORISON, W. L. 1991. PUVA therapy for chronic cutaneous graft-vs-host disease. *Arch Dermatol,* 127**,** 1673-8.

JOHNSON-HUANG, L. M., SUAREZ-FARINAS, M., SULLIVAN-WHALEN, M., GILLEAUDEAU, P., KRUEGER, J. G. & LOWES, M. A. 2010. Effective narrow-band UVB radiation therapy suppresses the IL-23/IL-17 axis in normalized psoriasis plaques. *J Invest Dermatol,* 130**,** 2654-63.

KEIJSERS, R. R., JOOSTEN, I., HENDRIKS, A. G., KOENEN, H. J., VAN ERP, P. E. & VAN DE KERKHOF, P. C. 2015. Balance of Treg versus T-effector cells during systemic treatment with adalimumab and topical treatment with calcipotriol-betamethasone dipropionate ointment. *Exp Dermatol,* 24**,** 65-7.

KEIJSERS, R. R., JOOSTEN, I., VAN ERP, P. E., KOENEN, H. J. & VAN DE KERKHOF, P. C. 2014. Cellular sources of IL-17 in psoriasis: a paradigm shift? *Exp Dermatol,* 23**,** 799-803.

KOLLISCH, G., KALALI, B. N., VOELCKER, V., WALLICH, R., BEHRENDT, H., RING, J., BAUER, S., JAKOB, T., MEMPEL, M. & OLLERT, M. 2005. Various members of the Toll-like receptor family contribute to the innate immune response of human epidermal keratinocytes. *Immunology,* 114**,** 531-41.

KORVER, J. E., VAN DUIJNHOVEN, M. W., PASCH, M. C., VAN ERP, P. E. & VAN DE KERKHOF, P. C. 2006. Assessment of epidermal subpopulations and proliferation in healthy skin, symptomless and lesional skin of spreading psoriasis. *Br J Dermatol,* 155**,** 688-94.

LAGGNER, U., DI MEGLIO, P., PERERA, G. K., HUNDHAUSEN, C., LACY, K. E., ALI, N., SMITH, C. H., HAYDAY, A. C., NICKOLOFF, B. J. & NESTLE, F. O. 2011. Identification of a novel proinflammatory human skin-homing Vgamma9Vdelta2 T cell subset with a potential role in psoriasis. *J Immunol,* 187**,** 2783-93.

LANDE, R., GREGORIO, J., FACCHINETTI, V., CHATTERJEE, B., WANG, Y. H., HOMEY, B., CAO, W., WANG, Y. H., SU, B., NESTLE, F. O., ZAL, T., MELLMAN, I., SCHRODER, J. M., LIU, Y. J. & GILLIET, M. 2007. Plasmacytoid dendritic cells sense self-DNA coupled with antimicrobial peptide. *Nature,* 449**,** 564-9.

LAPLANTE, M. & SABATINI, D. M. 2012. mTOR signaling in growth control and disease. *Cell,* 149**,** 274-93.

LARANGE, A., ANTONIOS, D., PALLARDY, M. & KERDINE-ROMER, S. 2009. TLR7 and TLR8 agonists trigger different signaling pathways for human dendritic cell maturation. *J Leukoc Biol,* 85**,** 673-83.

LEGAT, F. J., HOFER, A., QUEHENBERGER, F., KAHOFER, P., KERL, H. & WOLF, P. 2004. Reduction of treatment frequency and UVA dose does not substantially compromise the antipsoriatic effect of oral psoralen-UVA. *J Am Acad Dermatol,* 51**,** 746-54.

LEMSTER, B. H., CARROLL, P. B., RILO, H. R., JOHNSON, N., NIKAEIN, A. & THOMSON, A. W. 1995. IL-8/IL-8 receptor expression in psoriasis and the response to systemic tacrolimus (FK506) therapy. *Clin Exp Immunol,* 99**,** 148-54.

LEO, M. S. & SIVAMANI, R. K. 2014. Phytochemical modulation of the Akt/mTOR pathway and its potential use in cutaneous disease. *Arch Dermatol Res,* 306**,** 861-71.

LI, A. G., WANG, D., FENG, X. H. & WANG, X. J. 2004. Latent TGFbeta1 overexpression in keratinocytes results in a severe psoriasis-like skin disorder. *EMBO J,* 23**,** 1770-81.

LI, Y., MAN, X., YOU, L., XIANG, Q., LI, H., XU, B., CHEN, Z., ZHANG, X. & LIAN, S. 2014. Downregulation of PTEN expression in psoriatic lesions. *Int J Dermatol,* 53**,** 855-60.

LIN, Y. K., YANG, S. H., CHEN, C. C., KAO, H. C. & FANG, J. Y. 2015. Using Imiquimod-Induced Psoriasis-Like Skin as a Model to Measure the Skin Penetration of Anti-Psoriatic Drugs. *PLoS One,* 10**,** e0137890.

LING, T. C., CLAYTON, T. H., CRAWLEY, J., EXTON, L. S., GOULDEN, V., IBBOTSON, S., MCKENNA, K., MOHD MUSTAPA, M. F., RHODES, L. E., SARKANY, R. & DAWE, R. S. 2016. British Association of Dermatologists and British Photodermatology Group guidelines for the safe and effective use of psoralen-ultraviolet A therapy 2015. *Br J Dermatol,* 174**,** 24-55.

LIU, Y. J. 2005. IPC: professional type 1 interferon-producing cells and plasmacytoid dendritic cell precursors. *Annu Rev Immunol,* 23**,** 275-306.

MAEDA, K. & AKIRA, S. 2016. TLR7 Structure: Cut in Z-Loop. *Immunity,* 45**,** 705-707.

MANNELLO, F., LUCHETTI, F., FALCIERI, E. & PAPA, S. 2005. Multiple roles of matrix metalloproteinases during apoptosis. *Apoptosis,* 10**,** 19-24.

MENDONCA, C. O. & BURDEN, A. D. 2003. Current concepts in psoriasis and its treatment. *Pharmacol Ther,* 99**,** 133-47.

MOLLER, K. I., KONGSHOJ, B., PHILIPSEN, P. A., THOMSEN, V. O. & WULF, H. C. 2005. How Finsen's light cured lupus vulgaris. *Photodermatol Photoimmunol Photomed,* 21**,** 118-24.

MORHENN, V. B. 1997. Langerhans cells may trigger the psoriatic disease process via production of nitric oxide. *Immunol Today,* 18**,** 433-6.

NASHAN, B. 2002. Review of the proliferation inhibitor everolimus. *Expert Opin Investig Drugs,* 11**,** 1845-57.

NAST, A., BOEHNCKE, W. H., MROWIETZ, U., OCKENFELS, H. M., PHILIPP, S., REICH, K., ROSENBACH, T., SAMMAIN, A., SCHLAEGER, M., SEBASTIAN, M., STERRY, W., STREIT, V., AUGUSTIN, M., ERDMANN, R., KLAUS, J., KOZA, J., MULLER, S., ORZECHOWSKI, H. D., ROSUMECK, S., SCHMID-OTT, G., WEBERSCHOCK, T., RZANY, B., DEUTSCHE DERMATOLOGISCHE, G. & BERUFSVERBAND DEUTSCHER, D. 2012. S3 - Guidelines on the treatment of psoriasis vulgaris (English version). Update. *J Dtsch Dermatol Ges,* 10 Suppl 2**,** S1-95.

NESTLE, F. O., CONRAD, C., TUN-KYI, A., HOMEY, B., GOMBERT, M., BOYMAN, O., BURG, G., LIU, Y. J. & GILLIET, M. 2005. Plasmacytoid predendritic cells initiate psoriasis through interferon-alpha production. *J Exp Med,* 202**,** 135-43.

NESTLE, F. O., KAPLAN, D. H. & BARKER, J. 2009. Psoriasis. *N Engl J Med,* 361**,** 496-509.

NOONAN, F. P., BUCANA, C., SAUDER, D. N. & DE FABO, E. C. 1984. Mechanism of systemic immune suppression by UV irradiation in vivo. II. The UV effects on number and morphology of epidermal Langerhans cells and the UV-induced suppression of contact hypersensitivity have different wavelength dependencies. *J Immunol,* 132**,** 2408-16.

O'SHAUGHNESSY, R. F., WELTI, J. C., COOKE, J. C., AVILION, A. A., MONKS, B., BIRNBAUM, M. J. & BYRNE, C. 2007. AKT-dependent HspB1 (Hsp27) activity in epidermal differentiation. *J Biol Chem,* 282**,** 17297-305.

OBINATA, H. & HLA, T. 2012. Sphingosine 1-phosphate in coagulation and inflammation. *Semin Immunopathol,* 34**,** 73-91.

ORMEROD, A. D., SHAH, S. A., COPELAND, P., OMAR, G. & WINFIELD, A. 2005. Treatment of psoriasis with topical sirolimus: preclinical development and a randomized, double-blind trial. *Br J Dermatol,* 152**,** 758-64.

PANKOW, S., BAMBERGER, C., KLIPPEL, A. & WERNER, S. 2006. Regulation of epidermal homeostasis and repair by phosphoinositide 3-kinase. *J Cell Sci,* 119**,** 4033-46.

PATRA, V., BYRNE, S. N. & WOLF, P. 2016. The Skin Microbiome: Is It Affected by UV-induced Immune Suppression? *Front Microbiol,* 7**,** 1235.

POWELL, J. D., POLLIZZI, K. N., HEIKAMP, E. B. & HORTON, M. R. 2012. Regulation of immune responses by mTOR. *Annu Rev Immunol,* 30**,** 39-68.

PREVEL, N., ALLENBACH, Y., KLATZMANN, D., SALOMON, B. & BENVENISTE, O. 2013. Beneficial role of rapamycin in experimental autoimmune myositis. *PLoS One,* 8**,** e74450.

PUA, H. H., STEINER, D. F., PATEL, S., GONZALEZ, J. R., ORTIZ-CARPENA, J. F., KAGEYAMA, R., CHIOU, N. T., GALLMAN, A., DE KOUCHKOVSKY, D., JEKER, L. T., MCMANUS, M. T., ERLE, D. J. & ANSEL, K. M. 2016. MicroRNAs 24 and 27 Suppress Allergic Inflammation and Target a Network of Regulators of T Helper 2 Cell-Associated Cytokine Production. *Immunity,* 44**,** 821-32.

RACZ, E., PRENS, E. P., KUREK, D., KANT, M., DE RIDDER, D., MOURITS, S., BAERVELDT, E. M., OZGUR, Z., VAN, I. W. F., LAMAN, J. D., STAAL, F. J. & VAN DER FITS, L. 2011. Effective treatment of psoriasis with narrow-band UVB phototherapy is linked to suppression of the IFN and Th17 pathways. *J Invest Dermatol,* 131**,** 1547-58.

RADACK, K. P., FARHANGIAN, M. E., ANDERSON, K. L. & FELDMAN, S. R. 2015. A review of the use of tanning beds as a dermatological treatment. *Dermatol Ther (Heidelb),* 5**,** 37-51.

RAUKTYS, A., LEE, N., LEE, L. & DABORA, S. L. 2008. Topical rapamycin inhibits tuberous sclerosis tumor growth in a nude mouse model. *BMC Dermatol,* 8**,** 1.

RAVIC-NIKOLIC, A., RADOSAVLJEVIC, G., JOVANOVIC, I., ZDRAVKOVIC, N., MITROVIC, S., PAVLOVIC, S. & ARSENIJEVIC, N. 2011. Systemic photochemotherapy decreases the expression of IFN-gamma, IL-12p40 and IL-23p19 in psoriatic plaques. *Eur J Dermatol,* 21**,** 53-7.

RAYCHAUDHURI, S. K. & RAYCHAUDHURI, S. P. 2014. mTOR Signaling Cascade in Psoriatic Disease: Double Kinase mTOR Inhibitor a Novel Therapeutic Target. *Indian J Dermatol,* 59**,** 67-70.

REITAMO, S., SPULS, P., SASSOLAS, B., LAHFA, M., CLAUDY, A., GRIFFITHS, C. E. & SIROLIMUS EUROPEAN PSORIASIS STUDY, G. 2001. Efficacy of sirolimus (rapamycin) administered concomitantly with a subtherapeutic dose of cyclosporin in the treatment of severe psoriasis: a randomized controlled trial. *Br J Dermatol,* 145**,** 438-45.

RHO, O., KIGUCHI, K., JIANG, G. & DIGIOVANNI, J. 2014. Impact of mTORC1 inhibition on keratinocyte proliferation during skin tumor promotion in wild-type and BK5.AktWT mice. *Mol Carcinog,* 53**,** 871-82.

RODERBURG, C., URBAN, G. W., BETTERMANN, K., VUCUR, M., ZIMMERMANN, H., SCHMIDT, S., JANSSEN, J., KOPPE, C., KNOLLE, P., CASTOLDI, M., TACKE, F., TRAUTWEIN, C. & LUEDDE, T. 2011. Micro-RNA profiling reveals a role for miR-29 in human and murine liver fibrosis. *Hepatology,* 53**,** 209-18.

ROELANDTS, R. 2002. The history of phototherapy: something new under the sun? *J Am Acad Dermatol,* 46**,** 926-30.

ROELANDTS, R. 2005. A new light on Niels Finsen, a century after his Nobel Prize. *Photodermatol Photoimmunol Photomed,* 21**,** 115-7.

ROLLER, A., PERINO, A., DAPAVO, P., SORO, E., OKKENHAUG, K., HIRSCH, E. & JI, H. 2012. Blockade of phosphatidylinositol 3-kinase PI3Kdelta or PI3Kgamma reduces IL-17 and ameliorates imiquimod-induced psoriasis-like dermatitis. *J Immunol,* 189**,** 4612-20.

SALEM, S. A., BARAKAT, M. A. & MORCOS, C. M. 2010. Bath psoralen+ultraviolet A photochemotherapy vs. narrow band-ultraviolet B in psoriasis: a comparison of clinical outcome and effect on circulating T-helper and T-suppressor/cytotoxic cells. *Photodermatol Photoimmunol Photomed,* 26**,** 235-42.

SANTAMARIA, A. B., DAVIS, D. W., NGHIEM, D. X., MCCONKEY, D. J., ULLRICH, S. E., KAPOOR, M., LOZANO, G. & ANANTHASWAMY, H. N. 2002. p53 and Fas ligand are required for psoralen and UVA-induced apoptosis in mouse epidermal cells. *Cell Death Differ,* 9**,** 549-60.

SAUER, S., BRUNO, L., HERTWECK, A., FINLAY, D., LELEU, M., SPIVAKOV, M., KNIGHT, Z. A., COBB, B. S., CANTRELL, D., O'CONNOR, E., SHOKAT, K. M., FISHER, A. G. & MERKENSCHLAGER, M. 2008. T cell receptor signaling controls Foxp3 expression via PI3K, Akt, and mTOR. *Proc Natl Acad Sci U S A,* 105**,** 7797-802.

SAUNDERS, R. N., METCALFE, M. S. & NICHOLSON, M. L. 2001. Rapamycin in transplantation: a review of the evidence. *Kidney Int,* 59**,** 3-16.

SCHLAGER, S., GOERITZER, M., JANDL, K., FREI, R., VUJIC, N., KOLB, D., STROHMAIER, H., DOROW, J., EICHMANN, T. O., ROSENBERGER, A., WOLFLER, A., LASS, A., KERSHAW, E. E., CEGLAREK, U., DICHLBERGER, A., HEINEMANN, A. & KRATKY, D. 2015. Adipose triglyceride lipase acts on neutrophil lipid droplets to regulate substrate availability for lipid mediator synthesis. *J Leukoc Biol,* 98**,** 837-50.

SCHLAPBACH, C., GEHAD, A., YANG, C., WATANABE, R., GUENOVA, E., TEAGUE, J. E., CAMPBELL, L., YAWALKAR, N., KUPPER, T. S. & CLARK, R. A. 2014. Human TH9 cells are skin-tropic and have autocrine and paracrine proinflammatory capacity. *Sci Transl Med,* 6**,** 219ra8.

SCHON, M. P., SCHON, M. & KLOTZ, K. N. 2006. The small antitumoral immune response modifier imiquimod interacts with adenosine receptor signaling in a TLR7- and TLR8-independent fashion. *J Invest Dermatol,* 126**,** 1338-47.

SCHWARZ, T. 2008. 25 years of UV-induced immunosuppression mediated by T cells-from disregarded T suppressor cells to highly respected regulatory T cells. *Photochem Photobiol,* 84**,** 10-8.

SCHWEINTZGER, N., GRUBER-WACKERNAGEL, A., REGINATO, E., BAMBACH, I., QUEHENBERGER, F., BYRNE, S. N. & WOLF, P. 2015a. Levels and function of regulatory T cells in patients with polymorphic light eruption: relation to photohardening. *Br J Dermatol,* 173**,** 519-26.

SCHWEINTZGER, N. A., BAMBACH, I., REGINATO, E., MAYER, G., LIMON-FLORES, A. Y., ULLRICH, S. E., BYRNE, S. N. & WOLF, P. 2015b. Mast cells are required for phototolerance induction and scratching abatement. *Exp Dermatol,* 24**,** 491-6.

SHERR, C. J. & DEPINHO, R. A. 2000. Cellular senescence: mitotic clock or culture shock? *Cell,* 102**,** 407-10.

SHIMOBAYASHI, M. & HALL, M. N. 2014. Making new contacts: the mTOR network in metabolism and signalling crosstalk. *Nat Rev Mol Cell Biol,* 15**,** 155-62.

SHIRSATH, N., MAYER, G., SINGH, T. P. & WOLF, P. 2015. 8-methoxypsoralen plus UVA (PUVA) therapy normalizes signalling of phosphorylated component of mTOR pathway in psoriatic skin of K5.hTGFbeta1 transgenic mice. *Exp Dermatol,* 24**,** 889-91.

SHREEDHAR, V., GIESE, T., SUNG, V. W. & ULLRICH, S. E. 1998. A cytokine cascade including prostaglandin E2, IL-4, and IL-10 is responsible for UV-induced systemic immune suppression. *J Immunol,* 160**,** 3783-9.

SIDKY, Y. A., BORDEN, E. C., WEEKS, C. E., REITER, M. J., HATCHER, J. F. & BRYAN, G. T. 1992. Inhibition of murine tumor growth by an interferon-inducing imidazoquinolinamine. *Cancer Res,* 52**,** 3528-33.

SINCLAIR, L. V., FINLAY, D., FEIJOO, C., CORNISH, G. H., GRAY, A., AGER, A., OKKENHAUG, K., HAGENBEEK, T. J., SPITS, H. & CANTRELL, D. A. 2008. Phosphatidylinositol-3-OH kinase and nutrient-sensing mTOR pathways control T lymphocyte trafficking. *Nat Immunol,* 9**,** 513-21.

SINGH, T. P., HUETTNER, B., KOEFELER, H., MAYER, G., BAMBACH, I., WALLBRECHT, K., SCHON, M. P. & WOLF, P. 2011. Platelet-activating factor blockade inhibits the T-helper type 17 cell pathway and suppresses psoriasis-like skin disease in K5.hTGF-beta1 transgenic mice. *Am J Pathol,* 178**,** 699-708.

SINGH, T. P., MAYER, G. & WOLF, P. 2014. In vivo siRNA targeting of CD28 reduces UV-induced DNA damage and inflammation. *J Invest Dermatol,* 134**,** 861-4.

SINGH, T. P., SCHON, M. P., WALLBRECHT, K., GRUBER-WACKERNAGEL, A., WANG, X. J. & WOLF, P. 2013. Involvement of IL-9 in Th17-associated inflammation and angiogenesis of psoriasis. *PLoS One,* 8**,** e51752.

SINGH, T. P., SCHON, M. P., WALLBRECHT, K., MICHAELIS, K., RINNER, B., MAYER, G., SCHMIDBAUER, U., STROHMAIER, H., WANG, X. J. & WOLF, P. 2010. 8-methoxypsoralen plus ultraviolet A therapy acts via inhibition of the IL-23/Th17 axis and induction of Foxp3+ regulatory T cells involving CTLA4 signaling in a psoriasis-like skin disorder. *J Immunol,* 184**,** 7257-67.

SINGH, T. P., ZHANG, H. H., BOREK, I., WOLF, P., HEDRICK, M. N., SINGH, S. P., KELSALL, B. L., CLAUSEN, B. E. & FARBER, J. M. 2016. Monocyte-derived inflammatory Langerhans cells and dermal dendritic cells mediate psoriasis-like inflammation. *Nat Commun,* 7**,** 13581.

SNELLMAN, E., KLIMENKO, T. & RANTANEN, T. 2004. Randomized half-side comparison of narrowband UVB and trimethylpsoralen bath plus UVA treatments for psoriasis. *Acta Derm Venereol,* 84**,** 132-7.

SULLY, K., AKINDURO, O., PHILPOTT, M. P., NAEEM, A. S., HARWOOD, C. A., REEVE, V. E., O'SHAUGHNESSY, R. F. & BYRNE, C. 2013. The mTOR inhibitor rapamycin opposes carcinogenic changes to epidermal Akt1/PKBalpha isoform signaling. *Oncogene,* 32**,** 3254-62.

SWINDELL, W. R., JOHNSTON, A., CARBAJAL, S., HAN, G., WOHN, C., LU, J., XING, X., NAIR, R. P., VOORHEES, J. J., ELDER, J. T., WANG, X. J., SANO, S., PRENS, E. P., DIGIOVANNI, J., PITTELKOW, M. R., WARD, N. L. & GUDJONSSON, J. E. 2011. Genome-wide expression profiling of five mouse models identifies similarities and differences with human psoriasis. *PLoS One,* 6**,** e18266.

TANAKA, M., WATAYA-KANEDA, M., NAKAMURA, A., MATSUMOTO, S. & KATAYAMA, I. 2013. First left-right comparative study of topical rapamycin vs. vehicle for facial angiofibromas in patients with tuberous sclerosis complex. *Br J Dermatol,* 169**,** 1314-8.

TANEW, A., RADAKOVIC-FIJAN, S., SCHEMPER, M. & HONIGSMANN, H. 1999. Narrowband UV-B phototherapy vs photochemotherapy in the treatment of chronic plaque-type psoriasis: a paired comparison study. *Arch Dermatol,* 135**,** 519-24.

TIBERIO, R., MARCONI, A., FILA, C., FUMELLI, C., PIGNATTI, M., KRAJEWSKI, S., GIANNETTI, A., REED, J. C. & PINCELLI, C. 2002. Keratinocytes enriched for stem cells are protected from anoikis via an integrin signaling pathway in a Bcl-2 dependent manner. *FEBS Lett,* 524**,** 139-44.

TORTOLA, L., ROSENWALD, E., ABEL, B., BLUMBERG, H., SCHAFER, M., COYLE, A. J., RENAULD, J. C., WERNER, S., KISIELOW, J. & KOPF, M. 2012. Psoriasiform dermatitis is driven by IL-36-mediated DC-keratinocyte crosstalk. *J Clin Invest,* 122**,** 3965-76.

TYRING, S. 2001. Imiquimod applied topically: A novel immune response modifier. *Skin Therapy Lett,* 6**,** 1-4.

VACCHELLI, E., EGGERMONT, A., SAUTES-FRIDMAN, C., GALON, J., ZITVOGEL, L., KROEMER, G. & GALLUZZI, L. 2013. Trial Watch: Toll-like receptor agonists for cancer therapy. *Oncoimmunology,* 2**,** e25238.

VACCHELLI, E., GALLUZZI, L., EGGERMONT, A., FRIDMAN, W. H., GALON, J., SAUTES-FRIDMAN, C., TARTOUR, E., ZITVOGEL, L. & KROEMER, G. 2012. Trial watch: FDA-approved Toll-like receptor agonists for cancer therapy. *Oncoimmunology,* 1**,** 894-907.

VALLAT, V. P., GILLEAUDEAU, P., BATTAT, L., WOLFE, J., NABEYA, R., HEFTLER, N., HODAK, E., GOTTLIEB, A. B. & KRUEGER, J. G. 1994. PUVA bath therapy strongly suppresses immunological and epidermal activation in psoriasis: a possible cellular basis for remittive therapy. *J Exp Med,* 180**,** 283-96.

VAN AELST, B., DEVLOO, R., ZACHEE, P., T'KINDT, R., SANDRA, K., VANDEKERCKHOVE, P., COMPERNOLLE, V. & FEYS, H. B. 2016. Psoralen and Ultraviolet A Light Treatment Directly Affects Phosphatidylinositol 3-Kinase Signal Transduction by Altering Plasma Membrane Packing. *J Biol Chem,* 291**,** 24364-24376.

VAN BELLE, A. B., DE HEUSCH, M., LEMAIRE, M. M., HENDRICKX, E., WARNIER, G., DUNUSSI-JOANNOPOULOS, K., FOUSER, L. A., RENAULD, J. C. & DUMOUTIER, L. 2012. IL-22 is required for imiquimod-induced psoriasiform skin inflammation in mice. *J Immunol,* 188**,** 462-9.

VAN DER FITS, L., MOURITS, S., VOERMAN, J. S., KANT, M., BOON, L., LAMAN, J. D., CORNELISSEN, F., MUS, A. M., FLORENCIA, E., PRENS, E. P. & LUBBERTS, E. 2009. Imiquimod-induced psoriasis-like skin inflammation in mice is mediated via the IL-23/IL-17 axis. *J Immunol,* 182**,** 5836-45.

VAN WEELDEN, H., BAART DE LA FAILLE, H., YOUNG, E. & VAN DER LEUN, J. C. 1990. Comparison of narrow-band UV-B phototherapy and PUVA photochemotherapy in the treatment of psoriasis. *Acta Derm Venereol,* 70**,** 212-5.

VOGT, M., HAGGBLOM, C., YEARGIN, J., CHRISTIANSEN-WEBER, T. & HAAS, M. 1998. Independent induction of senescence by p16INK4a and p21CIP1 in spontaneously immortalized human fibroblasts. *Cell Growth Differ,* 9**,** 139-46.

WALDMAN, T., KINZLER, K. W. & VOGELSTEIN, B. 1995. p21 is necessary for the p53-mediated G1 arrest in human cancer cells. *Cancer Res,* 55**,** 5187-90.

WALKER, D. & JACOBE, H. 2011. Phototherapy in the age of biologics. *Semin Cutan Med Surg,* 30**,** 190-8.

WALTER, A., SCHAFER, M., CECCONI, V., MATTER, C., UROSEVIC-MAIWALD, M., BELLONI, B., SCHONEWOLF, N., DUMMER, R., BLOCH, W., WERNER, S., BEER, H. D., KNUTH, A. & VAN DEN BROEK, M. 2013. Aldara activates TLR7-independent immune defence. *Nat Commun,* 4**,** 1560.

WANG, S., UCHI, H., HAYASHIDA, S., URABE, K., MOROI, Y. & FURUE, M. 2009. Differential expression of phosphorylated extracellular signal-regulated kinase 1/2, phosphorylated p38 mitogen-activated protein kinase and nuclear factor-kappaB p105/p50 in chronic inflammatory skin diseases. *J Dermatol,* 36**,** 534-40.

WANG, Z., RUAN, Z., MAO, Y., DONG, W., ZHANG, Y., YIN, N. & JIANG, L. 2014. miR-27a is up regulated and promotes inflammatory response in sepsis. *Cell Immunol,* 290**,** 190-5.

WEI, K. C. & LAI, P. C. 2015. Combination of everolimus and tacrolimus: a potentially effective regimen for recalcitrant psoriasis. *Dermatol Ther,* 28**,** 25-7.

WEICHHART, T. & SAEMANN, M. D. 2008. The PI3K/Akt/mTOR pathway in innate immune cells: emerging therapeutic applications. *Ann Rheum Dis,* 67 Suppl 3**,** iii70-4.

WOLF, P. 2016. Psoralen-ultraviolet A endures as one of the most powerful treatments in dermatology: reinforcement of this 'triple-product therapy' by the 2016 British guidelines. *Br J Dermatol,* 174**,** 11-4.

WOLF, P., BYRNE, S. N., LIMON-FLORES, A. Y., HOEFLER, G. & ULLRICH, S. E. 2016a. Serotonin signalling is crucial in the induction of PUVA-induced systemic suppression of delayed-type hypersensitivity but not local apoptosis or inflammation of the skin. *Exp Dermatol,* 25**,** 537-43.

WOLF, P., MAIER, H., MULLEGGER, R. R., CHADWICK, C. A., HOFMANN-WELLENHOF, R., SOYER, H. P., HOFER, A., SMOLLE, J., HORN, M., CERRONI, L., YAROSH, D., KLEIN, J., BUCANA, C., DUNNER, K., JR., POTTEN, C. S., HONIGSMANN, H., KERL, H. & KRIPKE, M. L. 2000. Topical treatment with liposomes containing T4 endonuclease V protects human skin in vivo from ultraviolet-induced upregulation of interleukin-10 and tumor necrosis factor-alpha. *J Invest Dermatol,* 114**,** 149-56.

WOLF, P., NGHIEM, D. X., WALTERSCHEID, J. P., BYRNE, S., MATSUMURA, Y., MATSUMURA, Y., BUCANA, C., ANANTHASWAMY, H. N. & ULLRICH, S. E. 2006. Platelet-activating factor is crucial in psoralen and ultraviolet A-induced immune suppression, inflammation, and apoptosis. *Am J Pathol,* 169**,** 795-805.

WOLF, P., WEGER, W., PATRA, V., GRUBER-WACKERNAGEL, A. & BYRNE, S. N. 2016b. Desired response to phototherapy vs photoaggravation in psoriasis: what makes the difference? *Exp Dermatol,* 25**,** 937-944.

WONG, T., HSU, L. & LIAO, W. 2013. Phototherapy in psoriasis: a review of mechanisms of action. *J Cutan Med Surg,* 17**,** 6-12.

XU, R., JIN, J., HU, W., SUN, W., BIELAWSKI, J., SZULC, Z., TAHA, T., OBEID, L. M. & MAO, C. 2006. Golgi alkaline ceramidase regulates cell proliferation and survival by controlling levels of sphingosine and S1P. *FASEB J,* 20**,** 1813-25.

XU, R., SUN, W., JIN, J., OBEID, L. M. & MAO, C. 2010. Role of alkaline ceramidases in the generation of sphingosine and its phosphate in erythrocytes. *FASEB J,* 24**,** 2507-15.

YANG, F., TANAKA, M., WATAYA-KANEDA, M., YANG, L., NAKAMURA, A., MATSUMOTO, S., ATTIA, M., MUROTA, H. & KATAYAMA, I. 2014. Topical application of rapamycin ointment ameliorates Dermatophagoides farina body extract-induced atopic dermatitis in NC/Nga mice. *Exp Dermatol,* 23**,** 568-72.

YAO, Y., RICHMAN, L., MOREHOUSE, C., DE LOS REYES, M., HIGGS, B. W., BOUTRIN, A., WHITE, B., COYLE, A., KRUEGER, J., KIENER, P. A. & JALLAL, B. 2008. Type I interferon: potential therapeutic target for psoriasis? *PLoS One,* 3**,** e2737.

YONES, S. S., PALMER, R. A., GARIBALDINOS, T. T. & HAWK, J. L. 2006. Randomized double-blind trial of the treatment of chronic plaque psoriasis: efficacy of psoralen-UV-A therapy vs narrowband UV-B therapy. *Arch Dermatol,* 142**,** 836-42.

YOSHIDA, A., KANNO, H., WATABE, D., AKASAKA, T. & SAWAI, T. 2008. The role of heparin-binding EGF-like growth factor and amphiregulin in the epidermal proliferation of psoriasis in cooperation with TNFalpha. *Arch Dermatol Res,* 300**,** 37-45.

ZHAO, J., BENAKANAKERE, M. R., HOSUR, K. B., GALICIA, J. C., MARTIN, M. & KINANE, D. F. 2010. Mammalian target of rapamycin (mTOR) regulates TLR3 induced cytokines in human oral keratinocytes. *Mol Immunol,* 48**,** 294-304.